2018

Synthesis, Characterization and Molecular Dynamic Simulations of Aqueous Choline Chloride Deep Eutectic Solvents

Sampson Asare
South Dakota State University

SYNTHESIS,CHARACTERIZATION AND MOLECULAR DYNAMIC SIMULATIONS OF AQUEOUS CHOLINE CHLORIDE DEEP EUTECTIC SOLVENTS

BY

SAMPSON ASARE

A dissertation submitted in partial fulfillment of the requirements for the

Doctor of Philosophy

Major in Chemistry

South Dakota State University

2018

SYNTHESIS,CHARACTERIZATION AND MOLECULAR DYNAMIC SIMULATIONS OF AQUEOUS CHOLINE CHLORIDE DEEP EUTECTIC SOLVENTS

SAMPSON ASARE

This dissertation is approved as a creditable and independent investigation by a candidate for the Doctor of Philosophy in CHEMISTRY degree and is acceptable for the dissertation requirements for this degree. Acceptance of this dissertation does not imply that the conclusions reached by the candidate are necessarily the conclusion of the major department.

Douglas E. Raynie, Ph.D. Date

Dissertation Advisor

Department Head, Chemistry & Biochemistry

Dean, Graduate School Date

ACKNOWLEDGEMENTS

I express my profound gratitude and thanks to the Lord Almighty for finishing what He started. Secondly, I wouldn't be here without the enduring tutelage, advice, and instructions of my advisor Dr. Douglas E. Raynie. Sir, I am because you made it happen. I am forever indebted to you for your kindness and sense of responsibility.

I would also want to thank the Chemistry and Biochemistry department of South Dakota State University and the United States government. My sincere thanks and gratitude to my academic committee members Prof. Brian Logue, Dr. Suvobrata Chakravarty, Dr. Jihong Cole-Dai, and Dr. Larry Holler for their advice. A special thanks to Prof. Fathi Halaweish for his advice and encouragement.

I want to also thank my colleagues in the Green Chemistry lab as well as the Pharmacy, Mechanical Engineering and Ag. Engineering Departments for granting me access to their labs. Special thanks to Pastors Dave and Jeannie Kaufman of Holylife Tabernacle Church, Brookings. Above all, I dedicate this work to my parents Jacob Asuo Afram and Salomey Boamah for their love, prayers, support and encouragement. Agyasuo and Eno Abena, you gave me what you never had. I am forever indebted to you both. I owe a huge

debt of gratitude to my siblings Hagar, Joshua, Naomi, Emmanuel, Michael, Martha, and Gaspar. This is for all the love, support, encouragements, prayers and tolerance to all the troubles I did cause you.

Finally, Lois, Allen, and Eliana, this is for you. I love you all dearly. To God be all the glory!

CONTENT

LIST OF FIGURES

LIST OF TABLES

LIST OF EQUATIONS

LIST OF ABBREVIATIONS

α----------Hydrogen bond donor acidity

β----------Hydrogen bond accepter basicity

π*----------Dipolarity/polarizability parameter

ChCl----------Choline Chloride

H_2O ----------Water

Mg ----------milligram

µL ----------microliter

°C ----------Degree centigrade

% ----------Percentage

Cm ----------centimeter

DES ----------Deep eutectic solvent

DESs ----------Deep eutectic solvents

DMSO ----------Dimethyl Sulfoxide

D_2O ----------Deuterated water

Etc.----------Et cetera

FTIR ----------Fourier transformed infra-red

g ---------- gram

Kg ---------- Kilogram

HBA ----------Hydrogen bond acceptor

HBD ----------Hydrogen bond donor

Kcal ----------kilocalories

M ----------Molar

ΔHvap ---------- Enthalpy of vaporization

δ_H ----------Hildebrand solubility parameter

kJ ----------kilojoules

K_{OW} ----------Octanol/water partition coefficient

Mg ----------milligram

MHz ----------Megahertz

mL ----------milliliter

H^1-NMR ----------Proton nuclear magnetic resonance

Pa ---------- Pascal

RI ---------- Refractive Index

RPM/rpm ---------- Revolution per minute

RTILs ---------- Room temperature ionic liquids

T_d ---------- Decomposition temperature

T_f ---------- Freezing temperature

T_g ---------- Glass transition temperature

T_m ---------- Melting temperature

QAS ---------- Quaternary ammonium salts

UV ---------- Ultra violet

UV-Vis ---------- Ultra violet-visible

Wt ---------- Weight

LLE ---------- Liquid/liquid equilibrium

SLE ---------- Solid/liquid equilibrium

IL ---------- Ionic liquid

Org. solv ---------- Organic solvent

DMSO-d6 ---------- Deuterated dimethyl sulfoxide

ChCl:H_2O ---------- Choline chloride/water mixture

DFT ---------- Density functional theory

CTA ---------- Charge transfer analysis

VDD ---------- Voronoi deformation density

K-S ---------- Kohn-Sham

s ---------- Second

ρ ---------- Density

μS ---------- micro Siemens

H-bond ---------- Hydrogen bond

AIM ---------- Atoms in Molecules

ABSTRACT

SYNTHESIS,CHARACTERIZATION AND MOLECULAR DYNAMIC SIMULATIONS OF AQUEOUS CHOLINE CHLORIDE DEEP EUTECTIC SOLVENTS

SAMPSON ASARE

2018

Various forms of deep eutectic solvents have been synthesized with advantages of 100% atom economy, low vapor pressure, ease of preparation, cost efficiency, low toxicity, and tunability. Though several DESs have been synthesized and characterized, including binary and ternary solvents, none of the binary DESs have been formulated with water as the sole hydrogen bond donor(HBD). This is due to a couple of opinions. First, water is disruptive to the eutectic bond in tertiary DES. Secondly, the ubiquity and concentration of water even in natural systems have led to the assertion that a solution rather than a eutectic solvent will be formed.

The aims of the study were to explore the use of water as the sole HBD in the formulation of type III DES and to exploit the small size of water molecules to further probe the nature of the eutectic bonding system in DESs. To achieve these aims,

a system of solvents made up of choline chloride and water at varying molar ratios of water were formulated and characterized. The solvents included ChCl:H_2O (1:1) through to ChCl:H_2O (1:10) with the ratio of water increasing by one.

Spectroscopic analyses and physicochemical analyses were carried out to ascertain intermolecular hydrogen bonding between the choline chloride and water, as well as characterize the solvents. Also, molecular dynamic simulation (MDS) coupled with density functional theory were used to probe the nature of the interactions within the solvents formulated.

The results of the spectroscopic analyses indicated shifts in peaks and bands associated with weak hydrogen bond interactions. This was significant as it provides evidence of DES formation from the choline chloride and water. The largest shifts came in the ChCl:H_2O (1:3) followed by ChCl:H_2O (1:4). This suggested that the eutectic formulation is ChCl:H_2O 1:3. Freezing and melting point determinations confirmed the eutectic composition to be ChCl:H_2O (1:3) with eutectic point of -84.7^{o}C. The ChCl:H_2O (1:4) followed with freezing point of -82.9^{o}C.

The thermal stability studies involving DSC and TGA were as predicted, as the ChCl:H_2O (1:3) and ChCl:H_2O (1:4) solvents

exhibited high decomposition temperatures and high stabilities commensurate with the observed strengths of the hydrogen bonds found in the spectroscopic analyses.

The molecular dynamic and DFT simulations affirmed the formation of hydrogen bonding between the QAS and HBD in the order of the strengths observed in the spectroscopic analyses. Also, the simulated charge transfer analyses from Hirshfeld partial charges and Voronoi's deformation density charges indicate charge spreading from the chloride anion onto the organic backbone of the choline cation and HBD to facilitate the formation of Hydrogen bonds between the chloride ion and the HBD leading to DES formation. It is important to mention that other weaker interactions may also play a less significant role.

CHAPTER ONE

INTRODUCTION

The concept of sustainability and renewability of resources has gained traction in recent decades in the field of science and, specifically, chemistry[1-2]. This push received impetus through the work of Paul Anastas and John Warner when they documented the concept of 'green chemistry' in 1998. Key to their work was the development of the twelve principles of green chemistry[3-6](see Table 1.0). These twelve principles have been adopted by the American Chemical Society (ACS) and have been the bedrock for the promotion of the use, development, and design of chemical processes that have enhanced economic benefits, protects the environment, and promote sustainability.

The principles developed by Anastas and Warner have stretched beyond the field of science and chemistry to mainstream governance. Goal twelve of the United Nations Sustainable Development Goals (SDGs), 2015, of the Agenda 2030 for sustainable development, adopted in September 2015, engenders the promotion of sustainable consumption and production patterns[7]. Targets four and five of goal twelve of the SDGs seek to achieve an environmentally benign management of chemicals and all wastes. It also seeks to ameliorate waste

generation through use of renewable resources, prevention, recycling, and reuse of waste whenever possible.

Table 1.0. The Twelve Principles of Green Chemistry

Number	Principle
1	Prevent waste
2	Maximize atom economy
3	Less hazardous chemical syntheses
4	Safer chemicals and products
5	Safer solvents and reaction conditions
6	Increase energy efficiency
7	Use renewable feedstocks
8	Avoid chemical derivatives
9	Use catalysts
10	Design chemicals and products to degrade after use
11	Realtime analyses to prevent pollution
12	Minimize potential for accidents

Data on the amount of chemical waste generated globally suggest an annual waste of 1.3 billion metric tons at a cost of $205 billion. This is expected to rise to 2.2 billion tons by 2025 with an estimated cost of $375 billion[8]. It is, therefore, not a coincidence that the number one concern and item on the twelve principles of green chemistry is waste prevention. It suffices to say that while the ideal chemical

process should generate no waste, maximize atom economy and use less hazardous chemicals, this is often not achieved[5].

A major source of waste is liquid waste from academic laboratories and industrial chemical process; this is mostly from extraction, separation, chemical syntheses, and pre-treatment processes. These chemical processes consume large amounts of solvents. Among the solvents include acids, bases, petroleum-derived organic solvents, and other inorganic solvents[9-10]. Among these solvents, the petroleum-derived solvents are the most often used and, thus, generate the most waste in terms of volume. For instance, the mass allocation in a typical pharmaceutical process is 51% solvent, 46% process, 2% unreacted reagents, and only 1% product[11]. These statistics are similar in almost all chemical laboratories.

The safety profiles of most of these solvents are highly detrimental and therefore undesirable. They pose severe safety consequences to both humans and the environment. Acute exposure could be fatal, bioaccumulation from long-term exposure could lead to chronic diseases and fatality, and usually have long half-life leading to prolonged adverse effect on the environment.

The technology for the treatment of such hazardous wastes continues to evolve. Among the methods employed in

neutralizing and disposing of hazardous wastes include biological treatment (employing bacteria and fungi to act on these compounds to degrade them or turn them into environmentally innocuous compounds), incineration, and in recent times, employing nanotechnology[12]. Associated with these neutralization treatments and disposal is high cost. The cost can be viewed in three ways. The first is transport and treatment of the hazardous waste. The second involves the cost in the development of such technologies needed to effectively neutralize the waste before disposal. The third component involves the cost to life and environment reclamation.

Solvents serve an integral part of chemistry, in both physical and chemical processes. Solvents have historically served as reaction media, in extraction, and as reaction templates[12]. Generally, liquids are classified as solvents. However, gases can also be described as solvents. Supercooled gases have similar density ranges and viscosities as liquids to warrant their classification as solvents[13-14].

The role and choice of a solvent for a specific physical or chemical process is based on the physical and chemical properties of the solvent. Some of the physical properties that affect choice of a solvent include density, viscosity,

boiling and melting points, thermal stability, polarity, and volatility. The chemical properties include toxicity, flammability, chemical stability, acidity, and basicity. The large volumes of solvents used and wastes generated in chemical and physical processes pose significant human and environmental concerns due to their toxicity. There is a direct effect on soil nutrients and texture, affecting crop productivity when these wastes are released into the environment without appropriate treatment. Water bodies and the lives within them suffer similar debilitating effects. The cost of treating these toxic wastes is steadily increasing, placing severe financial burden on academic, industrial, and governmental institutions.

With the increasing environmental, financial, and social impacts of conventional solvents, the advocates for alternative solvents to these conventional solvents have grown louder in recent decades. Human and environmental impacts have not been the only driving factors toward the development of alternative solvents. Chemical reactions and processes have increasingly become complex. The syntheses and extraction of novel chemical compounds with peculiar chemical and physical properties have also driven the need for alternative solvents to conventional solvents that are

increasingly unable to help in the synthesis and or extraction of these novel compounds. It is important to stress that as a matter of course and need, chemical processes are going to be increasingly complex. It is trite, therefore, to suggest that designer solvents would become increasingly relevant and popular.

The concept of alternative solvents is not new. Alternative solvents have often been discussed in the search for alternative methods or chemical during the occurrence of chemical disasters or routine method developments. However, in the context of this project, alternative solvents refer to less hazardous, environmentally friendly or benign and biodegradable solvents with similar or better efficiency than the conventional petroleum solvents.

1.1 JUSTIFICATION

Challenges associated with conventional petroleum-based solvents have led to the search for alternative greener solvents. Among the challenges associated with petroleum-based solvents include high vapor pressure that leads to easy exposure through inhalation. Another challenge is their high level of toxicity. Highly lipophilic solvents are easily absorbed into fatty tissues and organs of the body to exert their adverse events. They could also bioaccumulate over long periods of time leading to chronic diseases and possible fatality. Some of the adverse events include chronic liver and kidney diseases, cancers, teratogenic mutations, and mental retardation.

Furthermore, most of these conventional solvents due to their high volatility are highly flammable, increasing the risk of fire or explosion when working with them. Also, the impact on the environment, cost of treatment, and disposal of wastes generated from conventional organic solvents have added to the need for the development of alternative solvents.

Many such green solvents have been developed. An example is ionic liquids. Ionic liquids are, as their name suggests, ions (cation and anion) which when combined form liquids. The asymmetric nature of the constituent ions weakens the

intermolecular forces of attraction, hence, their low melting temperature.

Several ionic liquids have been synthesized for numerous applications in diverse fields. Among the areas of application include pharmaceutical, as reaction media and template, separation and extraction, and synthesis of nanoparticles among others. The ionic liquids have the advantages of design tunability, low vapor pressure, and reusable. However, ionic liquids exhibit critical demerits such as high toxicity and high cost of preparation.

Therefore, there is the need for greener, cheaper, nontoxic, and low-vapor pressure solvents to be developed that are benign to humans and the environment. Deep eutectic solvents are the new area of attention in the quest for greener alternative solvents. This is due to their ease of preparation with 100% atom economy, cheaper cost of constituents, low vapor pressure, and environmental friendliness. Deep eutectic solvents are also known to be nontoxic or less toxic compared to conventional organic solvents and ionic liquids. Another advantage of deep eutectic solvents is the ability to formulate binary, ternary, and potentially quaternary constituent solvent systems.

There are four types of deep eutectic solvents:

i. Quaternary ammonium salt + metal chloride
ii. Quaternary ammonium salt + metal chloride hydrate
iii. Quaternary ammonium salt + hydrogen bond donor
iv. Metal chloride hydrate + hydrogen bond donor

The third type of DES has been the most prominent solvents formulated in recent times. The simple definition of a quaternary ammonium salt (QAS) and a hydrogen bond donor (HBD) suggests that a combination of compounds of these chemical descriptions, in their right molar ratios, should produce a deep eutectic solvent.

Thus far, 18 quaternary ammonium salts have been used for the formulation of type III deep eutectic solvents. Also, about 46 hydrogen bond donors have been employed in the formulation of DESs. Of the 18 quaternary ammonium cations, the most abundantly used is choline chloride, for its cost and nontoxicity as it is vitamin B_4. Again, in all the HBDs, water, in a relatively few DES, is used as a component of ternary DES systems. This begs the question, if water is the most common and abundant HBD, and certainly nontoxic, why is it not used as a sole HBD in the formulation of DESs with QAS?

Also, with over a decade of research in DESs, the molecular basis underpinning the phenomenon and behavior of DESs is yet to be fully understood. The conventional school of thought is that the phenomenon is as a result of hydrogen bonding. This school of thought is further entrenched by the idea or requirement of a hydrogen bond donor. However, it is important to examine critically the contributions of all forces of interaction and the extent of the hydrogen bonding contribution to this phenomenon.

What is more, we are unable as of now to predict precisely the molar ratios of the constituent components that would form DES. We still formulate DESs through the method of trial and error. This leads to the use of large amounts of compounds and waste. Quantum mechanics/quantum chemistry molecular dynamic simulations through density function theory and force field simulations studies have been helpful to the understanding and prediction of chemical properties and behavior. This work is meant to answer the above questions.

Also, while water is the most abundant, nontoxic and inexpensive HBD, its use in DES formulations have been limited to ternary systems. This is because water has been suggested to negatively modify the structure of the DES leading to breaking of the electrostatic interactions among the

components. Water as the sole HBD in the formulation of DES is explored. The physical and chemical properties of the DES formed are characterized. We also explore the small size of the water molecule to explore the molecular basis for the formation of DES through quantum chemistry molecular dynamic simulations.

1.2 DEEP EUTECTIC SOLVENTS

1.2.1 Definition

Deep eutectic solvents(DES) are systems of solvents formed from the eutectic mixture of Lewis or Bronsted-Lowry acids and bases which can contain a variety of anionic and cationic species. These DESs contain asymmetric ions that have low lattice energy, hence low melting point[15-16].

Charge delocalization occurring through the Lewis base (anion or hydrogen bond acceptor) and a hydrogen bond donor moiety is believed to be the cause of the observed low melting point of the solvent compared to the melting points of the individual components[17-18] (see Figure 1.0). The eutectic point represents the composition at the lowest temperature of the mixture. These DESs are distinct from ionic liquids (IL) which are composed primarily of one type of discrete anion and cation.

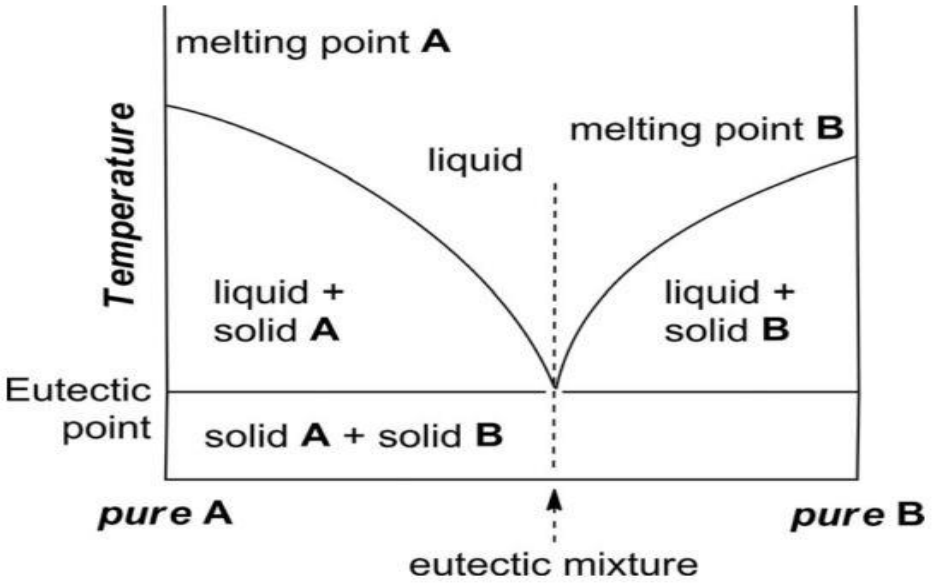

Figure 1.0. Phase diagram of a eutectic system of two components A and B with different melting points. The eutectic point represents the composition at the lowest temperature of the mixture.

Deep eutectic solvents can generally be described by the formula $Cat^{+}X^{-}zY$.[16]

Where Cat^{+} is the cation of the quaternary ammonium or phosphonium or sulfonium.

X^{-} is the Lewis base, generally a halide anion.

Y is the Bronsted-Lowry or Lewis acid and z is the number of Y molecules.

1.2.2 Classification

Deep eutectic solvents are classified based on the complexing agents used. There are four main classifications. A summary of the four classifications and their corresponding formulas is found in Table 1.1.

1.2.2.1 Type I: These include chloroaluminates imidazolium salts mixtures and imidazolium salts with metal halides. They are generally represented as $Cat^{+}X_z^{-}MCl_x$. MCl_x is the metal halide and M includes Fe, Zn, Sn, Al, Ga, and In. Examples of these imidazolium salts and metal halides include ethyl-3-methylimidazolium chloride(EMIC) and AgCl, CuCl, LiCl, $CdCl_2$, $SnCl_2$, $ZnCl_2$, $LaCl_3$, YCl_3, and $SnCl_4$[16, 19].

1.2.2.2 Type II: The type II DES expands the definition of DES to allow the incorporation of hydrated metal halides. They are generally represented as $Cat^{+}X_z^{-}MCl_x.yH_2O$. Here M include the following metals Cr, Co, Cu, Ni, and Fe. The hydrated metals possess two main advantages. First, they are cheap and easy to obtain. Secondly, they are less sensitive to air and moisture[16]. Examples include metal halides with choline chloride.

***1.2.2.3 Type III*:** This type of DES is by far the most versatile in terms of variety due to the possible number of hydrogen bond donors (HBD) available to prepare them. The

HBDs include amides, carboxylic acids, and alcohols. They are generally represented as $Cat^{+}X_z^{-}RZ$ where Z include $-CONH_2$, $-COOH$, and $-OH$[16-17, 20]. This type of DES reserve the advantages of ease of preparation, lower cost, biodegradability, and inertness to moisture. They are also adaptable or tunable for wide range of applications due to the chemical and physical properties of the various groups of HBDs available for their preparation. The physical and chemical properties of the solvents depend on the HBD. The cation is almost always choline chloride. Though the electrochemical window of this group of DES is narrow, it is enough for the electrodeposition of metals such as zinc with high efficiencies[16]. Type III DES have also been applied in areas such as the removal of glycerol from biodiesels[21-22], processing metal oxides[20, 23-24], and synthesis of organic compounds[25-26].

1.2.2.4 Type IV: This group of DESs is formed from metal halides and hydrogen bond donors. The general formula for this type of DESs is

$$MCl_x + RZ \rightarrow MCl_{x-1}^{+}.RZ + MCl_{x+1}^{-}$$

where an example of M are Al and Zn

An example of Z is $CONH_2$ and OH

Though inorganic cations do not generally form low melting point eutectics due to their high charge densities, Gambino et al 1987 was the first to show that metal halides react with urea to form eutectic system with a melting point below 150°C[27]. Abbot et al 2007 also confirmed the formation of eutectic systems between metal halides and HBDs when they successfully incorporated transition metal salts into DES by reacting with urea, acetamide, ethylene glycol, and 1,6-hexanediol[28].

Table 1.1. Categorization of deep eutectic solvents

Types	General formula	Terms	Example
Type I	$Cat^+X^- + zMCl_x$	M = Zn, In, Sn, Al, Fe	$ChCl + ZnCl_2$
TypeII	$Cat^+X^- + zMCl_x.yH_2O$	M = Cr, Ni, Cu, Fe, Co	$ChCl + CoCl_2.6H_2O$
TypeIII	$Cat^+X^- + zRZ$	Z = OH, COOH, $CONH_2$	ChCl + Urea
Type IV	$MCl_x + zRZ$	M = Zn, Al and Z = OH, $CONH_2$	$ZnCl_2$ + Urea

1.2.3 THE CASE OF NATURAL DEEP EUTECTICS SOLVENTS

Variations in climatic conditions have led to the development of various adaptive mechanisms for survival[29]. This is particularly true in extremophiles. An example of extremophiles is cryogenic organisms[30]. These organisms live in extremely cold environment. Several studies have been conducted on how cryogenic organisms avoid freezing and maintain cellular viability at such extremely cold temperatures[31]. It has been suggested that deep eutectic solvents formed from biomolecules such as amino acids and sugars sustain biochemical reactions and hence life in these organisms[31-32].

This is supported by the observation that cryogenic organisms have several aquaporin channels across the cell membranes that permit the flow of water, sugars, urea, and glycerol[33-34]. The sugars include mannitol and sorbitol. The unusually high level of these sugars and urea, and the expression of high thermal hysteria give credence to the suggestion that deep eutectic solvents may be formed intracellularly to aid survival[35]. All these molecules, in combination with amino acids and or water, are well known to form deep eutectic solvents.

Suffice to say that certain proteins, glycoproteins, and lipoproteins have been found to be produced in usually high levels or expressed ab initio in these organisms[36-37]. For instance, DeVries discovered that fish in Antarctica produce anti-freeze proteins (AFP)[38]. These AFPs bind to extracellular and intracellular water to prevent them from freezing. AFPs are known to prevent freezing, improve hemodynamics, and reduce apoptosis in studies involving cardiomyocytes[39].

Again, xylomannan, a biomolecule with β-mannopyranosyl-(1→4) β-xylopyranose backbone, extracted from *Upis ceramboides* is known to have antifreeze activity[35]. Another mechanism for survival at extremely cold environments involve the production of heat shock proteins (small hsp, hsp 70, and hsp 90) by the larvae of *Belgica antartica*[40]. Heat shock proteins are thought to facilitate protein folding in cryogenic organisms.

Another new but interesting area of DESs application that supports the idea of intracellular natural deep eutectic solvent is in DNA application. For instance, choline chloride:urea(1:2) has been used to study human telomere sequence DNA G-quadruplex folding with enhanced results[41]. Also, He et al.(2017) found that deep eutectic solvent facilitated information transfer from gene-length nucleic

acid in a model prebiotic replication[42]. This report was particular interesting as it suggested that viscous environment may have played a role in nucleic acid replication during the prebiotic era.

It against this background that suggestion for the existence of natural deep eutectic solvents (NADES) in biological species have been made[43]. The recent syntheses and applications of DESs from several biomolecules such as sugars, fatty acids, and amino acids provide impetus to the idea of existence[44-49].

1.2.4 CHOLINE CHLORIDE

Sulfonium and phosphonium cations can be used for the synthesis or formulation of DESs but quaternary ammonium salts (QAS) are the most commonly used[16, 50]. Choline [(2-hydroxyethyl)-N,N,N-trimethyl ammonium cation] chloride is by far the most widely used QAS. It is considered as a provitamin, B_4, and used as animal-food supplement. It is considered nontoxic to both humans and the environment and very cheap. It is a precursor to biologically active compounds such as acetylcholine (a neurotransmitter) and phosphatidylcholine (membrane component). It also serves as a methyl donor in animal systems. It is synthesized via a gas-phase reaction between HCl, ethylene oxide, and

trimethylamine with little or no waste[51-52]. Hence, an industrial use of choline chloride for the formulation of DESs raises no concern.

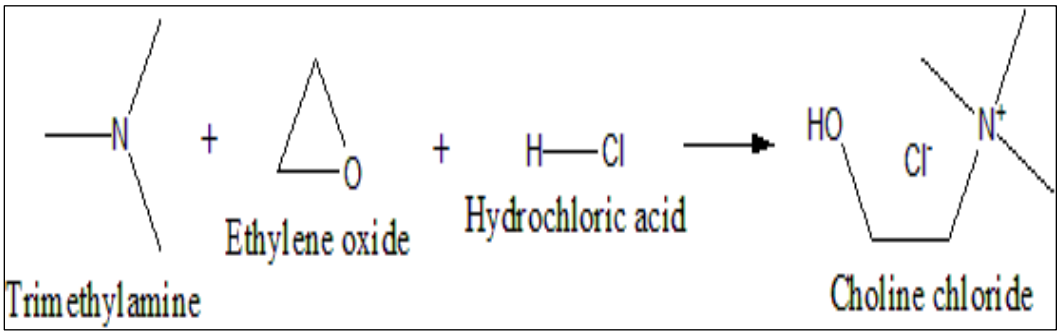

Figure 1.2. Gas phase synthesis of Choline Chloride

1.2.5 WATER

The most abundant molecule on earth is water covering about 75% of the earth's surface[52]. It is estimated that the oceans and the earth's crust contain about 1.4×10^{24} g and 0.8×10^{24} g of water respectively. Water is well known to be nontoxic and ubiquitous in biological systems. It is also by far the most used and desirable solvent in the laboratory.

Water is polar. The constituents of water are two hydrogen atoms and an atom of oxygen carrying a lone pair of electrons. Though very small in size (2.75 A), it has two hydrogen bond donors and one hydrogen bond acceptor. It acts both as an acid and base. Water molecules are interconnected by strong hydrogen bonds. This leads to water exhibiting unusual

physical and chemical properties (the water anomalies). For instance, water has an unusually high boiling and low freezing points of 100°C and 0°C. Again, upon freezing, the volume of water expands leading to a decrease in density.

1.3 ADVANTAGES OF DEEP EUTECTIC SOLVENTS

Deep eutectic solvents were developed as alternative green solvents to room-temperature ionic liquids (RTILs). Ionic liquids are made up of discrete ions (cations and anions). Though the major force interaction within the ILs is electrostatic, it is weakened by the asymmetric structure of the constituent ions which in turn weakens the lattice energy. Hence, they form liquids. Room-temperature ionic liquids form liquids at temperature 100°C or below[53-54].

RTILs have clear advantages over conventional organic solvents. RTILs are versatile and highly tunable. They can be task-specific designed for specific applications. RTILs and DESs have some similarities which include tunability, low vapor pressure, wide liquid range, and nonflammability[16, 55]. However, RTILs have shortcomings compared to DESs. Advantages of DESs over RTILs include ease of preparation, cheap cost of constituent compounds, less toxicity, and almost 100 percent atom economy[16, 56].

The formulation of DESs generally involves mixing and moderate heating at about 60°C or below for about 2 hours[55]. This however is not the case in RTILs. RTILs synthesis often involve multiple steps and under harsh chemical conditions. This is the major reason for the high cost of ionic liquids. A life cycle analysis on the synthesis of ionic liquids and DESs shows that ILs are less green than DESs[57]. Again, recent studies have shown that ILs are not nontoxic particularly to the environment. Ionic liquids are now known to inhibit enzymes and are cytotoxic, phytotoxic, and less biodegradable[58-60]. This is contrary to DESs which involves HBAs and HBDs that are generally less toxic. Also, DESs generally have zero E-factor as often 100% atom economy or mass efficiency is attained with no emissions.

1.3.1 NUMBER OF REFERENCES

There has been great interest in DESs since the first publication by Abbot et al 2003[15]. Data analytics from Web of Science and indicate that the decade immediately after Abbot's publication showed fewer than 100 publications in the DESs (see Figure 1.3). This was during the period of tremendous interest in ionic liquids as a greener, viable alternative to organic solvents. However, the turn of the decade has seen a steady growth in the DESs with applications in diverse fields of solvent chemistry.

This steady interest can be attributed to two main reasons. The first is the growing awareness of DESs and their vast areas of applicability. The second, however, has to do with a disinterest in ionic liquid borne from the realization their toxicity and high cost. For instance, data from Web of Science showed that in 2017, publications in the field of ionic liquids declined by 22% from 8154. During the same period, publications associated with DESs increased albeit at a low rate. Relatively, DESs research is still at the nascent stage but continuous to growth as more applications are reported and need for alternatives grow.

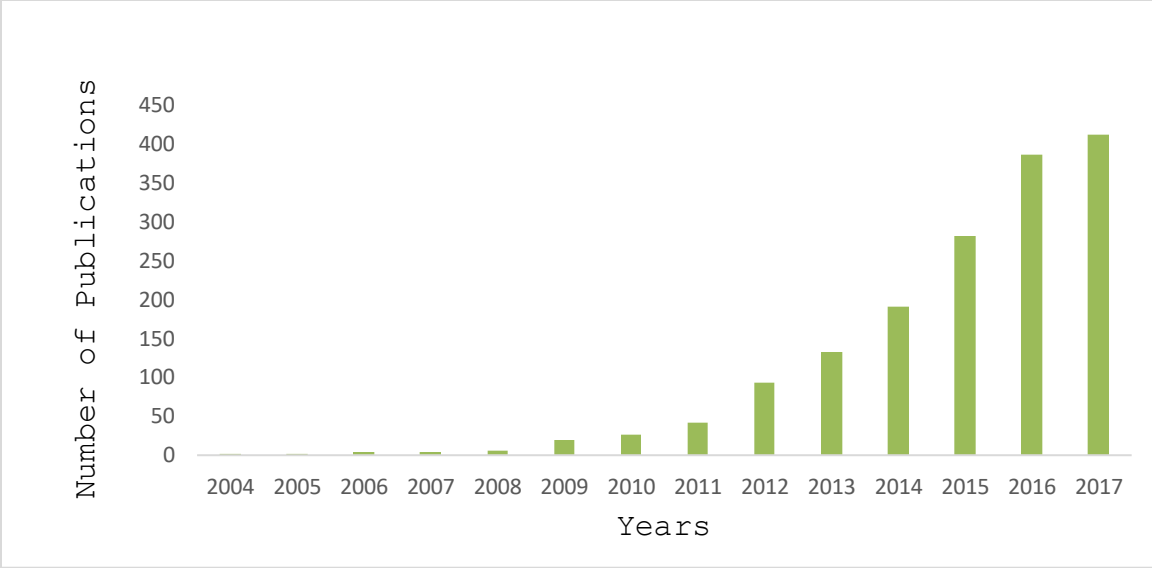

Figure 1.3. Number of publications containing the phrase 'deep eutectic solvent' in Web of Science over 14 years. The number of publications has markedly increased over the last five years.

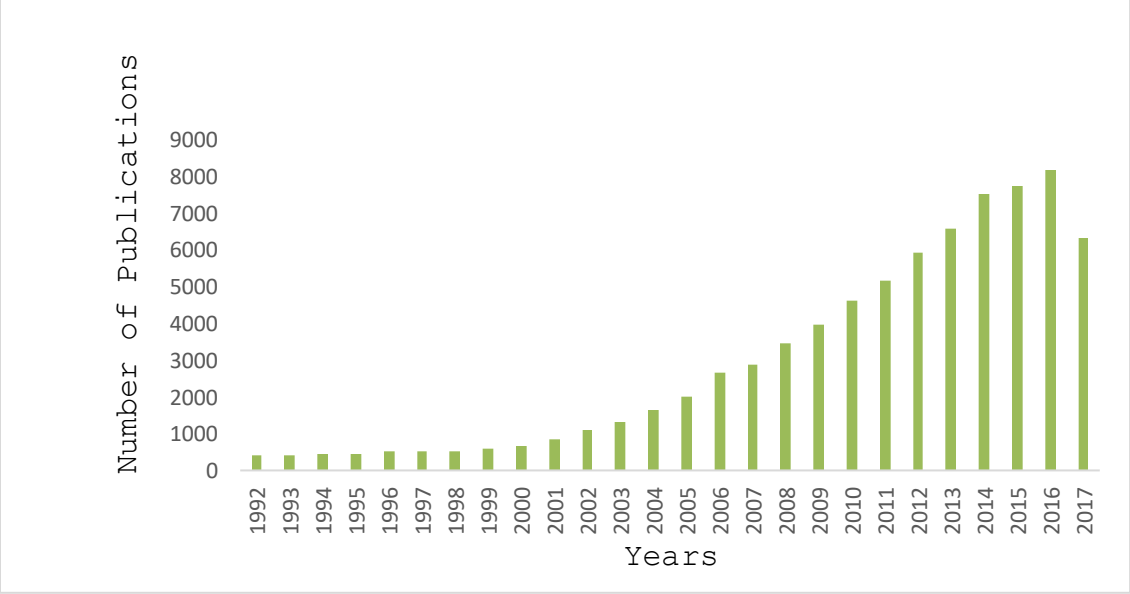

Figure 1.4. Number of publications containing the phrase 'ionic liquid' in Web of Science over the past two decades.

1.3.2 DISTRIBUTION OF RESEARCH FIELDS

Generally, DESs field of research and applications have been similar to those of ILs. There are eight main scientific areas that have drawn the most significant attention in both DESs and ILs research. In both DESs and ILs, synthesis and property characterization have received the most interest according to data from Web of Science and Scifinder. The two fields account for 53% and 48% in DESs and ILs respectively(see figures 1.5 and 1.6).

Also, analysis and separation are the next significant research fields to see application of both DESs and ILs. Together, the two fields account for 26% and 30% of areas or fields that have received attention in DESs and ILs respectively. Other notable areas or fields that have seen DESs and ILs research are sample preparations and nanotechnology. In recent times, DESs and ILs have received attention in the biological sciences for different reasons. In the case of ionic liquids, tags to biology have been more to the study of their toxicity. However, ever since the suggestion of possible formation and or existence of natural deep eutectic solvents (NADES)in cells of extremophiles using biomolecules, there have been growing studies of DESs from the biological sciences. This is accentuated by the observation that certain enzymes show increased activity and

selectivity in DESs than conventional media[61]. It is reasonable to expect high increase and expansion in the fields of application of DESs and particularly with NADES.

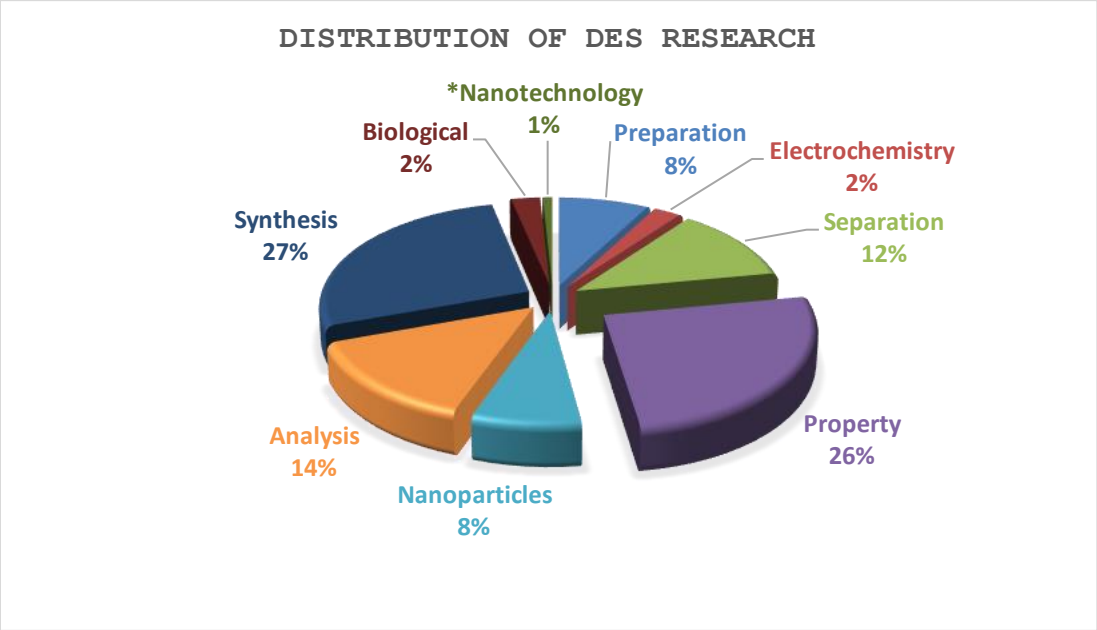

Figure 1.5. A chart of the distribution of the scientific fields that has observed possible application of deep eutectic solvents. The highest interests have been the synthesis and characterization of physical and chemical properties of DES

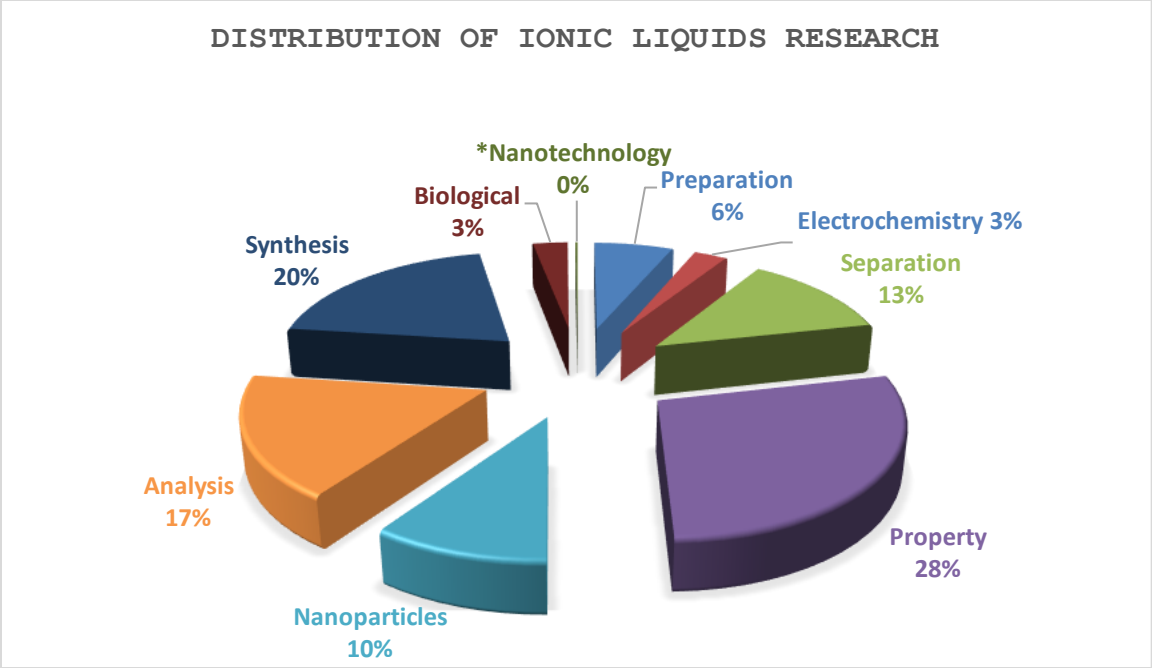

Figure 1.6. A chart of the distribution of the scientific fields that has observed possible application of ionic liquids. The fields of interest are the same in both ILs and DESs

1.4 APPLICATIONS OF DEEP EUTECTICS SOLVENTS

Several scientific fields have seen applications of deep eutectic solvents. These fields of application are similar to those of ionic liquids. This is expected as DESs were developed as alternative to ILs. Deep eutectic solvents have been applied as reaction media or template for organic synthesis. These include the Knoevenagel condensation synthesis of diphenyl amine[62], selective alkylation of aromatic primary amines[63], and synthesis of cinnamic acid[64].

Deep eutectic solvents have also been used in polymer synthesis. For instance, choline chloride (ChCl)-urea and ChCl-acrylic acid DESs have been used as media for frontal polymerization with superior yields than ILs and conventional organic solvents[65]. Also, polyanilines have been synthesized using ChCl-1,2-ethanediol(1:2)as media[66]. Deep eutectic solvents have been used to synthesize polyoctanediol-co-citrate elastomers[67], thermoplastic starch[68], and cellulose-based polymers[69].

Another area that has seen the application of deep eutectic solvents is electrochemistry. Here, the DESs have served as electrolytes for mostly electrodeposition of metals[70-73]. Also, synthesis of nanomaterials including star-shaped gold nanoparticles[74], ZnO nanorods[75-76], Ag nanoporous

films[77], carbon nanotubes[78], and CuCl nanoparticles[79] have been reported using DESs.

In the field of biochemistry, where DESs have recently been applied, enzyme kinetics and activity have been the focus areas. Deep eutectic solvents have served as media for the study of the activity of hydrolases[80] and lipase. Additionally, DESs have served as solvents for biocatalysis[81-82] and medium for storage of biologically active substances[83-84]. Again, DESs have been used as templates to immobilize complex polymers[85].

Another significant area of application of DESs is separation and analysis. For instance, ChCl-based and triphenylphosphonium DESs have been successfully used to remove glycerol from biodiesels and palm oils[22, 82, 86]. Again, DESs have been used to separate benzenes and phenols from mixtures[87-90] and to absorb hyaluronic acid[91]. Furthermore, Fe, Cu, and Zn in fish have been successfully analyzed with 95% recovery using ChCl-oxalic acid (1:2) as digestion medium[92].

CHAPTER TWO

FORMULATION AND SPECTROSCOPIC ANALYSIS OF DEEP EUTECTIC SOLVENT

2.0 INTRODUCTION

The most obvious advantages of DESs over ILs and conventional liquids are the safety and ease of preparation. Ionic liquids involve complex and multiple steps of synthesis. Also, the final products often contain by-products that render the ILs impure. Hence, purification is needed to achieve purities of 99% or higher. The combined effect is that ILs are expensive, difficult to prepare, and time consuming compared to DESs.

The first formulation or synthesis involving a quaternary ammonium salt and a hydrogen bond donor was by Abbot et al. 2002[15]. Abbot and his colleagues found that a 1:2 molar ratio of choline chloride and urea produced a eutectic solvent with melting point of 12°C compared to their respective melting points of 306°C (choline chloride) and 133°C (urea). The synthesis was done by simply heating and stirring, to a homogeneous liquid at 80°C, the choline chloride and urea in a 1:2 molar ratio.

Since Abbot's report, several methods have been developed for the formulation or synthesis of DESs. Most of these newly developed methods fundamentally involve heating and stirring. Methods that have been developed for synthesis of DESs include

freeze-drying, microwave irradiation, sonication, and vortexing. While most developed methods were for exploratory reasons to better understand the molecular basis of DES formation, others have been on the functionality or application. Also, other methods have focused on recovery and recyclability of the DESs. For instance, the freeze-drying method was developed to explore incorporation of bacteria into DESs for purposes of preservation. Ganesh Degam have extensively studied these various formulation methods[93]. The synthesis of DESs can be categorized into two main methods, thermal treatment and non-heat treatment.

2.1.0 THERMAL (HEAT) TREATMENT

The most common method of DESs preparation is the thermal or heat-treatment method. The method was employed in the synthesis of the first type III DES by Abbot et al. 2002. The method involves heating and stirring of the DES components together to homogeneity at a define temperature. Thermal treatment is often used to formulate DESs with melting points below 80°C. The formation of the DES complex depends on the DES components, temperature at which heating done, the length of heating, and/or stirring.

The heating is often carried out between 6-80°C with slow stirring. This is to avoid breaking the hydrogen bonds so

formed. Heating sources include hot plates, microwave irradiation, and rotary evaporator.

2.1.1 NON-HEAT TREATMENT METHODS

Nonthermal methods have also been used to prepare DESs. These modes of preparation often involve agitation at high speeds. These methods are best used in the synthesis or formulation of DESs with melting points at or below ambient temperature. Nonthermal methods include sonication, vortex mixing, and freeze-drying.

2.2 METHODOLOGY

2.2.1 MATERIALS

Choline chloride(ChCl) (99%) was purchased from Thermo-Fisher Scientific (Dubuque, IA). Deuterium oxide (D_2O) (99.8 atom% D) was purchased from Sigma-Aldrich (St Louis, MO). Dry ice was purchased from Hy-Vee (Brookings, SD). Ultrapure water was obtained from a Thermo-Fisher Scientific Barnstead E-Pure ultrapure water purifier system (Waltham,MA) set at 18.2 ΩM cm-1. D_2O and dry ice were used as received.

2.2.2 SYNTHESIS OF AQUEOUS CHOLINE CHLORIDE DES

The solubility of choline chloride in water is very high (620g/L). Indeed, choline chloride is highly hygroscopic. Therefore, aqueous choline chloride DESs were readily prepared by dissolving a defined molar amount in water with 100% atom economy. However, it must be stated that the objective was to determine whether water (H_2O) could be used as HBD and that whether choline chloride could form DES. Therefore, different molar ratios (1:1, 1:2, 1:3, 1:4, 1:6, 1:8) of choline chloride and water respectively were prepared. The melting points of these solvents were measured to determine the eutectic point.

2.2.3 DETERMINATION OF HYDROGEN BOND FORMATION

Central to the molecular description of deep eutectic systems is the existence or formation of hydrogen bonds within the solvent system. The energy-associated hydrogen bond varies from 1-40kcal/mol depending on the HBA or HBD, the geometry or orientation (distance and angle) of the H-bond, and the chemical environment. Therefore, the first objective was to establish the formation or otherwise of hydrogen bond in the aqueous choline chloride DES. The other objective was to establish which of the molar ratios or solvents had the strongest hydrogen bond interactions. Formation of hydrogen

bonds was studied using spectroscopic techniques viz FTIR, H^1-NMR, and Raman spectroscopy.

2.2.4 FTIR SPECTROSCOPY

Thermo-Fisher Scientific Nicolet 380 FTIR spectrometer (Waltham, MA) was used to obtain FTIR spectra of all the DESs formulated. The resolution was set at 8 nm^{-1}. The measurement spectrum range was 4000-400cm^{-1}. The spectra were produced and processed with EZ OMNIC software by Thermo-Fisher Scientific.

2.2.5 RAMAN SPECTROSCOPY

Raman spectra of all the DESs were obtained using Horiba Scientific LabRam HR Raman spectrometer (Edison, NJ) in a totally dark room. An Euromex fiber optic light source EK-1 (Euromex Holland) laser under the following parameters was used: x50 objective; 532 nm, DI filter; 1000 nm hole; grating: 1800; range: 300 nm – 1000 nm; and time = 5s. The spectra were obtained with Horiba Yvon LabSpec and processed with Originlab-Pro SR2(Northampton, MA).

2.2.6 PROTON (H^1)-NMR

Proton NMR(H^1-NMR) spectra were obtained for all the DESs and the constituent compounds. A Bruker 400 MHz spectrometer (Billerica, MA) equipped with QNP 5 mm probe at 400 MHz and 22°C was used to obtain the ^{1}H-NMR spectra. Deuterated DMSO (DMSO-d_6) and deuterated water (D_2O) were used as solvents for the DESs. The D_2O were used directly. In the case of DMSO-d_6, 5 µl of the DESs prepared with deionized water were added to sufficient amounts of DMSO-d_6. The ^{1}H-NMR parameters were set as follows: 90° pulse angle, 25 pulse rate, and 512 scans. All DESs were kept in a desiccator prior to the H^1-NMR scan.

2.2.7 FREEZING POINT

The freezing points of the aqueous choline chloride DESs were ascertained by transferring 5ml each into scintillation vials. A thermocouple temperature probe connected to a Vernier Labquest 2 (Beaverton, OR) was used for measuring the freezing temperature. The freezing was instigated in a dry ice bath insulated with polystyrene. The freezing points were conducted in triplicate and the average reported.

2.2.8 WATER CONTENT ANALYSIS

The available free water content in the DESs were determined via Karl Fischer coulometric method. A Metrohm 831 Karl Fischer coulometric titrator (Herisau, Switzerland) was used. The accuracy of the Karl Fischer titrator was ascertained using Hydranal CMR water standard 1.00 mg/g (St.Louis, MO). The percent water contents were measured in triplicate and the average reported. The DESs were prepared at 20 percent equivalent mass to cut down on amounts of choline chloride (0.200 mol) used.

Table 2.0. Molar ratios and mole fraction of aqueous choline chloride deep eutectics solvents.

SAMPLE	MOLAR RATIO	MOLAR FRACTION OF $CHCl^-$
Choline Cl^-:H_2O	1:1	0.50
Choline Cl^-:H_2O	1:2	0.33
Choline Cl^-:H_2O	1:3	0.25
Choline Cl^-:H_2O	1:4	0.20
Choline Cl^-:H_2O	1:5	0.17
Choline Cl^-:H_2O	1:6	0.14
Choline Cl^-:H_2O	1:8	0.11
Choline Cl^-:H_2O	1:10	0.09

2.3 RESULTS AND DISCUSSION

2.3.1 FTIR SPECTROSCOPY ANALYSIS

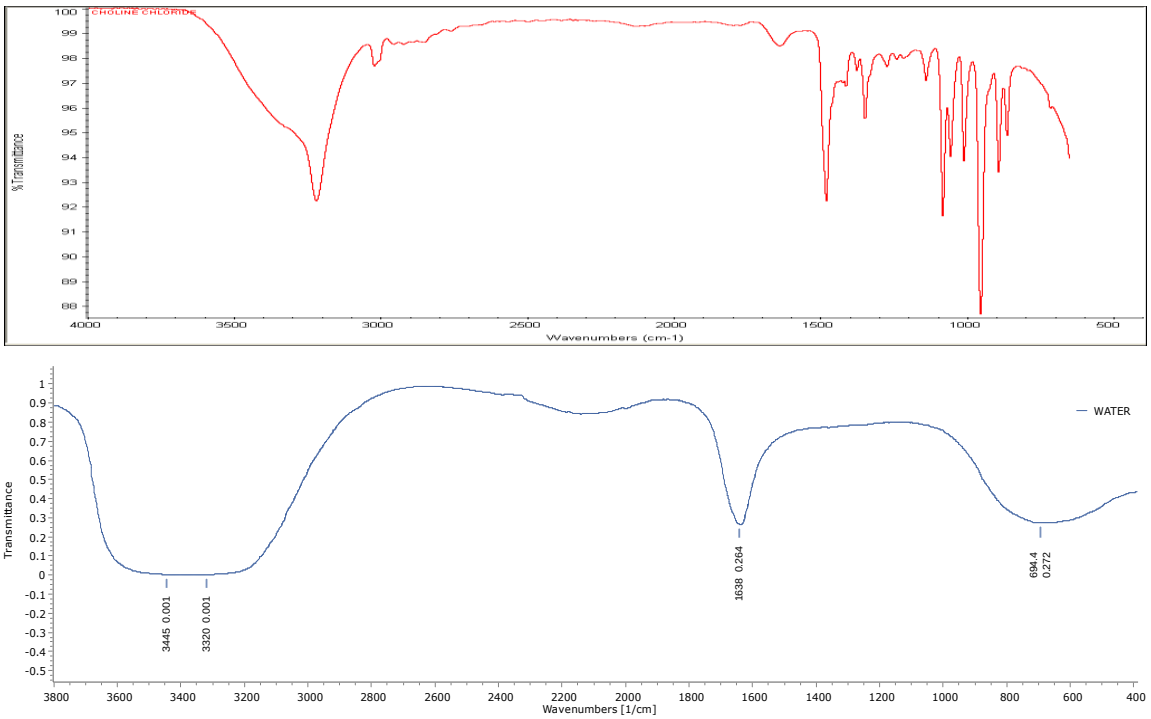

Figure 2.0. The FTIR spectra of choline chloride (above) and water (below). The -OH peak in the choline chloride and water are at 3225 cm^{-1} and 3445 cm^{-1} respectively.

Hydrogen bonding leads to significant changes to the frequency shifts in the infrared bands and the intensity of the vibrational modes of the groups involved in the hydrogen bond[94]. Hydrogen bonding also leads to band broadening. Free -OH stretching appears as a sharp band at ≈3600 cm^{-1} but reduces upon hydrogen bonding[95]. Area under the -OH stretching peak in solid ChCl at 3025 cm^{-1} as the water molecules increase is indicative of hydrogen bonding. The -OH band area

broadening at 3025 cm^{-1} increased from 8567 in ChCl:H_2O (1:1) to 12920 in ChCl:H_2O (1:10). However, the most significant finding is the fact that the rate of increase in band broadening from ChCl:H_2O (1:1) to ChCl:H_2O (1:4) compared to the increase observed from ChCl:H_2O (1:5) through ChCl:H_2O (1:10).

Also, the band/peak observed at about 1380 cm^{-1} in solid choline chloride is conspicuously absent in the DESs (Figures 2.0, 2.1, and 2.2). This coupled with the band broadening observed in the peak at 1650 cm^{-1} also indicates interaction between the water molecules and choline chloride.

This shows that the strength of the hydrogen bond is higher within the lower molar ratios of the ChCl and H_2O with the most seen within ChCl:H_2O (1:3) and ChCl:H_2O (1:4). Excess water molecules account for the insignificant and weak hydrogen bond observed in the DESs with higher molar ratio of H_2O.

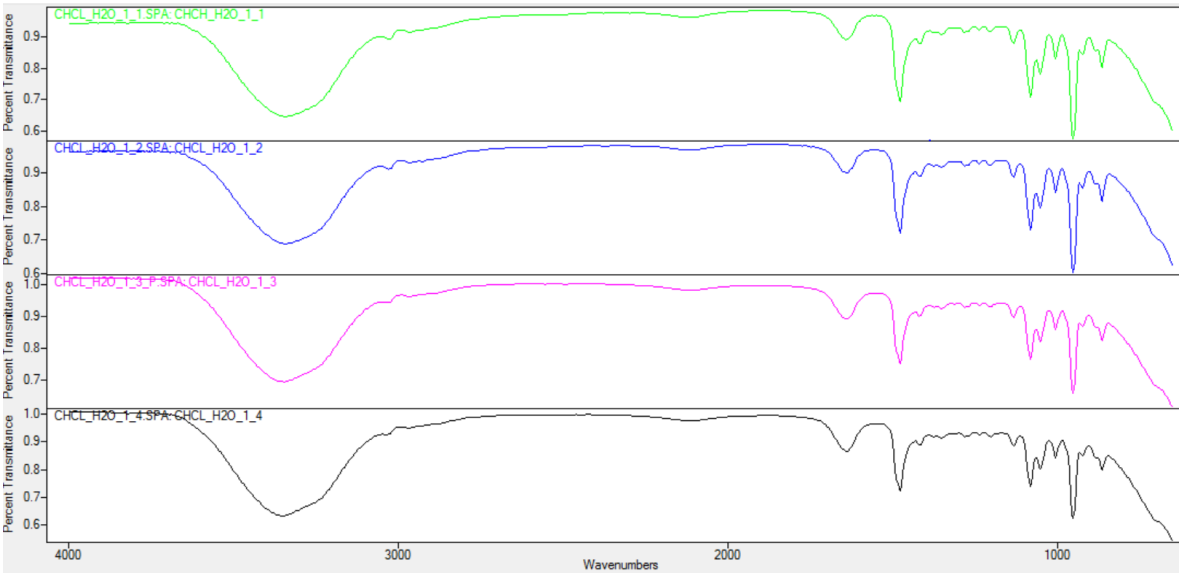

Figure 2.1. FTIR spectra of the ChCl:H_2O (1:1)(green), 1:2 (blue), 1:3 (cyan), and 1:4 (black). The -OH band area broadening increases with increasing water ratio.

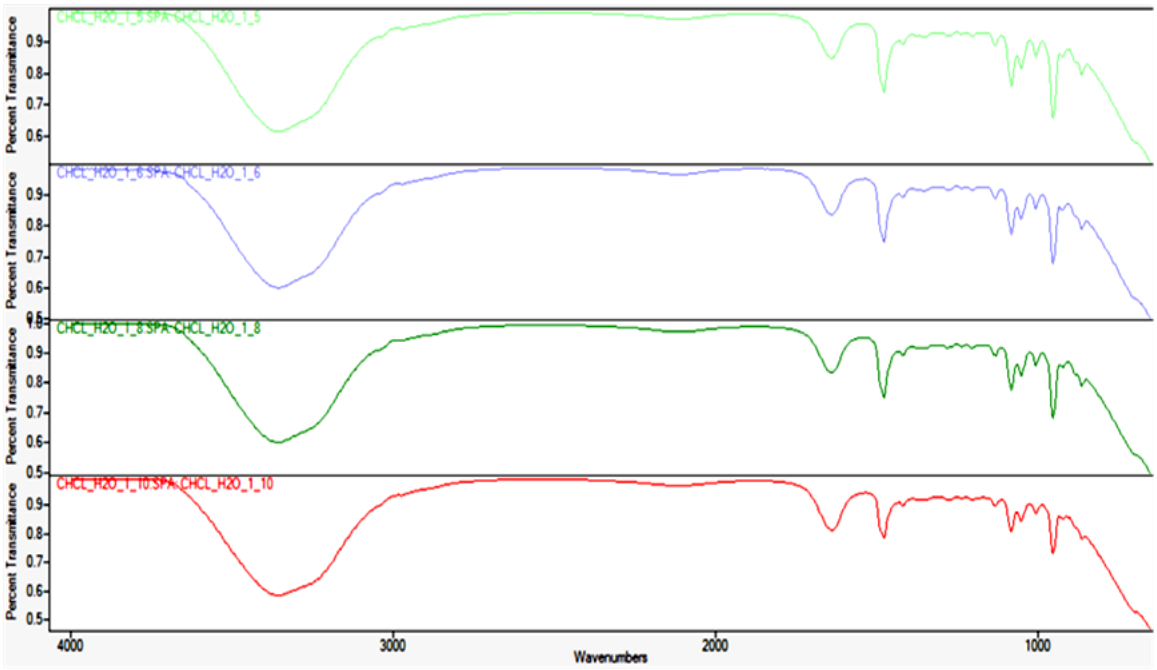

Figure 2.2. FTIR spectra of the ChCl:H_2O (1:5)(light green), 1:6 (blue), 1:8(deep green), and 1:10(red).

Another indication of the formation of H-bonding is the bathochromic shift observed at the same band peak compared to the band in the solid ChCl. The pure water molecule (HBD) expresses hypsochromic shift. This is due to changes in the environment of both the HBD and HBA caused by change in dipole moment as a result of hydrogen bonding. Also, the observation of new peaks at 2106cm^{-1} and 2118cm^{-1} in ChCl:H_2O (1:3) and ChCl:H_2O (1:4) due to increased band intensity suggest that the observed hydrogen bonding is relatively stronger in the two DESs compared to the other solvents.

2.3.2 PROTON (H^1)-NMR SPECTROSCOPY

There are very few studies reported in literature involving DESs using NMR. NMR studies suggest the protons around the quaternary nitrogen of choline chloride express shifts in frequency with the presence of an HBD[96]. The chemical shifts observed in the DESs are summarized in Table 2.1.

Table 2.1. Frequency shifts of the NMR spectra of all DESs

DES	δ/ppm			
ChCl:H_2O (1:1)	3.16	3.48	4.00	4.7
ChCl:H_2O (1:2)	3.15	3.47	4.00	4.7
ChCl:H_2O (1:3)	3.13	3.44	3.98	4.7
ChCl:H_2O (1:4)	3.12	3.44	3.97	4.7
ChCl:H_2O (1:5)	3.12	3.44	3.97	4.7
ChCl:H_2O (1:6)	3.11	3.43	3.97	4.7
ChCl:H_2O (1:8)	3.11	3.43	3.97	4.7
ChCl:H_2O (1:10)	3.10	3.43	3.97	4.7

Incidentally, the positive charge around the quaternary nitrogen attracts the negative Cl^- ions to that region. As a result, hydrogen bonding is observed as shifts in frequency of the protons of the trimethyl groups bonded to the quaternary nitrogen. The shifts between δ=3.16-3.10 represent the trimethyl groups. These shifts confirm the presence of hydrogen bonding. The shifts for the native -OH group in the ChCl is masked by the shift for the D_2O solvent at δ=4.7.

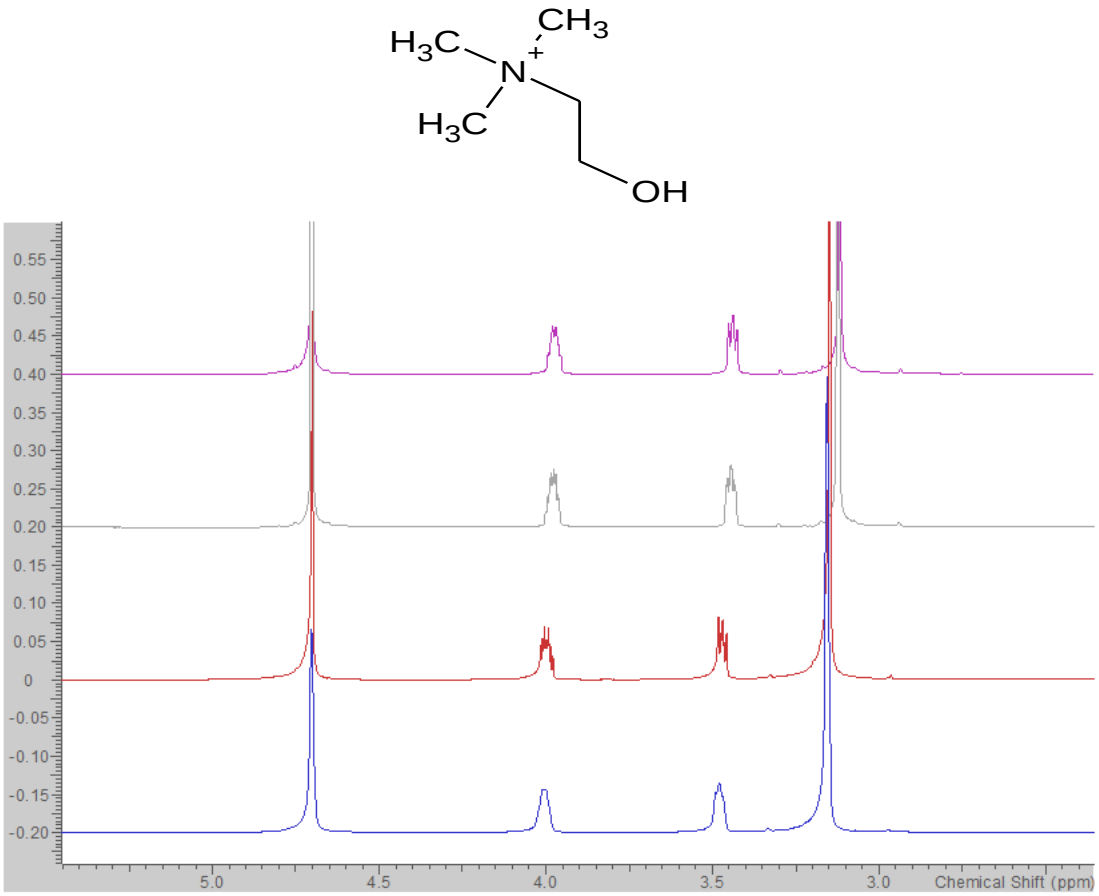

Figure 2.3. NMR of all choline Cl:water DESs. From bottom, 1:1, 1:2, 1:3, and 1:4. The frequency shifts indicative of the presence of hydrogen bonding is observed between δ=3.16-3.10.

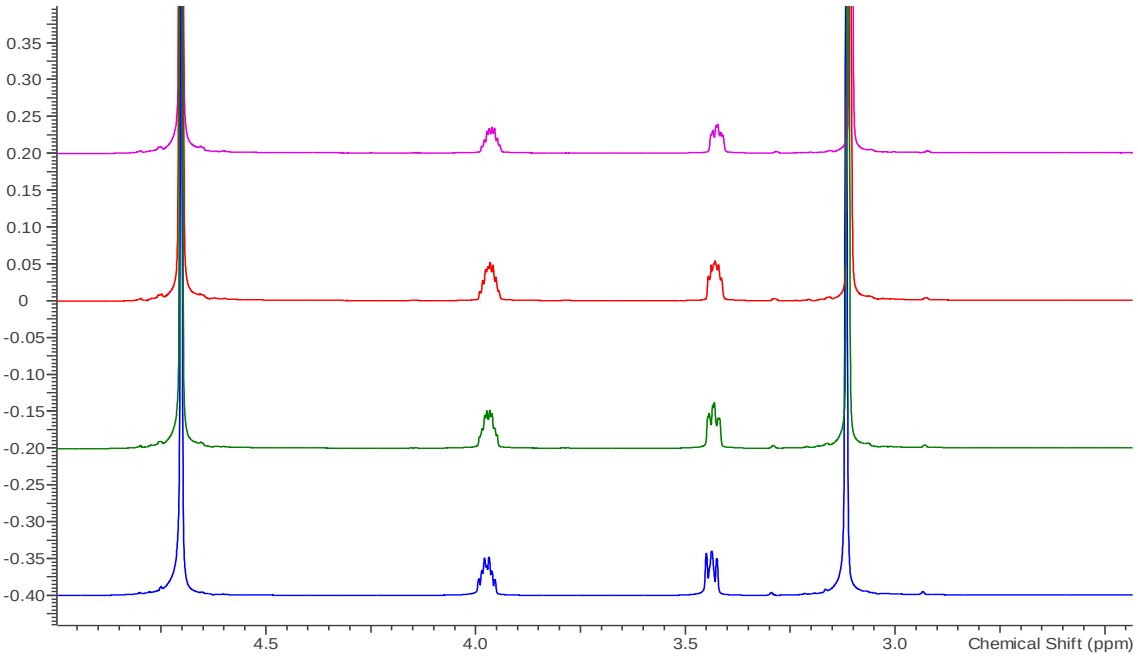

Figure 2.4. NMR of all choline Cl:water DESs. From bottom, 1:5, 1:6, 1:8, and 1:10.

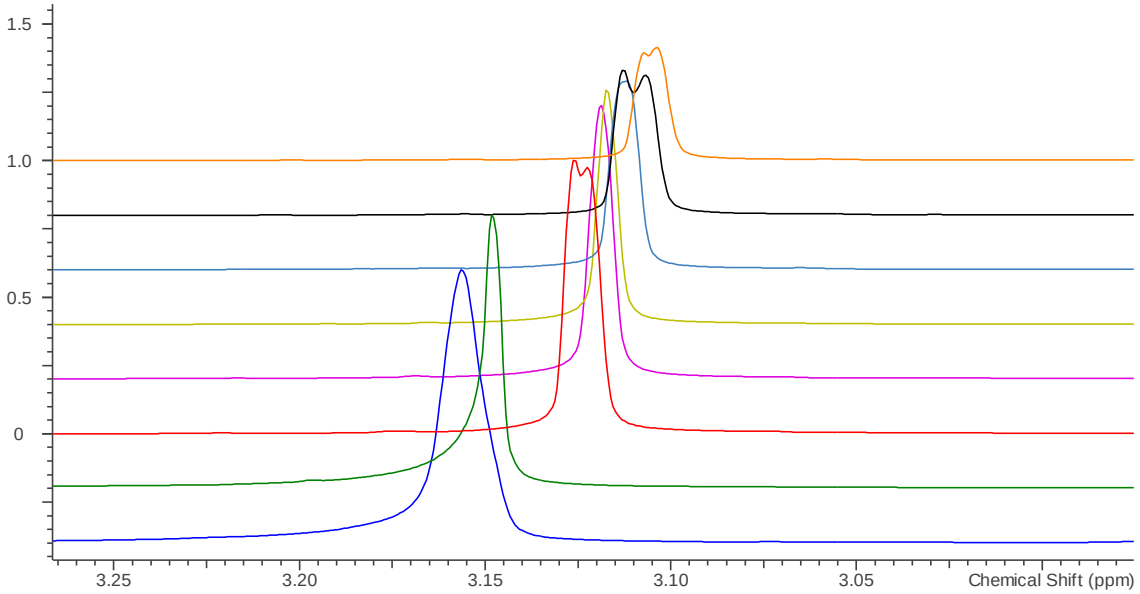

Figure 2.5. An enlarge segment of the NMR spectra of all the DESs showing the frequency shifts. From bottom, 1:1, 1:2, 1:3, 1:4, 1:5, 1:6, 1:8, and 1:10.

2.3.3 RAMAN SPECTROSCOPY ANALYSIS

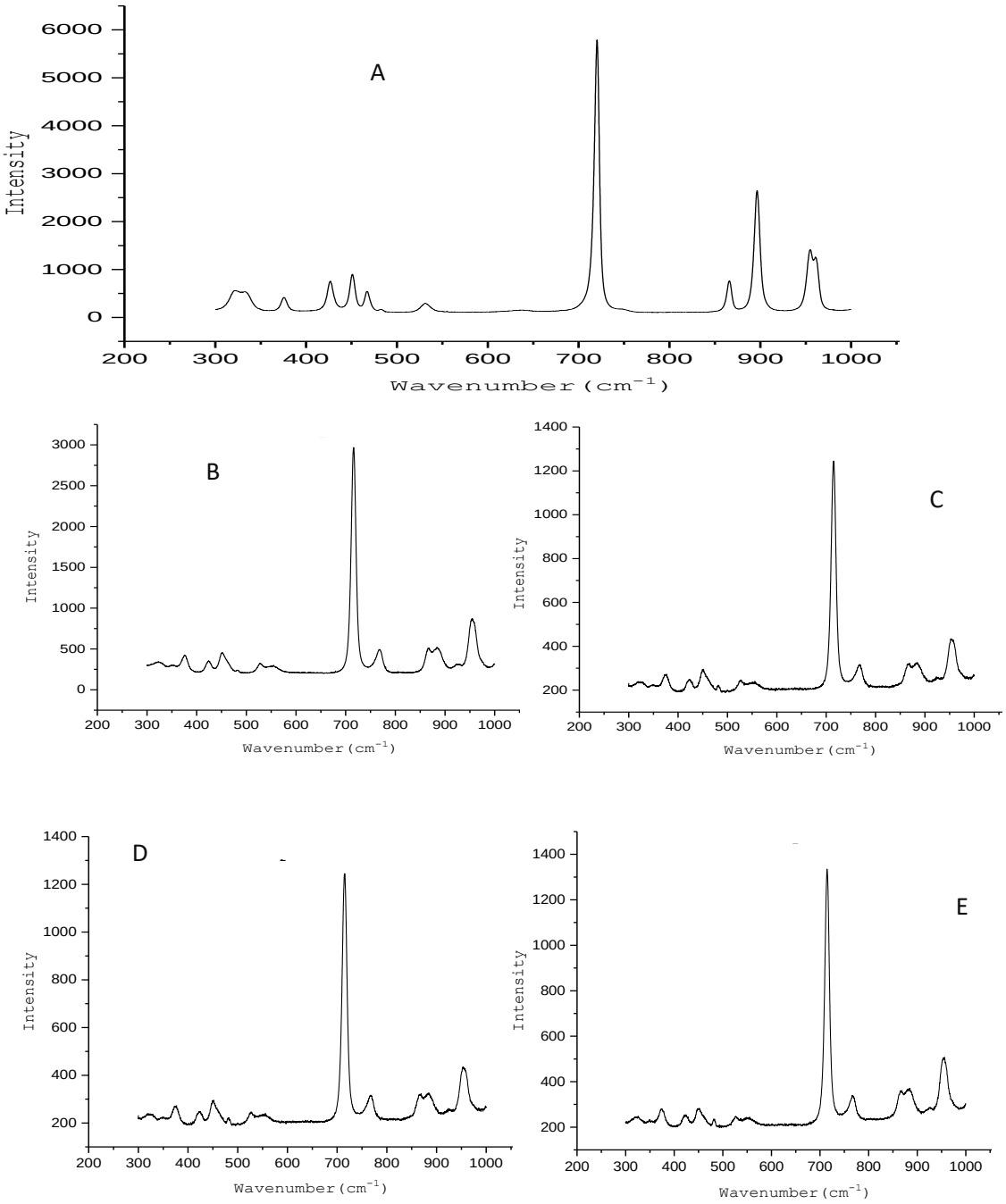

Figure 2.6. Raman spectra of ChCl:H_2O deep eutectic solvents. Choline chloride(A),1:1(B), 1:2 (C), 1:3 (D), and 1:4 (E).

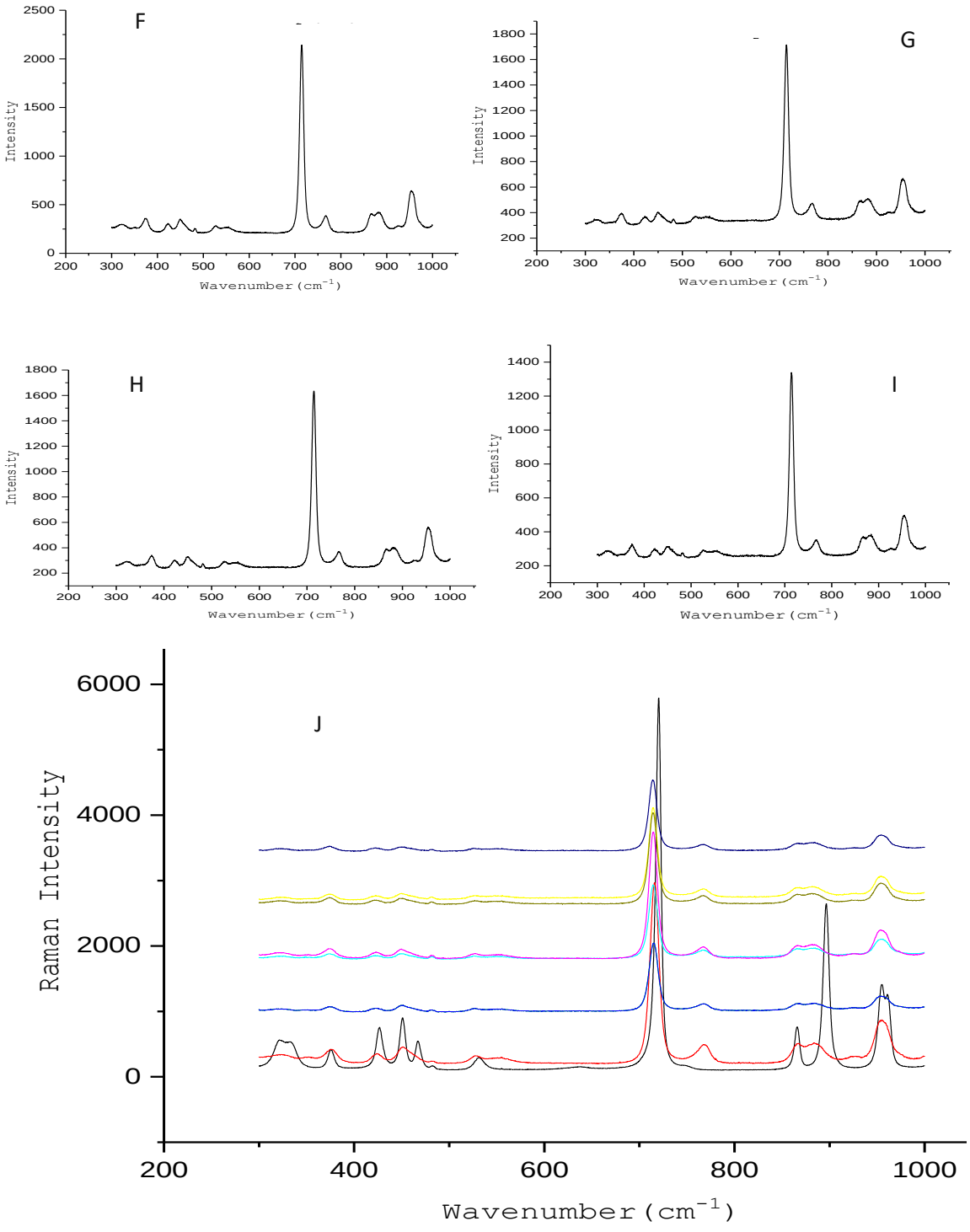

Figure 2.7. Raman spectra of four of the ChCl:H_2O DESs(top) and an overlay of Raman spectra of all the ChCl:H_2O DESs (J). *Top four spectra*: 1:5(F), 1:6 (G), 1:8 (H), and 1:10 (I)

Raman and infrared spectroscopies are both vibrational. An excited electron by light of a particular energy moves between vibrational energy levels or modes. The excitation and relaxation of the electrons in a molecule produce a fingerprint that is unique to the molecule, and hence could be used to identify the molecule. The spectrum provides information among others on noncovalent interactions.

Hydrogen bonding in Raman is often observed as relatively small shifts at low frequency regions. The HBD, water, is not Raman active since it is nonpolarizable. The Raman spectroscopy analysis of the DESs were compared to the Raman spectrum of the pure dried choline chloride. The results indicate a significant peak shift to the left of the peak at 897 cm^{-1} of between 6-11 cm^{-1}. This shift is attributable to hydrogen bonding. Also, the largest shift was observed in ChCl:H_2O (1:3) with the lowest shift in ChCl:H_2O (1:1). Again, a shift of 5 cm^{-1} observed at peak 720 cm^{-1} in all the DESs is attributable to hydrogen bonding. A new peak was observed at 771 cm^{-1} which was nonexistent in the choline chloride spectrum. This peak may be as a result of stretching of the -OH group on the second carbon of the choline chloride, a consequence of weak hydrogen bonding.

2.3.4 FREEZING POINT AND WATER CONTENT ANALYSIS

Central to the definition of DES is their very low freezing or melting point compared to melting or freezing points of the individual components. Indeed, in the formulation of DESs, the eutectic composition is the molar ratio of the constituent compounds that yields the lowest freezing point. Therefore, to find the eutectic point is to find the lowest freezing point. Cryogenic, vitrification, and biocatalytic studies have driven the quest for very low freezing temperature solvents. Table 4 gives a summary of the freezing points and percent free water content of the aqueous choline chlorides DESs.

Table 2.2. Summary of the freezing points of the aqueous choline chloride DESs

DES SAMPLE	FREEZING POINT(°C)	WATER CONTENT (%)
ChCl:H_2O (1:1)	-61.6	17.2 ± 2.4
ChCl:H_2O (1:2)	-65.2	22.3 ± 1.8
ChCl:H_2O (1:3)	-84.7	27.9 ± 1.4
ChCl:H_2O (1:4)	-82.9	35.5 ± 2.7
ChCl:H_2O (1:5)	-71.7	41.1 ± 2.1
ChCl:H_2O (1:6)	-68.9	46.5 ± 3.0
ChCl:H_2O (1:8)	-63.3	49.3 ± 2.6
ChCl:H_2O (1:10)	-62.2	51.8 ± 4.0

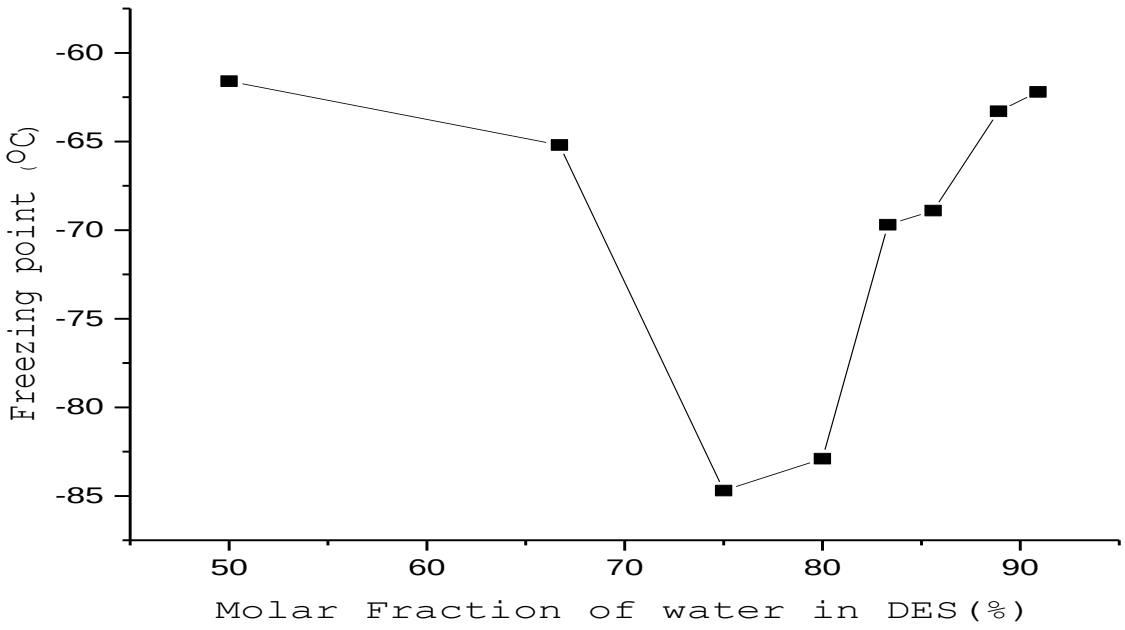

Figure 2.8. The eutectic point, eutectic composition and eutectic temperature of ChCl:H_2O DESs.

The eutectic point is with ChCl:H_2O (1:3) with a freezing temperature of -84.7°C. This was closely followed by ChCl:H_2O (1:4) with freezing temperature of -82.9°C. The formulations with the highest freezing point is ChCl:H_2O (1:1) and ChCl:H_2O (1:10). The data confirms the earlier findings that indicated that ChCl:H_2O (1:3) and ChCl:H_2O (1:4) have relatively stronger hydrogen bonding than the other formulations. Compared to other DESs found in literature, the ChCl:H_2O DESs account for some of the lowest freezing temperatures for DESs[16,55].

A cursory look at the percent water content indicate an expected increase in the water content with increasing molar ratio of water in the DES. However, this increase appears nonlinear (see Figure 2.9). The water contents measured constitute the available free water in the DES.

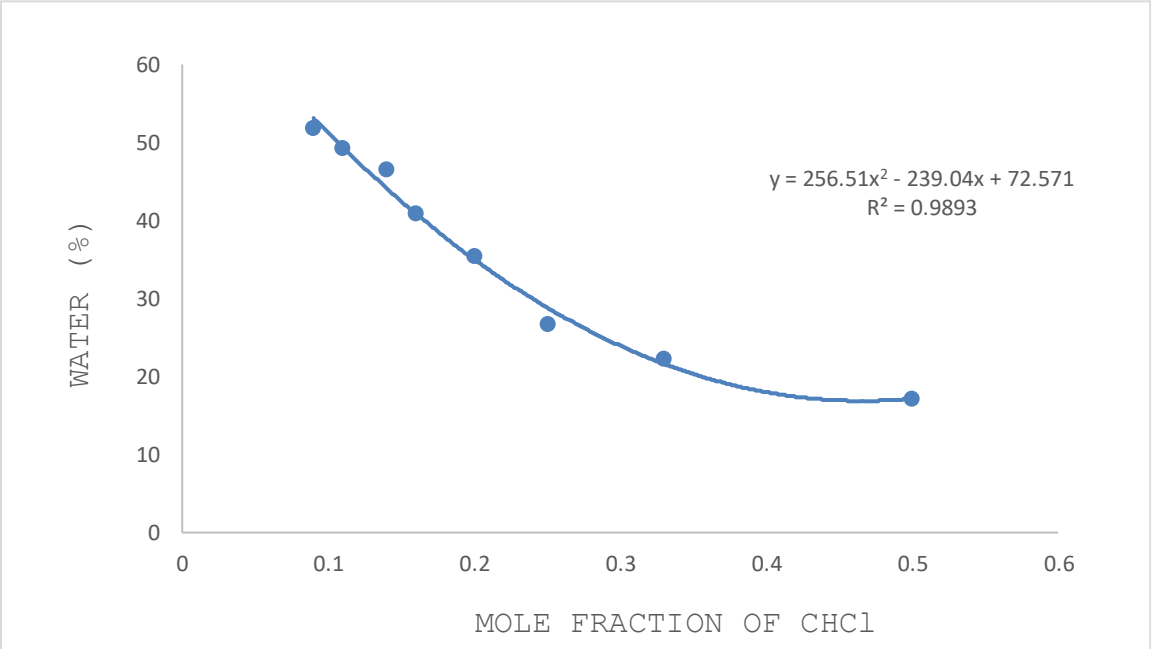

Figure 2.9. Water content of the ChCl:H_2O DESs. The DESs are represented as mole fraction of choline chloride.

2.4 CONCLUSION

Eight different solvent systems were successfully formulated using quaternary ammonium salt, choline chloride, as the HBA and water as solely the HBD with 100% atom economy. The eutectic temperature were found within the ratios of ChCl:H_2O (1:3) and ChCl:H_2O (1:4). From the freezing point analysis, ChCl:H_2O (1:3) was found to have the lowest freezing point of -84.7^{o}C. Spectroscopic analyses involving FTIR, NMR, and Raman established interaction between the HBD and HBA, suggesting hydrogen bond formation. This was determined through band broadening and frequency shifts with equivalent energies within the range of hydrogen bonding. The band broadening and frequency shifts were significantly prominent within the ChCl:H_2O (1:3) and ChCl:H_2O (1:4). Later studies through molecular dynamic simulations would confirm this observation.

CHAPTER THREE

CHARACTERIZATION CHOLINE CHLORIDE:WATER DES

3.0 INTRODUCTION

The applications of novel compounds depend on their thermal and physicochemical properties. These properties are both intrinsic and extrinsic. There are several thermal and physicochemical parameters that depend on the state of the compound. Therefore, the knowledge of these properties informs the choice and manner of application.

Among these physicochemical and thermal properties include density, conductivity, pH, refractive index, surface tension, viscosity, water content, partition coefficient, melting point, boiling point, solvatochromism, and decomposition temperature.

3.1.0 DENSITY

The density of a compound is an intrinsic property that permits the determination of other important derived thermophysical parameters such as isobaric thermal expansivity, isothermal compressibility, isentropic compressibility, and isochoric molar heat capacity. The density of a solvent affects the mass flow and hence suitability of the solvent for specific chemical reactions or separations.

The densities of the aqueous choline chloride DESs were determined via the direct method at 22.1°C. A 1.00 ml sample of the DESs were slowly pipetted using a calibrated micropipette (margin of error ±0.002) into a pre-weighed vial and the mass measured using Mettler Toledo analytical balance (Columbus, OH). The densities were determined in triplicate at room temperature and atmospheric pressure.

3.1.1 CONDUCTIVITY

The polarity of solvents permits electrical conductivity for applications in electrochemistry, separations, and chemical synthesis. The conductivities of the DESs were determined using Vernier Labquest 2 (Beaverton, OR) connected to a conductivity probe. A 0.5M NaCl solution was used as the reference. The measurements were conducted in triplicate at room temperature. The conductivity maximum range of the instrument was 20,000 µS/cm.

3.1.2 pH

The concentrations of proton ions in a solvent (acidity or basicity) affect reactivity and may affect the suitability of a solvent as a reaction media. Again, the pH of a solvent can affect its effectiveness during extraction and separation. The pH of the DESs were determined using a Mettler Toledo FEP20 pH meter (Columbus, OH) at room temperature. The pH meter was calibrated using standard buffers of pH 4, 7, and 10. The average uncertainty associated with the measurements was calculated to be ±0.03.

3.1.3 REFRACTIVE INDEX

The refractive index, the measure of the relative speed of light in a medium compared to the speed of light in a vacuum, is an intrinsic property of a substance that allows the penetration of light. It is important in confirming purity, measuring concentration, and building materials with photo applications. The refractive indices of all the DESs were determined in triplicate using a Bausch and Lamb Abbe-3L refractometer (Rochester, NY) at room temperature. Deionized water was used as a calibrator. The average uncertainty associated with the measurements was ±0.001.

3.1.4 SURFACE TENSION

A Fisher Scientific tensiomat 21 (Dubuque, Iowa) was used in measuring the surface tensions of all the DESs using the DuNouy ring method 151. A flame-dried platinum-iridinium ring was employed. Also, all glassware was washed and dried with acetone after each measurement. Deionized water was used to calibrate the tensiometer. The standard uncertainty after triplicate measurements was ±0.5 dynes/cm. All measurements were done at room temperature (23 ± 1°C).

3.1.5 VISCOSITY

The viscosity of all the DESs were measured as a function of temperature. A Brookfield DV-III Ultra rheometer (Toronto, Canada) was used to determine the viscosities between 25°C-60°C at 5°C increments. The temperature variation was obtained by employing an external water bath containing 50/50 antifreeze and water with a TC Brookfield TC-502 circulator (Toronto, Canada). Also, the measurements were conducted with a CP40 spindle at a speed of 0.2 rpm. The standard uncertainty after triplicate measurements was ±0.001 Pa.s and ±0.01°C for the viscosity and temperature respectively.

3.1.6 DECOMPOSITION TEMPERATURE

The heat tolerance of the DESs were analyzed through thermogravimetric analysis (TGA) and differential scanning calorimetry (DSC). The TGA was conducted using a Seiko 220 TG/DTA (Tokyo, Japan). A sample size of 5-10 mg was placed in an aluminum pan and heated. The samples (DESs) were heated from 30°C to 300°C at a temperature ramp of 10°C/min under nitrogen.

The DSC was conducted using a TA instrument DSC Q200 (New Castle, DE). TA instruments Tzero aluminum pans with Tzero hermetic aluminum lids were used to collect 5-10 mg samples of DESs for analysis. The thermal analyses were conducted between the temperatures of -40°C and 300°C with a ramp of 10°C/min under nitrogen. The data was analyzed using TA Advantage Universal Analysis 2000 software ver4.5A build 4.5.0.5.

3.1.7 FREEZING TEMPERATURE

The freezing temperatures of the DESs were analyzed via two methods. The first method is as described in Chapter 2. The second method was via DSC analysis. The DSC method was under the same conditions as described above (section 2.2.7) with the temperature range from -80°C and 40°C. Again, the data was

analyzed or evaluated using TA Advantage Universal Analysis 2000 software ver4.5A build 4.5.0.5.

3.1.8 BOILING POINT

The boiling points of the DESs were determined using DSC. The data obtained from the decomposition analysis of the DESs via DSC were used for the boiling point determination.

3.2 RESULTS AND DISCUSSION

3.2.1 DENSITY

The density distributions of deep eutectics are affected by the HBD and the HBA. Relatively little information on densities of DESs are available in literature compared with organic solvents or ionic liquids[97]. Types I and II DESs have relatively higher densities compared to type III DESs due to the use of metals in their formulations[98]. Figure 3.0 shows the relative distribution of the densities of DES (1.04-1.38 g/ml) and ILs (1.04-1.65g/ml) obtained from literature to the formulated ChCl:H_2O DESs.

The densities of the ChCl:H_2O DESs were as expected. The densities decreased linearly with increasing water molar ratio (see Figure 3.1). This is because there is a greater increase in the molar volumes of the DESs as more water was

added relative to the mass. Also, the addition of more water increases the void volume which in turn reduces the density. The densities ranged between 1.05627 g/cm^3-1.13427 g/cm^3 .

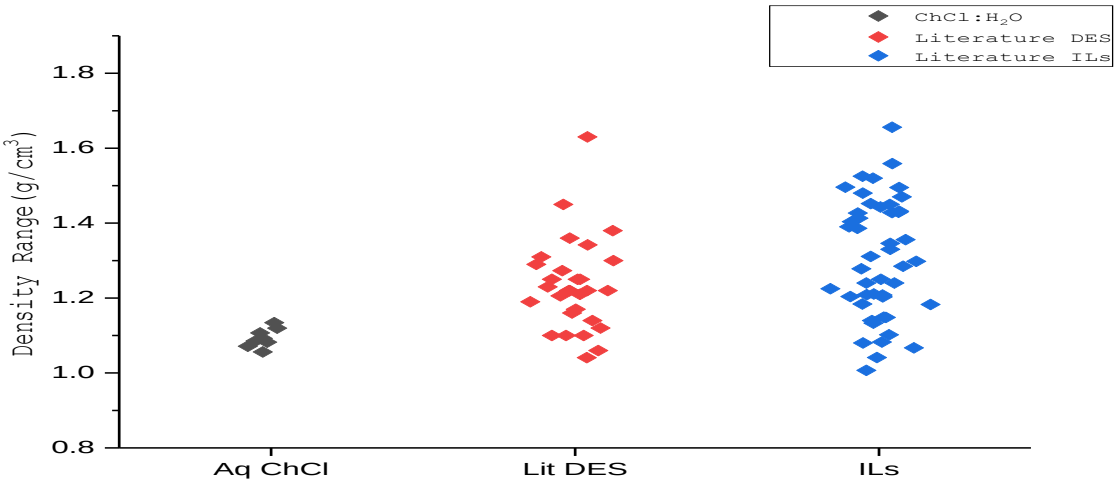

Figure 3.0. A comparison of the density distributions in DES[97] and ionic solvents[99] obtained from literature to ChCl:H_2O DESs.

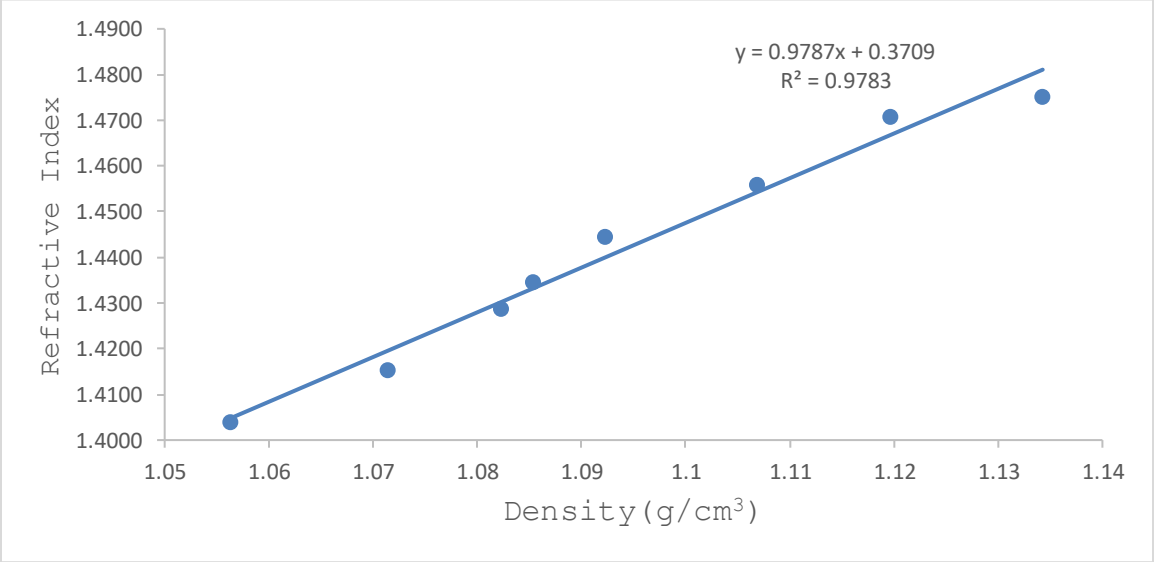

Figure 3.1. The relationship between the density and refractive index of the ChCl:H_2O DESs. A strong linear correlation exists between the two physical properties.

3.2.2 REFRACTIVE INDEX(RI)

The refractive indices of the ChCl:H_2O DES ranges from 1.4041 in ChCl:H_2O(1:10) to 1.4752 in ChCl:H_2O(1:1). The RI decreased with increasing water content. This is expected as the denser a medium, the greater the difficulty of light penetration. The RI and density are directly and linearly related (see Figure 3.1). The RI data obtained for ChCl:H_2O DESs are comparable to literature values of DESs[100-101] and higher than the RI of water.

3.2.3 VISCOSITY

Viscosity affects mass flow. High-density solvents are expected to have high viscosities. The viscosities of the ChCl:H_2O DESs were directly related to the density (Figure 3.2b). Strong hydrogen bonding and other intermolecular forces of attraction, such Van der Waals, reduce mobility of the DESs by causing compactness as a result reduced void volume[102-103]. This increases the viscosity of the solvents. The effect of these forces lead to reduction in the linearity of density and viscosity as seen in Figure 3.2b. The viscosities of ChCl:H_2O DESs decreased with increasing water(see Figure 3.2a). This is expected as net hydrogen bonding between the water molecules and the choline chloride ions reduces with increasing water. The viscosities

determined for the ChCl:H_2O DESs were comparable to literature values of DESs.

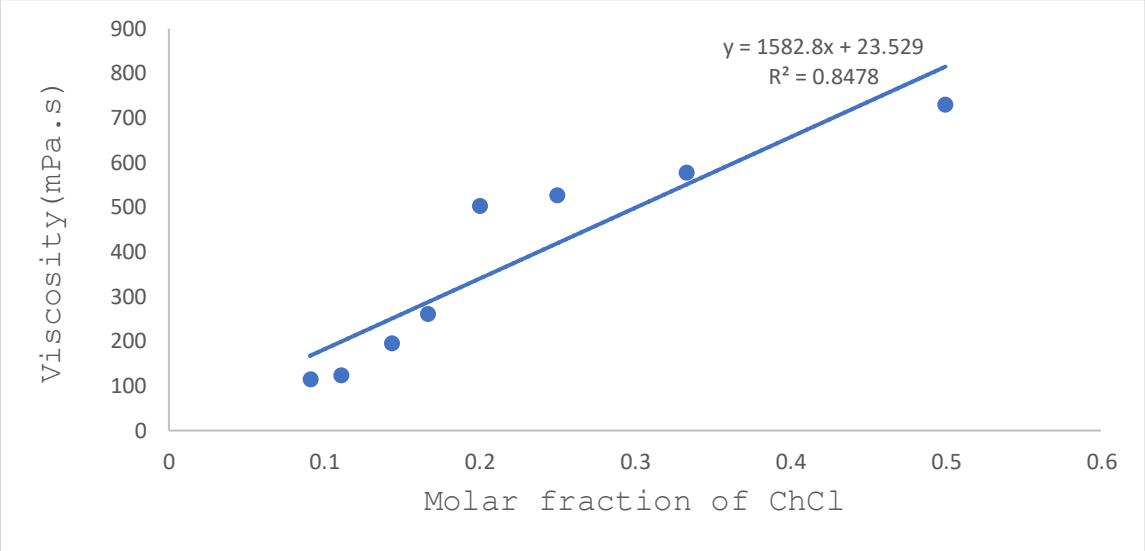

Figure 3.2a. Viscosity of the ChCl:H_2O DES. Hydrogen bonding is the cause of elevated viscosities in 0.25 and 0.20.

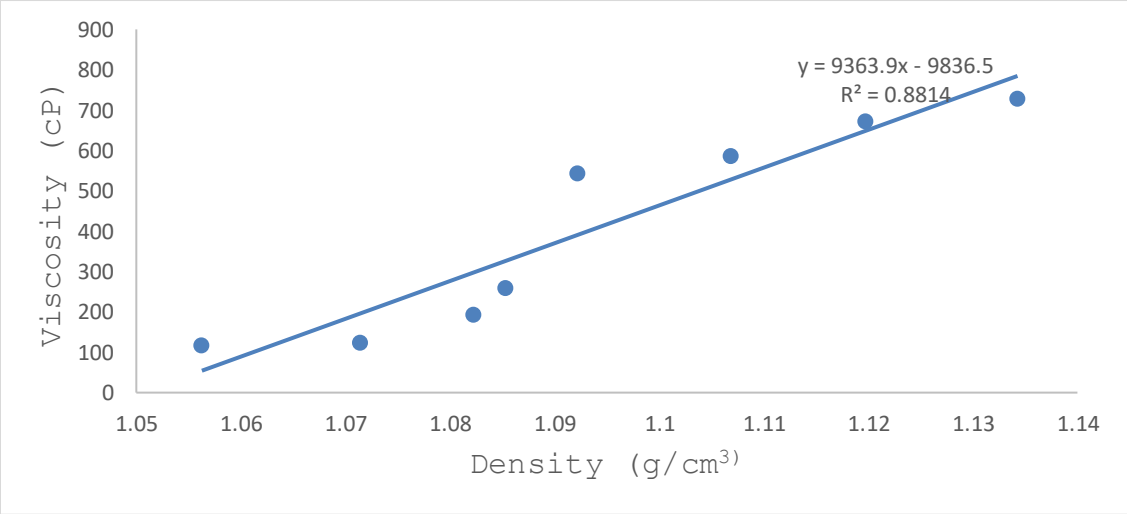

Figure 3.2b. The relationship between the density and viscosity of the ChCl:H_2O DESs. The effect of relative high hydrogen bonding in ChCl:H_2O 1:3 and ChCl:H_2O 1:4 reduces the linearity of the two physical properties.

3.2.4 FREEZING AND BOILING POINTS

The freezing and boiling points analyses determined through differential scanning calorimetry(DSC) is summarized in Table 3.

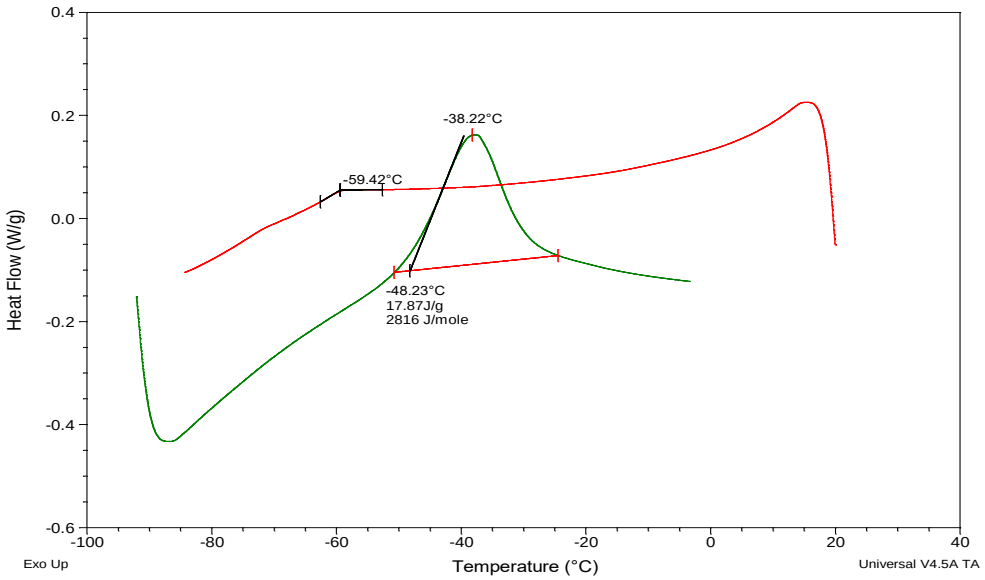

Figure 3.3a. Differential thermograms of freezing(red) and thawing(green) processes for ChCl:H_2O (1:1).The thawing temperature range was -90°C-20°C. The freezing temperature range was 20°C— -90°C.

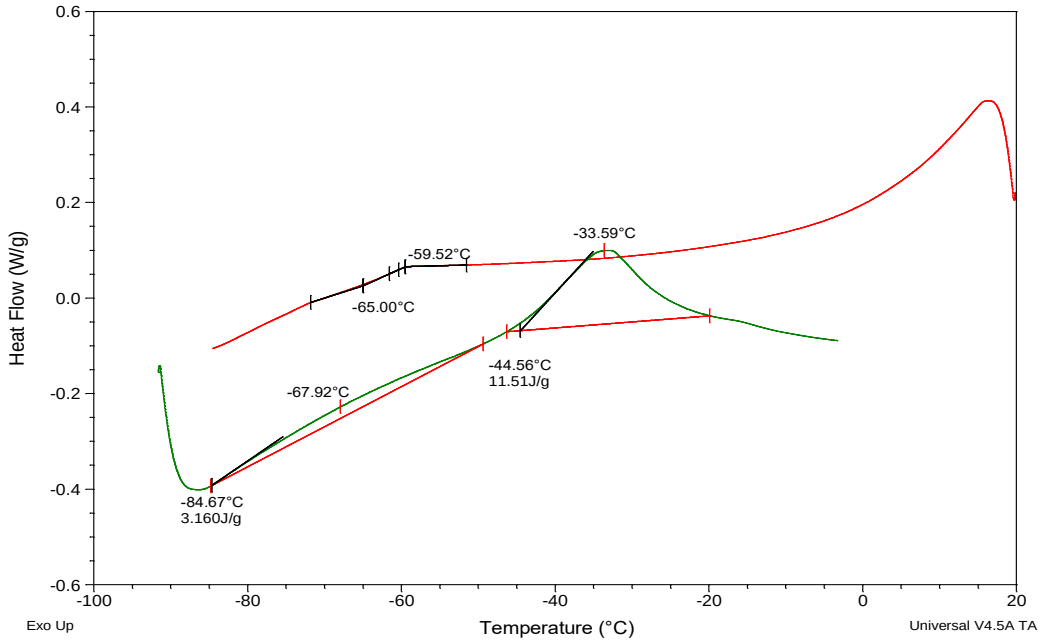

Figure 3.3b. Freezing(red) and thawing(green) processes for ChCl:H_2O (1:2).

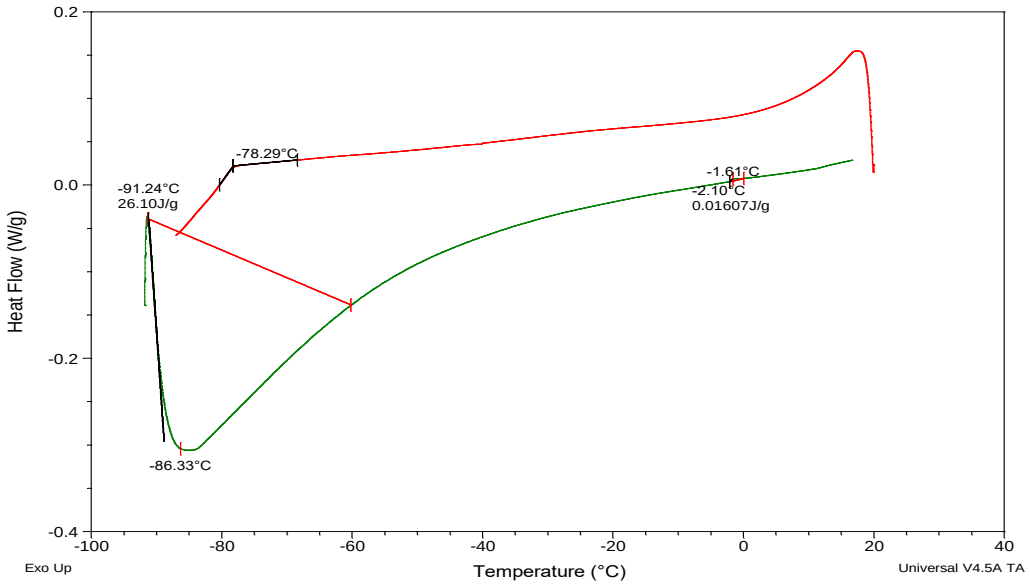

Figure 3.3c. Freezing(red) and thawing(green) processes for ChCl:H_2O (1:3).

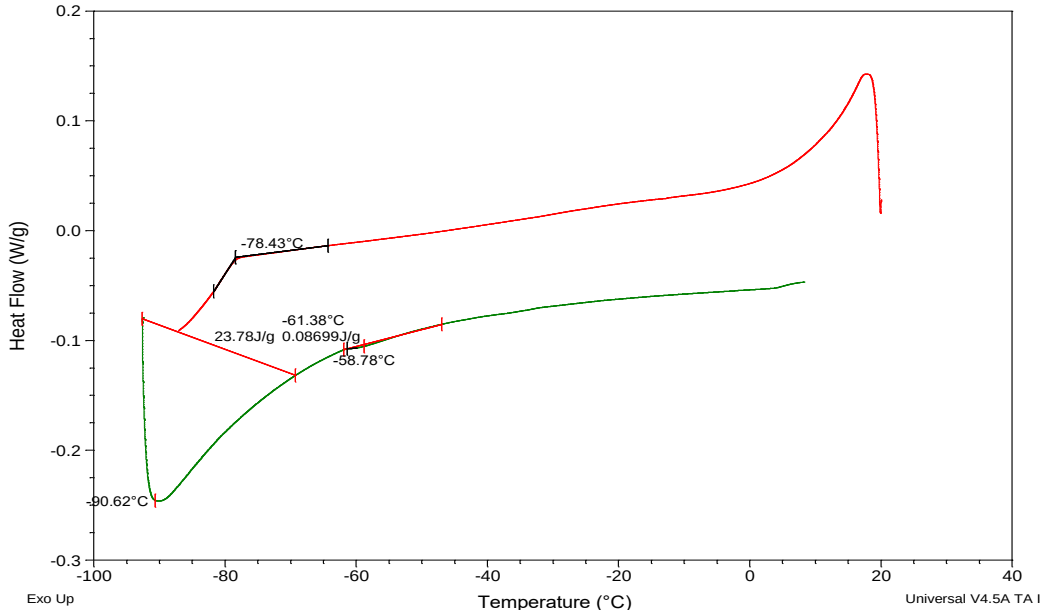

Figure 3.3d. Freezing(red) and thawing(green) processes for ChCl:H_2O (1:4).

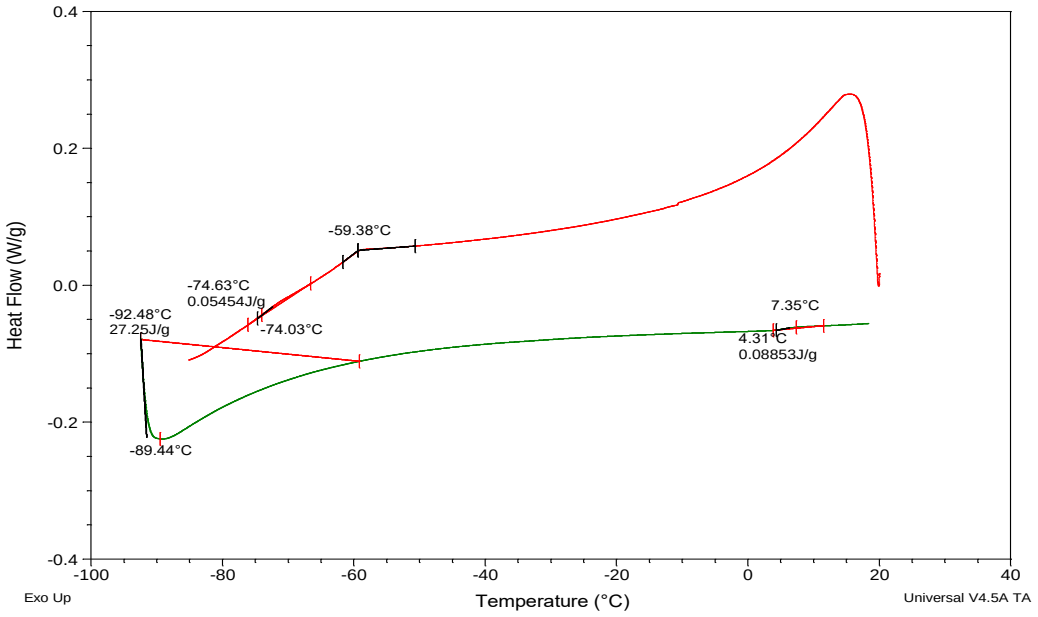

Figure 3.3e. Freezing(red) and thawing(green) processes for ChCl:H_2O (1:5).

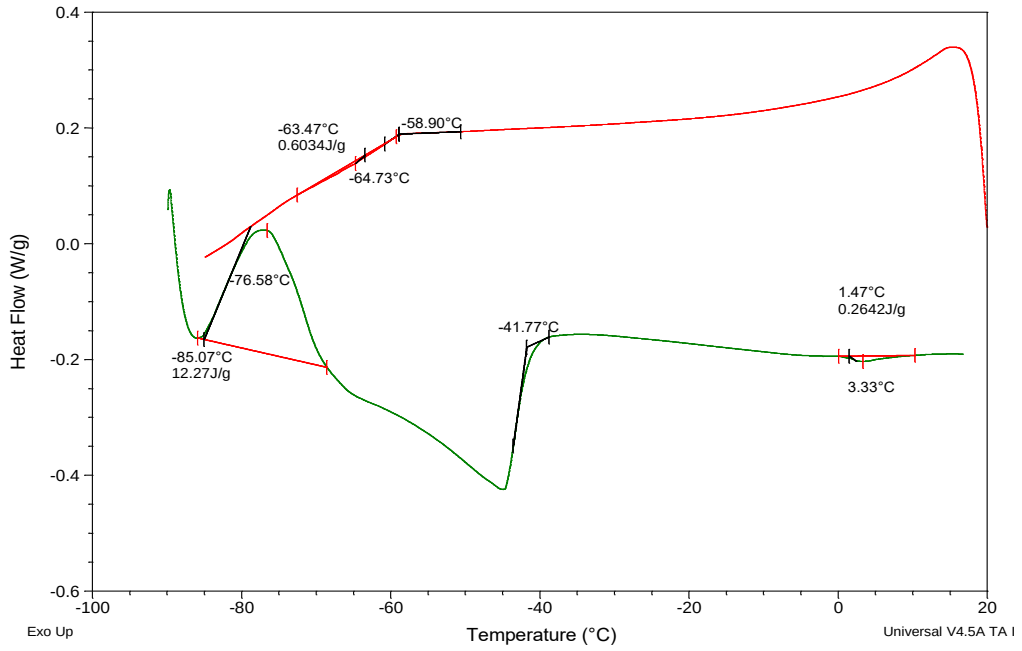

Figure 3.3f. Freezing(red) and thawing(green) processes for ChCl:H_2O (1:6).

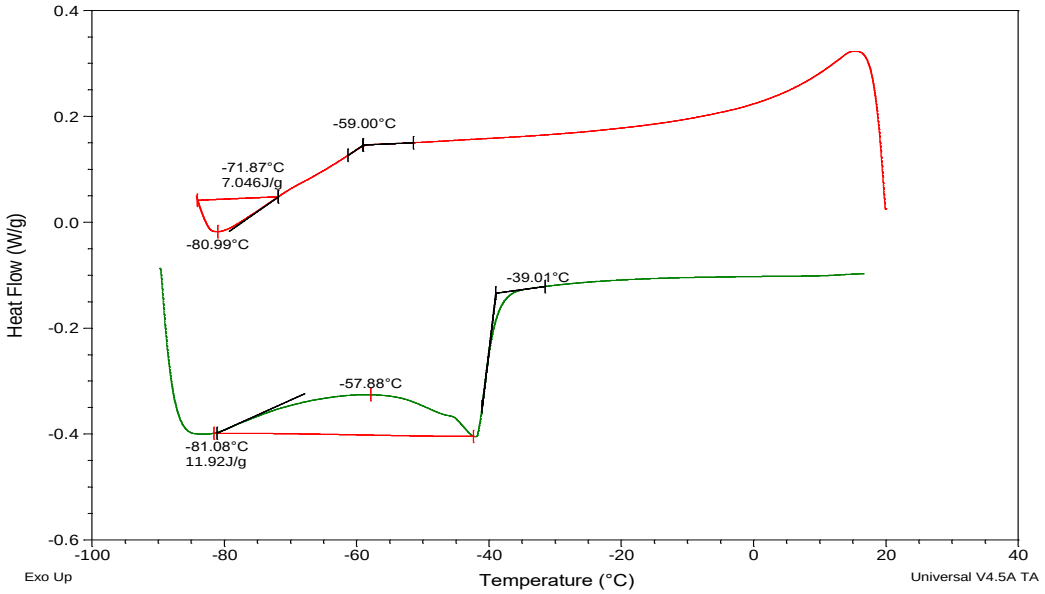

Figure 3.3g. Freezing(red) and thawing(green) processes for ChCl:H_2O (1:8).

Freeze-thaw processes of all the DESs were studied to understand the thermal behavior of the solvents under the

stresses of reduced temperature and melting. The study was also used to determine the freezing points and boiling points using differential scanning calorimetry. Freeze-thaw process is particularly important in vitrification. Desirable vitrification solvents produce no crystalline amorphous solids during freezing. The freezing and thawing were done at a rate of 10°C/min.

The thermograms of freezing and thawing are dissimilar though reversible. During freezing, the kinetic energy of the atoms and molecule reduces, the molecules become more constricted and intermolecular forces of attraction dominate. Ice formation, interfacial transitions, and changes in chemical and electrostatic interactions are the causes of the freeze-thaw variations or instability.

The freezing and thawing processes profiles (thermograms of ChCl:H_2O (1:1) and ChCl:H_2O (1:2)) were very similar with the onset of freezing, -59.4°C and -59.5°C respectively. The initial smooth profile curve suggests that the ChCl:H_2O eutectic undergoes a consistent molecular rearrangement and further relaxation during the freezing process. There is no formation of non-crystalline amorphous states. Again, the thawing thermograms of the two DESs were similar but different from the freezing thermograms. At the onset temperatures of

-48°C and -44.5°C in ChCl:H_2O (1:1) and ChCl:H_2O (1:2) respectively, the intermolecular forces weaken causing expansion of the DESs and melting begins at -38°C and -33°C respectively. The change in enthalpy of melting were 17.87 J/g and 11.51 J/g respectively.

The DESs ChCl:H_2O (1:3), ChCl:H_2O (1:4), and ChCl:H_2O (1:5)have similar freezing and thawing profiles. All three solvents show no initial formation of glass transition and no amorphous states prior to total freezing and throughout thawing. The significant difference pertains to the onset temperatures of freezing which were -78.3°C, -78.4°C, and -59.4°C respectively. Again, this is attributed to the nature of the intermolecular forces of attraction between the molecules. The relatively weaker hydrogen bonding and Van der Waals forces cause a further depression in the freezing points of these solvents.

The ChCl:H_2O (1:6)and ChCl:H_2O (1:8) DESs thermograms provide a typical profile. Multiple phase transitions are observed including crystallization, freezing, and melting. The effect of free water molecules is also observed. In ChCl:H_2O (1:6), the melting temperature of ice(T_{ice}) is observed at about 1.5°C with a latent heat of melting of 0.26 J/g. Also, a slushy nonhomogeneous amorphous crystal of ice

and DES molecules is observed between -64°C and -41°C. This is typical of very weak interactions between the choline chloride ions and water molecules. This phenomenon of weak interaction between the choline chloride ions and water molecules is also observed in ChCl:H_2O (1:8) at temperatures between -81°C and -39°C. It is worth noting that the freezing temperature (T_f) falls within this phase.

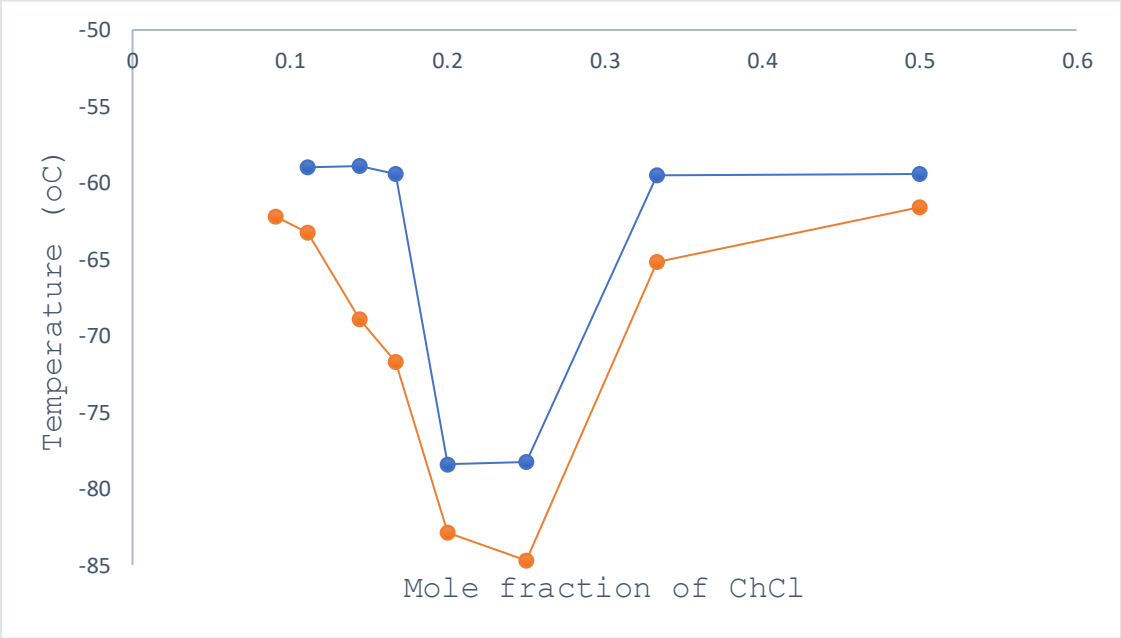

Figure 3.3h. Comparison of the freezing points determined obtained through DSC (blue) and conventional (orange) methods. Though the profiles look similar the DSC data are slightly elevated.

3.2.5 DECOMPOSITION ANALYSIS

The thermal stabilities and decomposition of the DESs were analyzed using DSC and TGA. The thermal stability is a function of the strength of the interactive forces within the solvent molecules. Strong electrostatic interactions, hydrogen bonding, and Van der Waals forces imposes high thermal stability to molecules or compounds. Figures 3.3a and 3.3b represent the DSC thermogram of H_2O and ChCl respectively. The major physical transitions in the water molecules are observed as endothermic freezing (-3.5°C-4.5°C) and evaporation at 145°C. The results are expected. The high pressure within the capped Al pan and surrounding enclosure of the pans is the cause of the elevated evaporation in water molecules. The DSC thermogram of the ChCl conspicuously shows the glass transition of ChCl at onset temperature of 66°C caused by molecular rearrangement within the ChCl crystal lattice. The only other transition expressed by choline chloride is decomposition at 302-312°C. Table 3.0 provides the summary of the physical and chemical transitions of all studied solvents.

The results of the DSC analysis indicate that thermal stability of the solvents is directly related to the water content. This is clearly observed in the ChCl:H_2O (1:1)and ChCl:H_2O (1:2) which decompose at 216°C and 221°C respectively

compared to the ChCl:H_2O (1:8) and ChCl:H_2O (1:10) which dissociate at 107°C and 104°C respectively. The higher the water content, the weaker the interactions within and between the water molecules and choline chloride molecules. However, ChCl:H_2O (1:3), ChCl:H_2O (1:4), and ChCl:H_2O (1:5) exhibited relatively high thermal stability due to the already established strong hydrogen bonding and other intermolecular forces decomposing at 215°C, 231°C, and 189°C respectively. By this, the ChCl:H_2O (1:4) shows the largest capacity to absorb heat.

The DSC data is supported by the TGA studies(see Figure 3.5). The percent weight loss at a specific temperature was calculated using the formula below:

$$\%\, Weight\ loss = \frac{Weight_{initial} - Weight_{specific\ temperature}}{Weight_{initial}} \times 100 \qquad \textit{Equation 3. 1}$$

The most thermally stable solvents with the least weight loss as temperature increased were ChCl:H_2O (1:3) and ChCl:H_2O (1:4). At 294°C, only 33% of the weight of ChCl:H_2O (1:4) was lost. Also at 234°C, only 26% of the weight of ChCl:H_2O (1:3) was lost. This observation is similar to those made in the DSC analysis. This confirms spectroscopic analyses that indicated that the ChCl:H_2O (1:3) and ChCl:H_2O (1:4) solvents had relatively stronger hydrogen bonding compared to the other solvents.

Again, confirming the observations in the DSC analysis, the higher the water content, the less thermally stable the solvent was. ChCl:H_2O (1:6), ChCl:H_2O (1:8), and ChCl:H_2O (1:10) solvents are typified by large weight loss at relatively similar or even lower temperatures compared to ChCl:H_2O (1:3) and ChCl:H_2O (1:4) solvents. For instance, at 240^{o}C, ChCl:H_2O (1:6) lost 90% of its weight. Similarly, ChCl:H_2O (1:8) and ChCl:H_2O (1:10) at 102^{o}C and 107^{o}C respectively, had already lost 41% and 49% of their total weight. The loss of weight is as a result of loss of water. The profile of water loss indicates that free unbonded water and weakly bound water molecules are first lost followed by tightly held water molecules(see Figure 3.5).

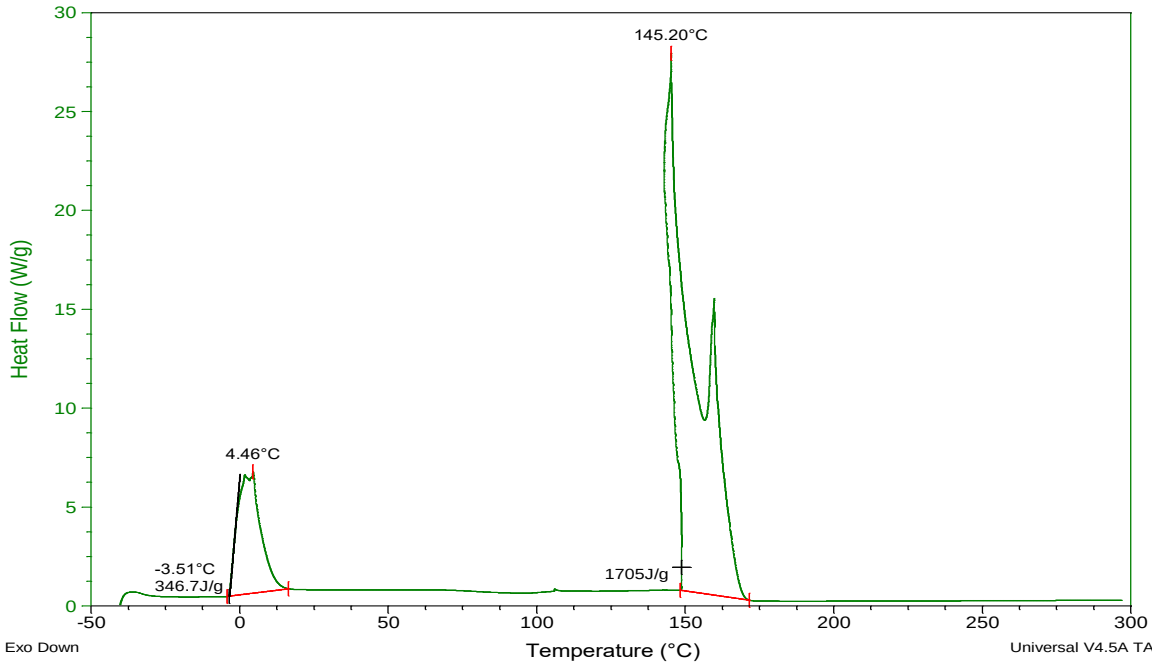

Figure 3.4.0. DSC thermogram of pure water determined from -40°C to 300°C. Onset freezing temperature is ~4.5°C. High pressure causes liquid-gas phase transition to occur at higher temperature.

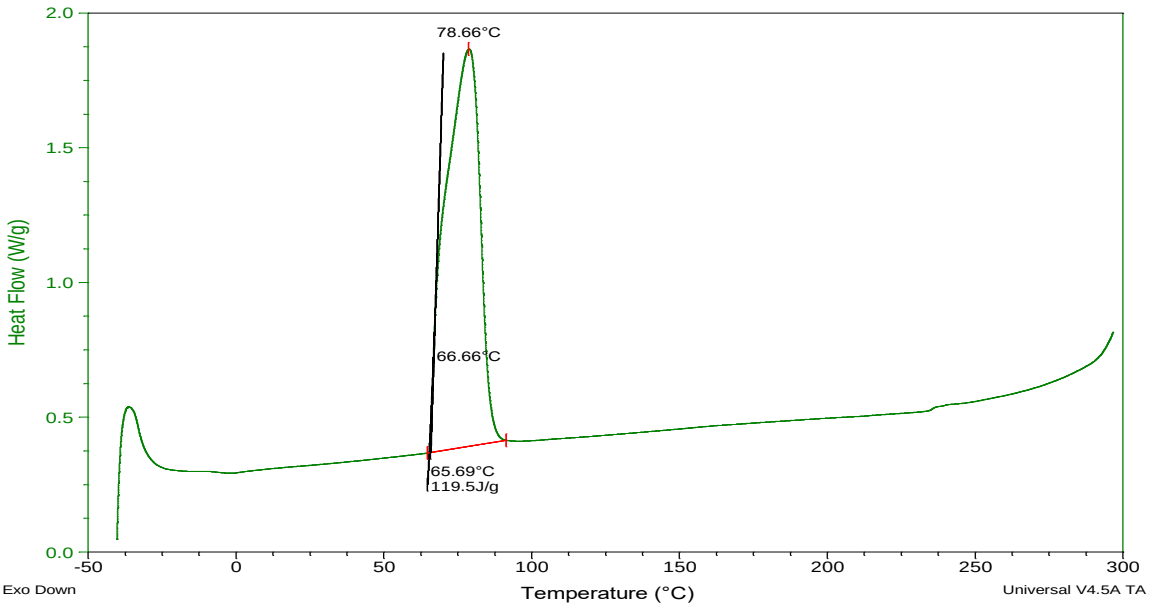

Figure 3.4.1. DSC thermogram of choline chloride indicating the glass transition(T_g)at 66°C.

Table 3.0. Summary of TGA decomposition analysis of ChCl:water DES

Sample	Temperature(°C)	Weight Loss(%)
Choline Cl^-	111	3.4
$ChCl:H_2O(1:1)$	234	19
	235	95
$ChCl:H_2O(1:2)$	221	12.5
	224	74
$ChCl:H_2O(1:3)$	234	26
	236	91
$ChCl:H_2O(1:4)$	107	25
	294	33
$ChCl:H_2O(1:5)$	104	29
	247	99
$ChCl:H_2O(1:6)$	107	32
	240	98
$ChCl:H_2O(1:8)$	102	41
	232	96
$ChCl:H_2O(1:10)$	107	49
	245	99

Table 3.1. Summary of DSC decomposition analysis of ChCl:Water DES.

Sample	Onset DES dissociation(°C)	Freezing (°C)	Free H_2O loss(°C)	T_g (°C)	Choline Cl decomposition(°C)
Choline Cl^-				66	308
H_2O		0	145		
ChCl:H_2O(1:1)	216	-59.4	155		312
ChCl:H_2O(1:2)	221	-59.5	172		303
ChCl:H_2O(1:3)	215	-78.3	155		313
ChCl:H_2O(1:4)	231	-78.4	151		289
ChCl:H_2O(1:5)	189	-59.4	148		313
ChCl:H_2O(1:6)	172	-58.9	142		226
ChCl:H_2O(1:8)	107	-59	66		314
ChCl:H_2O(1:10)	104		78		314

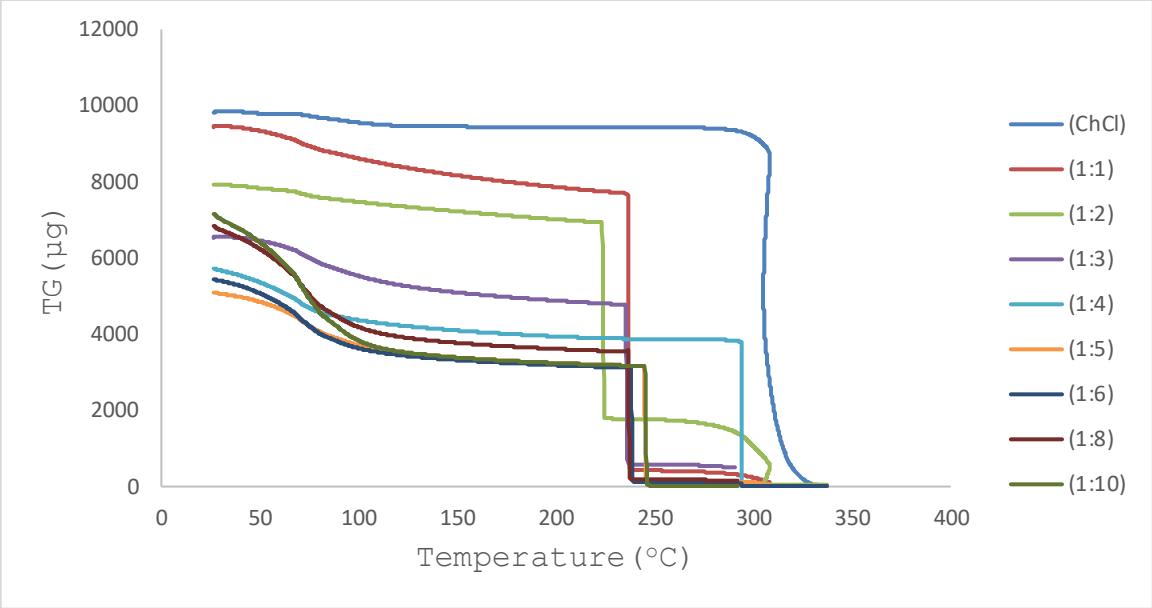

Figure 3.5. TGA thermogram of all ChCl:H_2O DESs. All DESs lost over 90% of their mass at 250°C except the 1:4 molar ratio.

Table 3.2. Summary of physicochemical properties of the Solvents

Sample	Conductivity (mS/cm)	Surface Tension (dynes/cm)	Water Content (%)	Density (g/cm^3)	pH
(1:1)	21.837	81.0	17.2	1.134	6.7
(1:2)	25.336	78.8	22.3	1.120	6.9
(1:3)	33.485	83.9	27.9	1.107	7.3
(1:4)	31.570	83.7	35.5	1.092	7.3
(1:5)	31.857	74.6	41.1	1.085	7.3
(1:6)	31.799	70.7	46.5	1.082	7.2
(1:8)	32.104	70.8	49.3	1.071	7.3
(1:10)	31.641	70.4	51.8	1.056	6.9

3.3 SOLVATOCHROMIC ANALYSES

3.3.1 INTRODUCTION

Solvents applications are generally based on the solubility of the compound of interest in the solvent or the polarity of the solvent. This is dictated by the chemical properties of the solvent. Deep eutectic solvents have gained attention in solvent chemistry due to their unique advantages that have led them to be considered greener alternative to organic solvents and ionic liquids.

Solvent-solvent, and solute-solvent interactions are the underlying principles for solvent activity and functionality. These interactions are dictated by the intermolecular forces of attraction including Van der Waals, hydrogen bonding, and dispersion as well as physical properties such as polarity and dipole moment[104-105].

Solvent selection for chemical processes is often challenging. However, solvent characterization with defined descriptors greatly aids in overcoming this challenge. Solvent polarity descriptors are estimated in two major ways, spectrometric and chromatographic[106]. Abraham et al first reported the chromatographic method using retention times of gas-liquid chromatographic data[107-108]. However, the most common polarity descriptors employ spectrometry[109].

3.3.2 SOLVATOCHROMISM

Chemical substances respond to various stresses by changing color. For instance, chemical substances can respond to pressure by color change (piezochromism)[110], temperature by color change (thermochromism)[111], pH by color change (halochromism)[112], and polarity by color change (solvatochromism)[113].

Solvatochromic analysis is a method for studying both bulk and localized polarity in chemical and biological solvents[113]. It is also effective for studying the effects of hydrogen bonding. The change in polarity leads to a shift in wavelength of maximum absorbance (λ_{max}) of the chemical probe. Negative solvatochromism (hypsochromism) corresponds to a blue shift and positive solvatochromism (bathochromism) corresponds to a red shift.

Electromagnetic waves within the UV/Vis and near-IR are often used to explore the interactions of chemically active probes with solvent molecules. The chemical interactions or forces exerted on these probes as they interact with solvent molecules cause changes in polarity of the probes. This change is observed as either bathochromic or hypsochromic shifts in the λ_{max} of the chemical probes and it is dependant on the solvent environment around the chemical probe. For instance,

the solvolysis rate of 2-chloro-2-methylpropane increases by $1x10^{11}$ fold from benzene to water[114]. Also, the IR absorption band of C=O stretching shifts by $\Delta\nu=29cm^{-1}$ from n-heptane to hexafluoro-2-propanol[115-116].

The energy change as a result of the shift in the λ_{max} is calculated and used for the empirical calculation of the polarity.

3.3.3 SOLVENT DESCRIPTORS

Descriptors characterizing solvents are an important tool for effective selection of solvents for purposes of chemical reactions, separations, extractions, and enzyme activation. These descriptors are used in isolation or in combination. Examples of solvent descriptors include Hildebrand solubility parameter, Kovat's index, Abraham parameters, Hansen parameters, and Kamlet-Taft parameters.

3.3.4 HILDEBRAND SOLUBILITY PARAMETER(δ_H)

According to the Hildebrand solubility parameter, three main dynamics are involved in the performance of solvent activity. These are solvent-solvent interactions, solvent-solute interactions, and solute-solute interactions. These interactions involve both intra- and intermolecular attractive forces which must be overcome or formed. The Hildebrand solubility parameter describes the internal cohesive energy density between solvent molecules that must be broken by the solute as it interacts with the solvent. It is a solvent-solvent descriptor and does not involve the solute.

The Hildebrand solubility parameter is defined as:

$$\delta_H = \sqrt{\frac{\Delta H - RT}{V_m}} \qquad \textit{Equation 3. 2}$$

δ_H = Hildebrand solubility

ΔH = Molar heat of vaporization

V_m = Molar volume

T = Temperature

R = Ideal gas constant

3.4 SOLVENT POLARITY AND KAMLET-TAFT PARAMETERS

Electric charge distortion or separation in a molecule induces dipole or multipole moment on the molecule or part of the molecule. This dipole or multipole induction in a molecule as a result of charge separation is called polarity. Differences in electronegativity and asymmetry of bonds are required for molecules to be polar. The main intermolecular forces of interaction within polar molecules are dipole-dipole and hydrogen bonding.

Polarity can be studied spectroscopically using organic compounds called probes that change polarity depending on their environment. These probes can be used for solvent polarity studies when irradiated using UV/Vis, IR, or NIR radiations. The probes provide detailed information on the chemical nature of the solvation system of a solute, and hence the solvent. The change in polarity of these probes in solvents have led to the development of polarity solvent scales for solvents.

Brooker et al. 1951, first suggested the probable use of probes for solvent polarity studies[117]. Thereafter, Kosower (1958) developed the first extensive solvent polarity scale[118]. Dimroth and Reichardt (1963) developed the $E_T(30)$

polarity scale using betaine dye as probe. The $E_T(30)$ is defined as the molar transition energy of the Reichardt's dye, measured with a UV/Vis[109, 119-120].

$E_T(30) = c\nu$

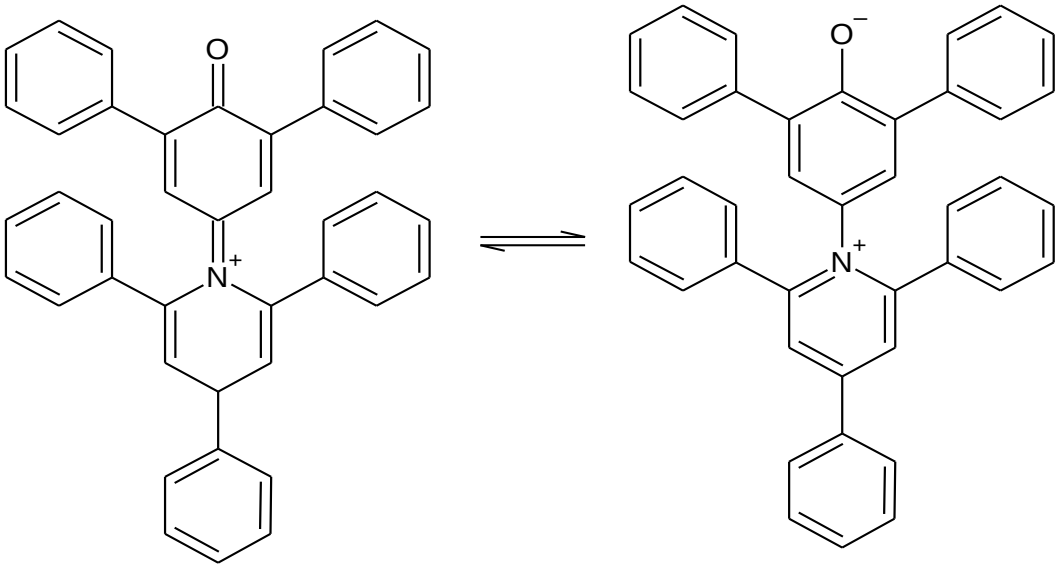

Figure 3.6.0. 2,6-Diphenyl-4-(2,4,6-triphenylpyridin-1-ium-1-yl) phenolate (Reichardt's dye/betaine 30) used by Dimroth and Reichardt to develop the $E_T(30)$ polarity scale. $E_T(30)$ measures the difference in solvation energies between the zwitterions.

Several organic compounds have served as probes for solvent polarity studies. These include 1-alkylpyridinium salts[118], 1-methyl-4-carbomethoxy iodide, 1-ethyl-4-carbomethoxy iodide, 1-methyl-4-cyano iodide, 1-ethyl-4-cyano iodide, merocyanines[121], and ketocyanines[122].

Kamlet-Taft parameters are solvent-solute interaction parameters that define solvent systems on three scales of solvent properties based on hydrogen bond donors and acceptors. These are the hydrogen-bond donor (HBD) acidity(α), hydrogen-bond acceptor (HBA) basicity(β), and dipolarity/polarizability (π*)[123-124]. The HBD acidity (α) provides a measure of the potential of the HBD to donate a proton to a solute. Whiles the HBA basicity (β) measures the potential to receive a proton from an HBD solute[125-126]. The polarity/polarizability parameter (π*) indicates the ability of the solvent to hold a charge due to its dielectric effect[124]. It is attributable to p→π* and π→π* transitions. It is worth mentioning, in single dominant dipole bonds of nonchlorinated nonprotic solvents, the value of π* is approximately the same as the molecular dipole moment of the solvent[124, 127].

3.5 METHODOLOGY

Four highly solvatochromic dyes were prepared for the solvatochromic analysis of all DESs. These were 9-diethylamino-5-benzo[α]phenoxazinone (Nile red) which has λ_{max} of 520nm, 4-nitroaniline with λ_{max} of 370 nm, N,N-diethyl-4-nitroaniline with λ_{max} of 410 nm, and, 2,6-diphenyl-4-(2,4,6-triphenylpyridin-1-ium-1-yl) phenolate (Reichardt's dye)

with λ_{max} of 580 nm . A $1.25x10^{-4}$ M solution each of 4-nitroaniline and N,N-diethyl-4-nitroaniline were prepared in methanol. A $4.0x10^{-3}$ each of Reichardt's dye and Nile red were also prepared in methanol. To each DES in separate wells of a 96 well plate was pipetted 200 µL of each probe in triplicates. The solvatochromic shifts were obtained using Biotek Synergy H1 UV/Vis microplate reader (Winooski, VT). The samples were scanned between 180 and 720 nm over the temperature range of 25°C and 50°C at 5°C increments.

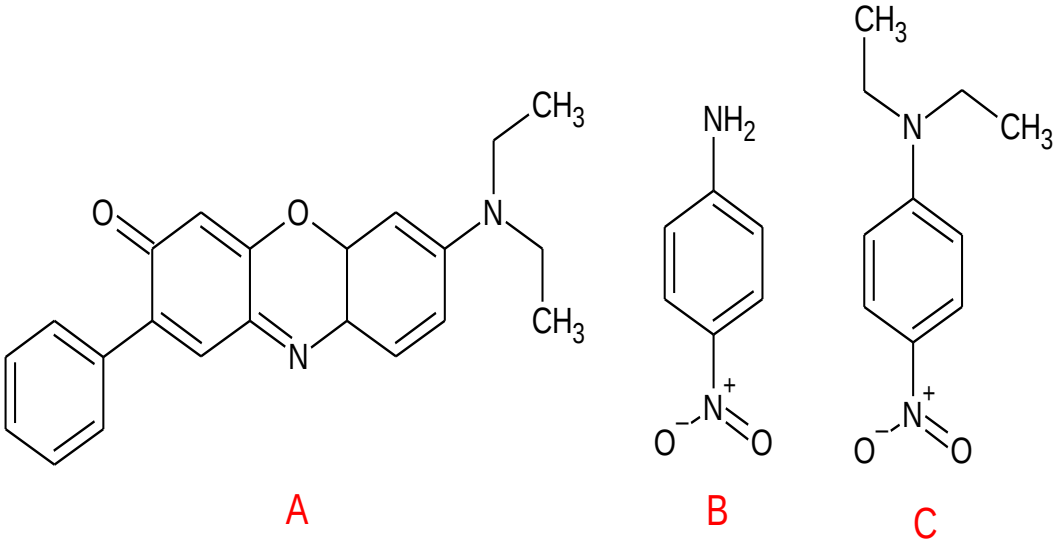

Figure 3.6.1. The three dyes used for the solvatochromic studies of the solvents. Nile red(A), 4-nitroaniline(B), and N,N-diethyl-4-nitroaniline(C).

3.6 RESULTS AND DISCUSSION

3.6.1 NILE RED E_T(NR) AND NORMALIZED E_T^N

The Nile red molar electronic transition energies(E_T(NR)) were calculated from Plank's law as modified by Kosower[118] and Reichardt[119]

$$hcV_{max}N_A$$

$$= (2.8591 \times 10^{-3})V_{max}(cm^{-1}) \qquad \textit{Equation 3. 3}$$

$$E_T(30)/(kcalmol^{-1}) = \frac{28591}{\lambda(3)_{max(nm)}} \qquad \textit{Equation 3. 4}$$

h = Plank's constant

c = Speed of light

V_{max} = Wavenumber

N_A = Avogadro's constant

$\lambda(3)_{max}$ = Wavelength of maximum absorbance of Reichardt's dye

The E_T(NR) developed by Reichardt and co-authors assumed trimethylsilane (TMS) as the least polar solvent and water as the most polar solvent. Consequently, E_T(NR) values range between 30.7 kcal/mol for TMS and 63.1 kcal/mol for water. To avoid the use of the non-SI unit kcal/mol and use SI units, normalized E_T(NR) was developed with the same assumptions of TMS as least polar and water as most polar solvents[128]. The normalized E_T(NR), E_T^N , is calculated as follows:

$$E_T^N = \frac{E_T(solvent) - E_T(TMS)}{E_T(water) - E_T(TMS)} \qquad \textit{Equation 3. 5}$$

$$\approx \frac{E_T(solvent) - 30.7}{32.4} \qquad \textit{Equation 3. 6}$$

Unlike the E_T(NR) scale, E_T^N scale ranges between 0.00 for TMS to 1.00 for water[129].

3.6.2 KAMLET-TAFT PARAMETERS

The Kamlet-Taft parameters α, β, and π* of the solvents were calculated through the following equations:

$$\alpha = 0.0649E_T - 2.03 - 0.72\pi^* \qquad \textit{Equation 3. 7}$$

$$\beta = \frac{(1.035\nu_{(2)} + 2.64 - \nu_{(1)})}{2.80} \qquad \textit{Equation 3. 8}$$

$$\pi^* = 0.314(27.52 - \nu_{(2)max}) \qquad \textit{Equation 3. 9}$$

Where,

α= hydrogen-bond donor acidity

β= hydrogen-bond acceptor basicity

π*= dipolarity/polarizability parameter

$\nu_{(1)}$= frequency or wavenumber of 4-nitroaniline

$\nu_{(2)}$= frequency or wavenumber of N,N-diethyl-4-nitroaniline

The α parameter ranges from 0.00 for non-HBD solvents such as aliphatic and aromatic solvents to 1.96 for hexafluoro-isopropyl alcohol. The β parameter ranges from

0.00 for cyclohexane to 1.00 for hexamethylphosphoric acid triamide. The dipolarity/polarizability parameter, π*, ranges from 0.00 for cyclohexane to 1.00 for dimethyl sulfoxide[129].

Figure 3.6.2. Solvents with the dye probes. Violet, light yellow, yellow, and magenta colors of Nile Red, 4-nitroaniline, N,N-diethyl-4-nitroaniline, and Reichardt's dyes respectively.

Table 3.3. Summary of the Solvatochromic parameters determined for all the solvents at 25°C.

SAMPLES	E_T(NR)	E_T^N	α	β	Π*
ChCl:H_2O(1:1)	58.92	0.87	0.93	0.44	0.71
ChCl:H_2O(1:2)	59.35	0.88	0.94	0.41	0.72
ChCl:H_2O(1:3)	59.78	0.9	0.96	0.39	0.73
ChCl:H_2O(1:4)	58.09	0.85	0.84	0.36	0.75
ChCl:H_2O(1:5)	60.19	0.91	0.98	0.36	0.75
ChCl:H_2O(1:6)	58.05	0.84	0.83	0.35	0.75
ChCl:H_2O(1:8)	59.01	0.87	0.9	0.35	0.75
ChCl:H_2O(1:10)	58.89	0.87	0.89	0.36	0.75

The E_T(NR) for all the solvents confirmed the high polarity of the solvents as expected. The polarity, however, was lower than that of water. Generally, no significant difference exists between the solvents in terms of E_T(NR). A statistical evaluation of the E_T(NR) for all solvents at five different temperatures yielded p-value greater than 0.05. The E_T(NR)values decrease minimally with temperature from 25°C to 40°C. The minimal changes in E_T(NR) observed suggests that choline cations and the chloride anions dominate the

interactions between solvent and the organic probe. Water content levels contribute little or no significant effect. See Figure 3.6.3 for effect of temperature on the E_T(NR) values.

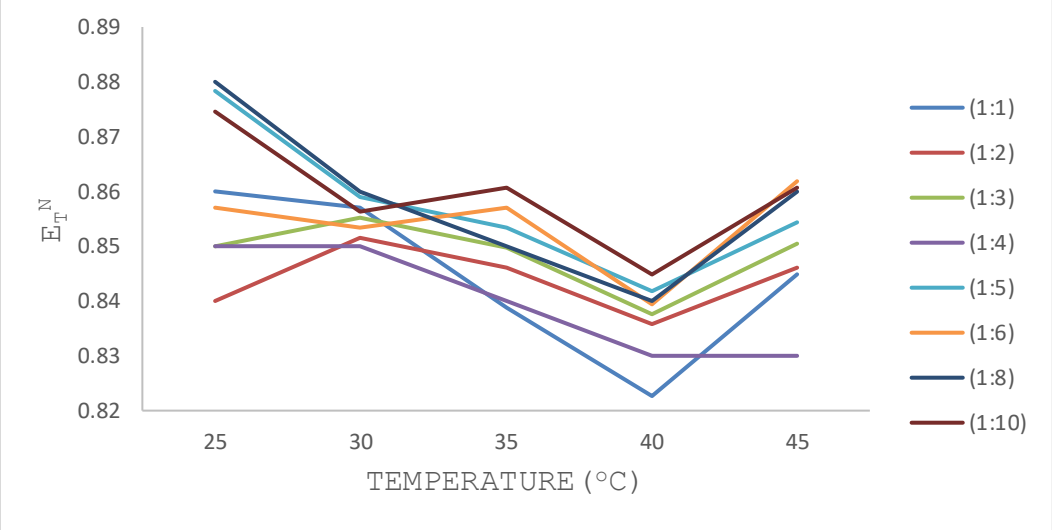

Figure 3.6.3. The effect of temperature on the E_T(NR) values of the solvents. The E_T(NR) values decrease minimally with temperature until at 40°C.

The hydrogen-bond donor acidity(α) values fall halfway within the α scale of 0.00-1.96. The reported α values range from 0.83 to 0.96. Also, the β and π* values ranged from 0.35-0.44 and 0.71-0.75 respectively. Statistically, the Kamlet-Taft parameters were not significantly affected by temperature in all the solvents studied (Figure 3.6.4). However, the β values decrease with increasing water content while the inverse is

observed in π*. The measured Kamlet-Taft parameters are within reported literature range of DESs.

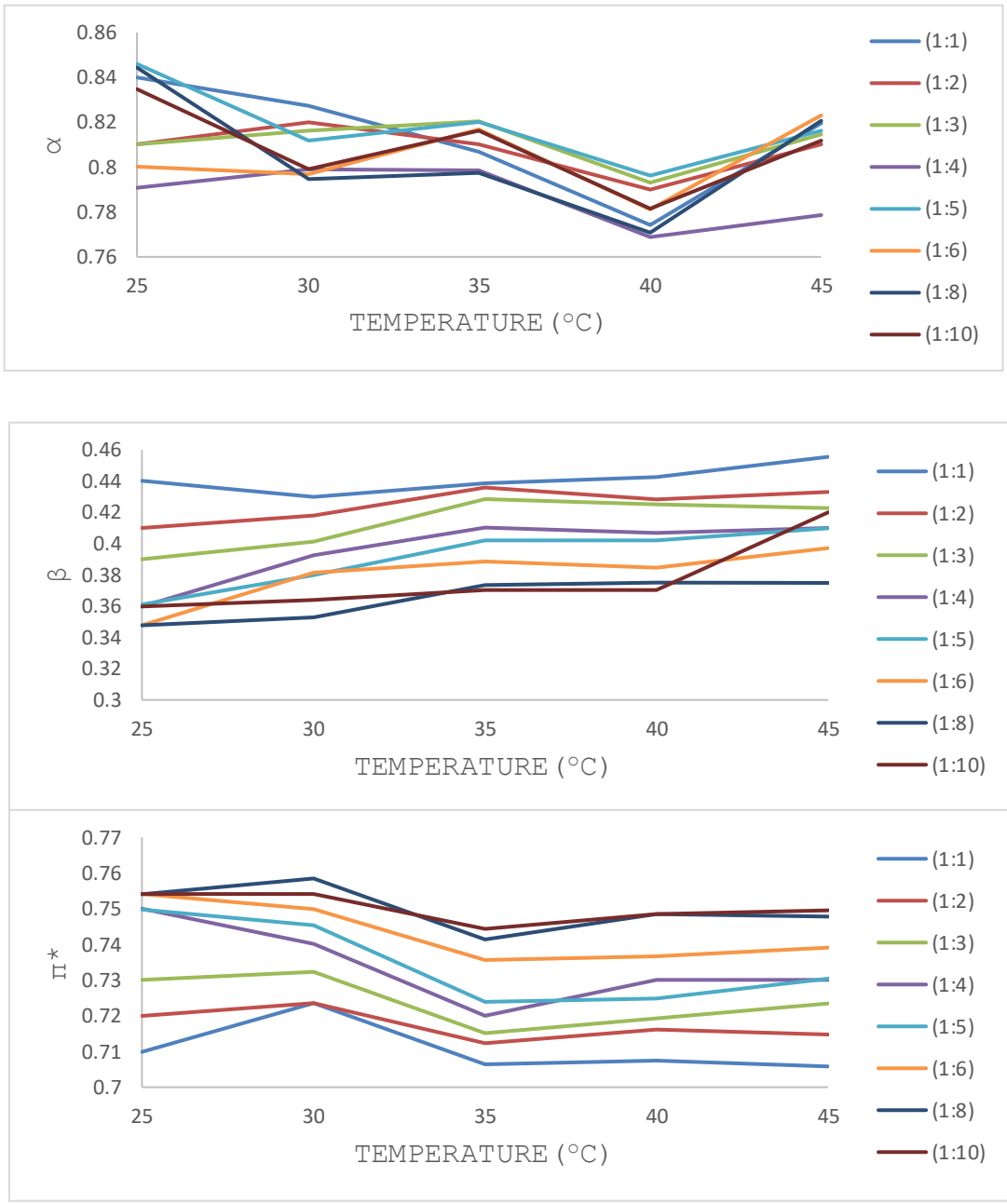

Figure 3.6.4. The Kamlet-Taft parameters of various ChCl:H_2O solvents. Temperature effect in insignificant in all the parameters but water content levels affect β and π*

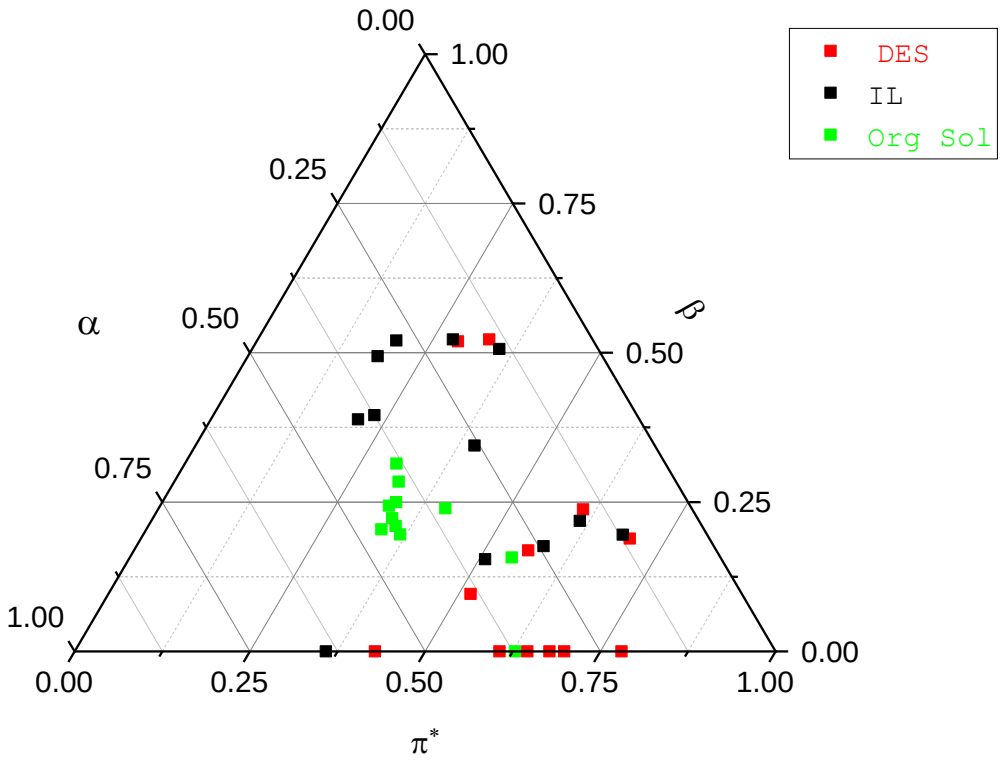

Figure 3.6.5. Comparison of the Kamlet-Taft parameters of DESs (red), ionic liquids (black), and organic solvents (green).

3.7 CONCLUSION

The physicochemical, thermal, and solvatochromic properties of the ChCl:water solvents were successfully characterized. The densities of the ChCl:water solvents were higher than that of water but the higher the water content, the closer the density was to that of water. Again, the densities of the solvents directly correlated with their refractive index

(R^2=0.99) but less so with the viscosities (R^2= 0.88). The relatively strong H-bonding in ChCl:water (1:3) and ChCl:water (1:4) caused them to have elevated viscosities compared to the other solvents except ChCl:water (1:1).

A freeze-thaw process analysis showed that the thermograms correlated with the measured freezing points of the solvents. The freeze-thaw profiles of ChCl:water (1:1) and ChCl:water (1:2) were similar whiles ChCl:water (1:3), ChCl:water (1:4), and ChCl:water (1:5) had similar profiles. But ChCl:water (1:6) and ChCl:water (1:8) profiles were different.

The thermal stability profiles studied through DSC and TGA indicated that ChCl:water (1:3)and ChCl:water (1:4) were the most thermally stable. The two solvents had decomposition temperatures of 215^{o}C and 231^{o}C respectively. It is worthy to mention that these two solvents have relatively strong H-bonding compared to the other solvents. These findings were also supported by the TGA analysis. The ChCl:water (1:3) and ChCl:water(1:4) had the lowest weight loss per temperature of 26% at 234^{o}C and 33% at 294^{o}C respectively.

All the solvents are highly polar as indicated by the E_T(NR) and E_T^N results as a result of H-bonding[130-132] and ionic interaction. The E_T(NR) values ranged from 58.05 in

ChCl:water (1:6) to 60.19 in ChCl:water (1:5). The E_T^N values range from 0.87-0.91. The Kamlet-Taft parameters do not significantly differ among the solvents. However, the hydrogen bond acceptor basicity (β) and the dipolarity/polarizability parameter (π*) are affected by percent water content and temperature, while E_T^N and α are not. The solvatochromic data for all the solvents are comparable to literature DESs values as shown in the ternary plot of α, π, and β for organic solvents, ionic liquids, and DES(Figure 3.6.5).

CHAPTER FOUR

MOLECULAR DYNAMICS SIMULATIONS

4.0 INTRODUCTION

Molecular dynamics simulations (MDS)involve the use of quantum chemistry to study the molecular dynamics and intra- and intermolecular conformational rearrangements of atoms within a molecule as the molecule interacts with the environment[133]. MDS provide a cheaper, effective, time-saving, and accurate mode for atomic and molecular studies to inquire and predict behavior of molecules[133]. MDS employing quantum chemistry provide better understanding of the nature of bonding, forces involved, and electron density shifts in a molecular reaction system[134-135]. MDS have been applied to various fields including drug discovery, theorical chemistry, solute-solvent systems, protein studies, and membrane studies[136-139].

An important component for the development of a green solvent alternative to conventional organic solvents and ionic liquids is the elimination of waste by-products or attainment of 100% atom economy[3,6]. More importantly, the underlying molecular basis for such solvents should be properly understood. Despite increased interest, the fundamental molecular basis of their formation and

interactions of DESs are yet to be fully understood. The general assertion of hydrogen bonding being solely the main cause of formation of DESs have come under scrutiny[134, 140].

Charge transfer analyses have called into question the source of the H-bonding and nature of the interactions or forces within DESs systems[140]. Indeed, Kempter et al. cautions the oversimplification, generalization, and attribution of the interactive forces within imidazolium ionic liquids and DESs[141].

Force field studies and density functional theory (DFT) are powerful tools that have provided better understanding and insight into several chemical phenomenon such as ionic liquid formation and interactions between proteins. The application to DESs is still in the nascent stage with the first report occurring in 2014[142-143]. Garcia et al.(2015), in a study employing DFT and AIM and involving ChCl:urea (1:2), ChCl:glycerol (1:2), ChCl:glycerol (1:3), and ChCl:malonic acid (1:1) suggested that charge delocalization due to hydrogen bonding causes low electron density which in turn leads to low melting points observed in DESs[144]. However, Zahn et al.(2016) raise questions about this suggestion[140]. Again, in a recent study by Ashworth et al.(2016), the choline chloride and urea are said to form multiple complexes

involving choline and urea and urea and chloride. This challenges the commonly held assertion that chloride anion and urea form the H-bonds that is known to be the major force of interaction underpinning DES formation. There is therefore a need for further studies into the molecular basis of DES formation.

Aqueous choline chloride DES is a very good model for studying the molecular mechanisms of DES formation. The small size of the HBD, water, has strong intermolecular hydrogen bonds. The small size of the HBD should amplify the hydrogen bonds between the HBD and HBA due to the short distance between them, if any existed. Also, the strength of the H-bond should follow a predictable pattern as the HBD ratio increases. Again, this pattern should confirm other measured properties such as thermal analyses. The pattern, if established, could lead to the predictability of the molar ratios of HBD and HBA needed to form the DES. This avoids the current trial-and-error method used in DESs discovery and formulation which consumes more chemicals. The aim of this part of the research was to understand and predict the effect of hydrogen bonding in the formation of aqueous choline chloride deep eutectic solvents using molecular dynamic simulations.

4.1 DENSITY FUNCTIONAL THEORY(DFT)

Density functional theory provides computational description of the ground state properties or electronic structure using electron density. DFT is used for the description of spin polarized systems, multicomponent systems such as nuclei and electron hole droplets, free energy at finite temperature, time-dependent phenomena and excited states, bosons, and molecular dynamics[135, 145-146].

The central basis of DFT is to describe a system based on the electron density (ρ) rather than the wavefunction (ϕ). This reduces the load of calculations that have to be done and therefore time. The solution to the Schrodinger equation, whether time-dependent or time-independent, for a system with N electrons calculated via wavefunctions have 3N variables while DFT has only 3 variables. The other advantage of DFT is that it provides information on other chemical properties such as electronegativity (chemical potential), hardness or softness, and Fukui function (describes ρ in frontier orbital with small change in total electrons)[146-147].

4.1.1 DEFINITIONS IN DFT

In a simple time-independent Hamiltonian, the Schrodinger equation for the wavefunctions is given as;

$$\left[\frac{\hbar^2}{2m}\sum_{i-1}^{N}\nabla_i^2 + \sum_{i-1}^{N}V(r_i) + \sum_{i-1}^{N}\sum_{j<i}U(r_i,r_j)\right]\psi = E\psi \qquad \textit{Equation 4. 1}$$

m= mass of electron

$\hbar$= Reduced Planck's constant

N= Number of electrons

r= Position vector

i and j= imaginary units

V= Potential energy

The first term is the kinetic energy. The second term refers to interaction energy between each electron and the collection of nuclei. The third term refers to interaction energy between different electrons.

However, in DFT, two fundamental principles underpin the equations. First, the ground-state energy from the Schrodinger equation is a unique functional of the electron density. Secondly, the electron density that minimizes the energy of the overall functional is the true electron density corresponding to the full solution of the Schrodinger equation. It is worth noting that the wavefunction is not

real but complex, unlike the electron density which is observable. The electron density is described as

$$n(r) = 2\sum_i \psi_i^*(r)\psi_i(r) \qquad \textit{Equation 4. 2}$$

The DFT expression or Kohn-Sham (K-S) equation is given as

$$\left[\frac{\hbar^2}{2}\nabla^2 + V(r) + V_H(r) + V_{XC}(r)\right]\psi_i(r) = \varepsilon_i\psi_i(r) \qquad \textit{Equation 4. 3}$$

The three variables describing the electron density are V, V_H, and V_{XC}.

V= the potential energy that describes the interaction between an electron and the collection of atomic nuclei

V_H (Hartree potential)= describes the coulomb repulsion between the electron under consideration in the K-S equation and itself, and the total electron density defined by all electrons in the problem.

V_H is mathematically expressed as

$$V_H(r) = e^2\int \frac{n(r')}{|rr'|}d^3r' \qquad \textit{Equation 4. 4}$$

V_{XC}= exchange and correlation contribution to the single electron equation. It is a functional derivative of the exchange correlation energy.

$$V_{XC}(r) = \frac{\delta E_{XC}(r)}{\delta n(r)}$$ *Equation 4. 5*

4.1.2 THE HYDROGEN BOND

The hydrogen bond is an intermolecular force of attraction lesser in strength to ionic and covalent bonds and yet stronger than Van der Waals and London forces. In quantum chemistry, the hydrogen bond is described to be an inherent property of matter itself resulting from nonlinear coupling of quantified energy levels and electromagnetic field[148]. However, the IUPAC defines the hydrogen bond as an attractive interaction between the hydrogen atom from a molecule or a fragment of it in which the hydrogen is attached to a more electronegative atom, and an atom or group of atoms in a molecule in which evidence of a bond formation is observed[149]. Representatively, the hydrogen bond can be described as X—H---Y—Z where X—H is the hydrogen bond donor and Y is the hydrogen bond acceptor.

The hydrogen bond may include electrostatic forces, charge transfer between the HBD and HBA, as well as dispersion forces[150]. The H---Y bond strength increases with electronegativity of X. The interaction energy correlates with the extent of charge transfer. Therefore, charge

transfer analyses via DFT can be used to determine the formation and strength of hydrogen bonds.

4.1.3 CHARGE TRANSFER ANALYSIS (CTA)

Charge transfer analysis in DFT involves arbitrary assignment of charges to nuclei or bond orders by partitioning their wavefunctions or electron density. The assigned charges provide a better understanding of the electron density distribution as they relate to the proximity of the electrons to the nucleus at a particular time[151]. For instance, the charges provide an effective way of predicting molecular interactions such as sites that are amenable to nucleophilic or electrophilic attack[152]. More importantly, these partial charges correspond very well with the nature and direction of bonds (ionic, covalent or hydrogen bonds) as well as their polarity[153].

The proximity of atoms, group of atoms, or a molecule to another during bond formation or breaking distorts the electron cloud density around the atom or group of atoms thus affecting the partial charges assigned to them. These changes in charges is what is analyzed via population analysis to predict the nature of bonds, bond type, polarity, etc[151].

The distortion in the electron density distribution is quantified in energy terms as the interaction energy. The interaction energy provides useful information on the nature of the interaction or bond. In this research, the CTA and population analysis conducted are Hirschfeld and Voronoi's deformation density and are used to better understand the nature and directions of interactions within the choline Cl:water DES. These two methods have the advantage of being independent of the basis set.

4.2 COSMO-RS

The chemical potentials, free energies, dominant forces, solubility, and other thermodynamic parameters of fluids are very relevant to solvent characterization and applications. Conductor-like screening model for realistic solvents (COSMO-RS) is a thermodynamic computation method for fluid systems[154]. COSMO-RS forms part of the dielectric continuum solvation models but employs both DFT and statistical thermodynamics and considers solvent effects[155].

COSMO-RS works by applying statistical thermodynamics to the interacting surfaces of the solvent molecules calculated from their screening charge densities to develop a sigma (σ)-profile of the solvent[154]. The σ-profile indicates the amount of surface area $p(\sigma)$ as a function of the polarization charge

density(σ). The molecular interactions account for in COSMO-RS computations include Van der Waals forces, electrostatic interactions, and hydrogen bonding. Therefore, the contributions or effects of each of these interactions can be isolated and evaluated[155].

COSMO-RS computations lead to an accurate estimation of solubility parameters such as LogP or K_{ow}, pKa, solvation free energies, Henry's law constant, vapor pressures, boiling points, vapor-liquid phase diagrams, and binary and ternary mixture (VLE/LLE and SLE)[156].

4.2.1 METHODOLOGY

The quantum mechanics/quantum chemistry software was used for the molecular dynamic simulations. These were Amsterdam density function (ADF) by SCM (Amsterdam, Holland), CosmothermX and TmoleX by COSMOlogic Predicting Solutions (Leverkusen, Germany).

All calculations were ab initio. Structural optimizations using ADF were obtained with MOPAC2012.12.237 with PM7-TS method. The basis function applied was XC-GGA Becke-Pardew with ZORA relativistic scalar. The nuclear charge densities were calculated using the point-charge nuclei model. The optimized structures were used to develop Cosmo files using Klamt 2005 model. All hydrogen-bond

profiles were obtained from the Cosmo files calculated using ADF. Hirschfeld and Voronoi deformation charge transfer analyses were calculated using ADF under the above conditions.

CosmothermX version 17.0.2 was used for σ-profile and σ-potentials calculations under BP-TZVP_C30_1701 parameterization. TmoleX version 4.2.1 was used for structural optimization using MOPAC2012 prior to generation of COSMO-RS files. All calculations were done at room temperature.

4.3 RESULTS AND DISCUSSIONS

4.3.1 EQUATIONS AND CALCULATIONS

Van der Waals forces were computed using the expression;

$E_{vdw}^{x} \cong \sum_{\alpha} \tau_{el(\alpha)} A_{\alpha}^{x}$ or

$$E_{vdw} = a_{eff}(\tau_{vdw} + \tau'_{vdw}) \qquad \textit{Equation 4. 6}$$

where,

α= general constant

A_{α}^{x} *or* a_{eff} = effective contact area

τ= element-specific coefficient for dispersion

For unlike segment pairs, the electrostatic energy is given by;

$$\Delta E_{misfit} = a_{contact} c_{misfit} (\sigma + \sigma')^2$$ *Equation 4. 7*

Where,

$(\sigma + \sigma') =$ net charge

$a_{contact} =$ surface segment contact area

$c_{misfit} =$ coefficient from electrostatics

The hydrogen-bond interaction energy is computed as;

$$\Delta E_{HB} \cong a_{contact} c_{HB} min(0, \sigma\sigma' - \sigma_{HB}^2)$$ *Equation 4. 8*

ΔE_{HB} = Hydrogen bond interaction energy

$a_{contact} =$ Surface segment contact area

σ_{HB}= Polarization charge density threshold for hydrogen bond

$\sigma\sigma'$= correction for hydrogen bond (*it ensures that hydrogen bond term increases with polarity of the HBD and HBA*)

c_{HB}= interaction strength coefficient

* Only contributions from sufficiently polar segments pairs contribute to the H-bond

For a solute X in solvents, the chemical potential of solute X in solvent S is calculated as

$$\mu_s^x = \int d\sigma p^x(\sigma)\mu_s(\sigma) + RTln(x\gamma_{comb,s}^x) \qquad \textit{Equation 4. 9}$$

where,

$\mu_s^x =$ Chemical potential of solute X

$\mu_s(\sigma)$= polarization charge density of solvent

$\gamma_{comb,s}^x =$ combinatorial activity coefficient

x = molar fraction of solute X

$p^x(\sigma) =$ σ-profile of X

The sigma(σ)- profile of a mixture is given as the additive of the pure mixtures;

$$p_s(\sigma) = \sum_i \frac{x_i p_s^{x_i}(\sigma)}{x_i A^{x_i}} \qquad \textit{Equation 4. 10}$$

Activity coefficient of a segment is given as;

$$ln\gamma_s(\sigma) = -ln\left[\int d\sigma' p_s(\sigma)\gamma_s(\sigma') \times exp\left\{\frac{-a_{eff}e(\sigma,\sigma')}{RT}\right\}\right] \qquad \textit{Equation 4. 11}$$

The combined activity coefficient is given by:

$$ln\gamma_{i/s} = n_i \sum_{\sigma_m} p_i\,(\sigma_m)[ln\gamma_s(\sigma_m) - ln\gamma_i(\sigma_m)] + \gamma_{comb,s}^i \qquad \textit{Equation 4. 12}$$

$ln\gamma_s(\sigma_m) =$ segment activity coefficient of s

$ln\gamma_i(\sigma_m)$ = segment activity coefficient of i

$\gamma^i_{comb,s}$ = combinatorial activity coefficient

$p(\sigma_m)$ = sigma profile of the mixture

4.3.2 STRUCTURAL OPTIMIZATION

The structures of choline chloride, water, and all the solvents were optimized using MOPAC2012. The hydrogen-bonding distance were automatically generated ab initio for equivalency. The red-colored surface charge densities indicate high electronegativity whiles the blue color represents electropositive atoms or groups. The neutral groups are depicted in the green shade.

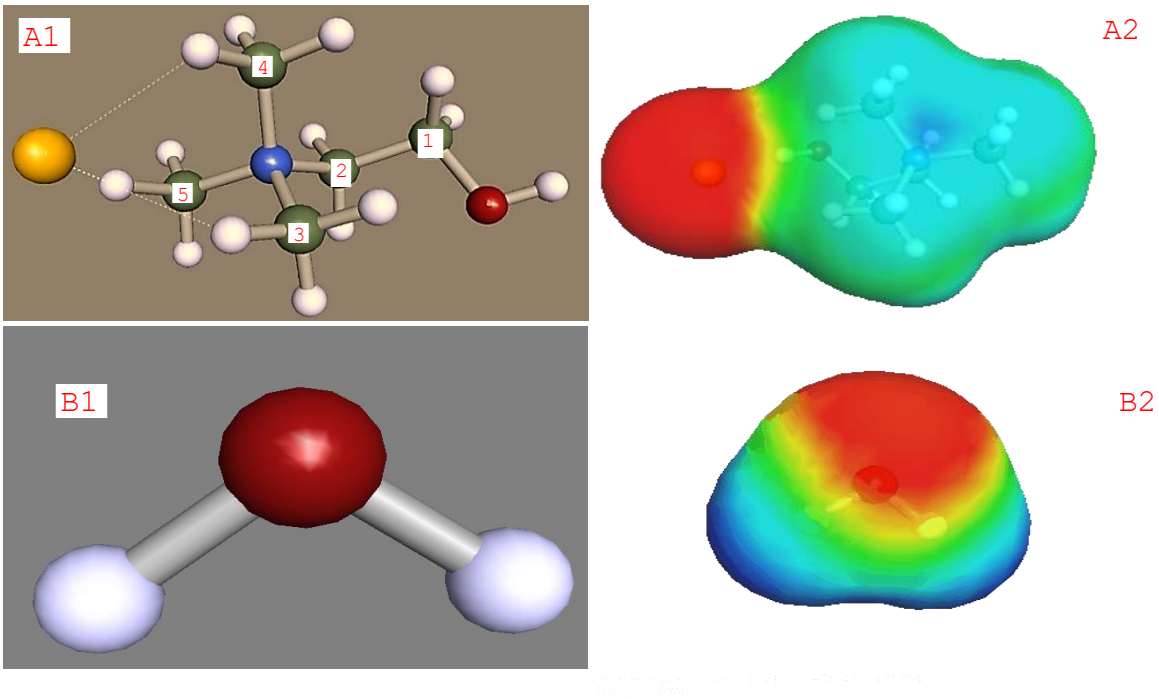

Figure 4.0. The optimized structures and σ-surface potentials of choline chloride(A1 and A2)and water molecule(B1 and B2). The dashed lines represent hydrogen bonding occurring between the chloride anion and adjacent hydrogen atoms within choline chloride. [C (green), H (white), O (red), N (blue) and Cl^- (yellow)].

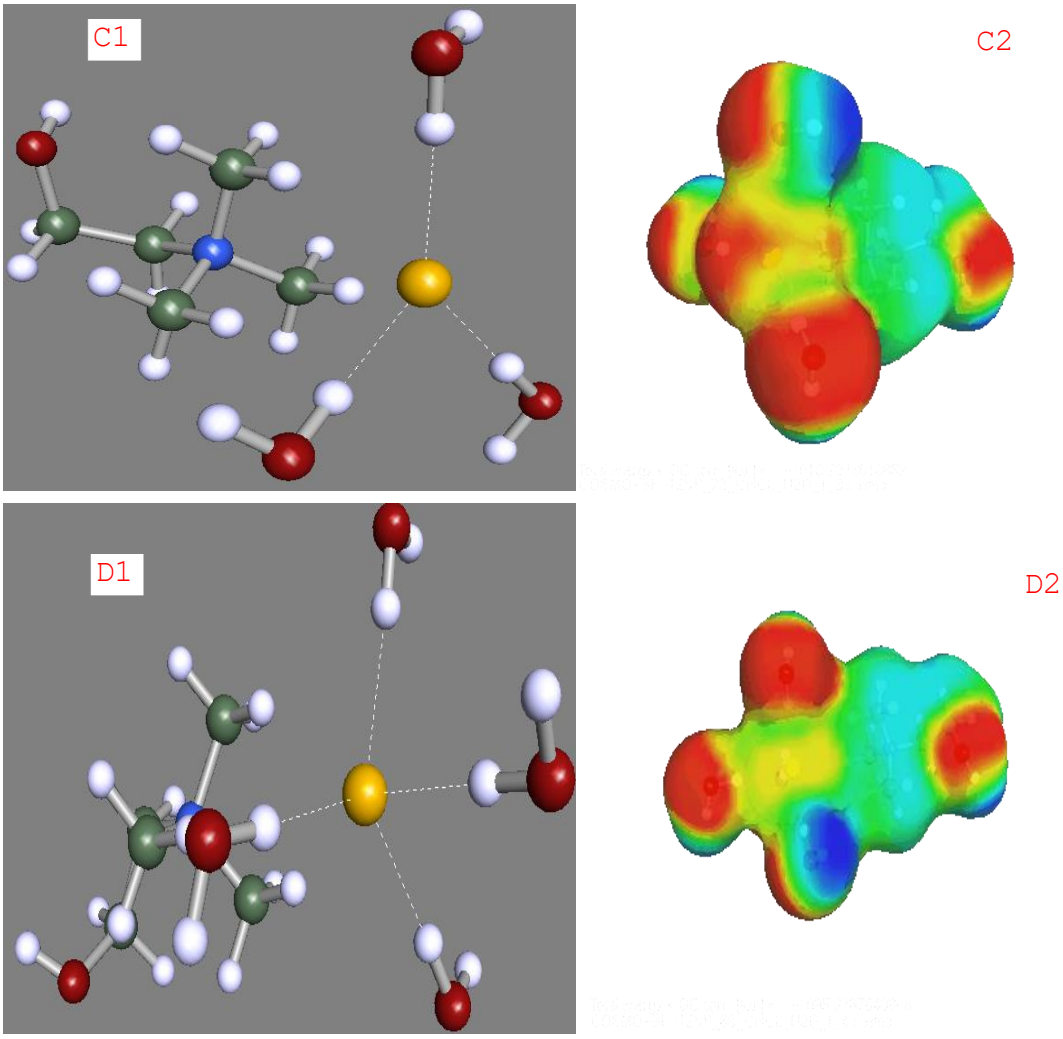

Figure 4.1. The optimized structures and σ-surface potentials of ChCl:H_2O(1:3)(C1 and C2)and ChCl:H_2O(1:4)(D1 and D2). The dashed lines represent hydrogen bonding occurring between the chloride anion and hydrogen atoms of water.

4.3.3 σ-PROFILES AND σ-POTENTIALS

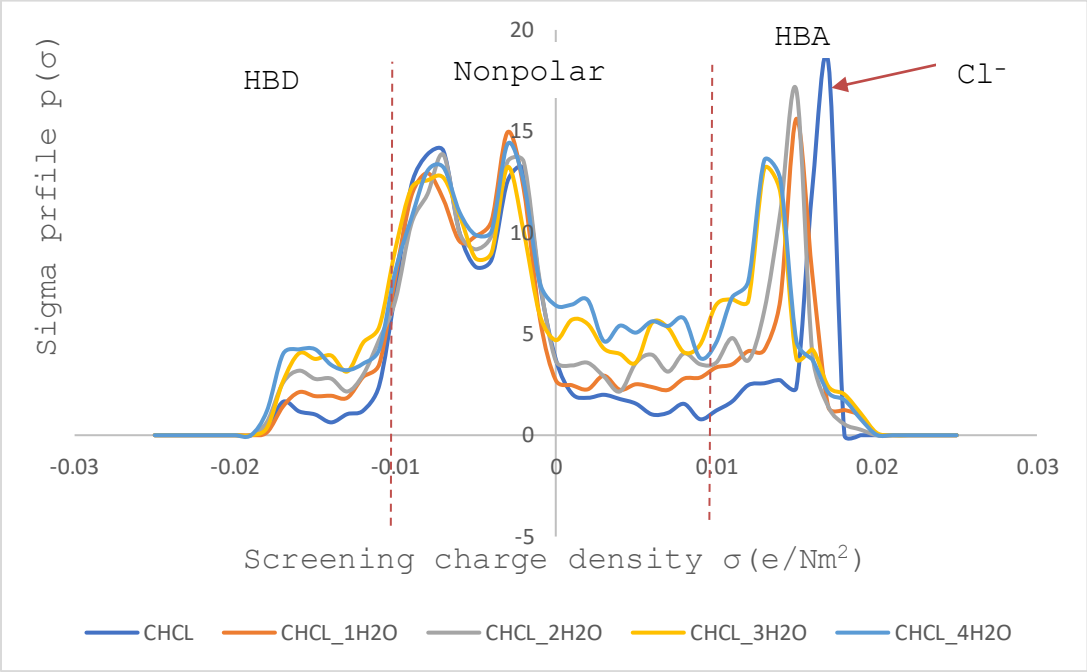

Figure 4.2. σ-Profile of ChCl and ChCl:water solvents

The σ-profile represents the probability distribution of the surface charges, or screening charge densities of all the components of the solvent mixture or molecule. The electronegative groups represent the positive side of the plot as they serve as counter ions or charges for the electropositive groups which are represented as negative charges on the plot.

The σ-profile of all the solvents and choline chloride ranges between -0.02 to +0.02 (see Figure 4.2). The asymmetrical choline chloride σ-profile has four maxima corresponding to, from right, the gaussian chloride ion at

+0.017 e/Nm^2, the almost neutral hydrogen atoms on carbons 1 and 2, the partially positive nine hydrogen atoms of the three methyls on the nitrogen, and the positive charge of the nitrogen at -0.017 e/Nm^2. Also, the σ-profile shows that the positive charge on the nitrogen is spread around the methyl groups. The maxima for the lone pair of electrons on the oxygen in the hydroxyl group is seen at +0.011 e/Nm^2.

As the ratio of water molecules increase, the screening charge on the chloride ion reduces and it becomes more positive. This is significant because reduction in the surface charges of the chloride ion is spread towards the neutral region. This should lead to increase in the affinity of the solvent molecules for each other, and hence increase in surface tension. Also, increased surface tension should enhance hydrogen bonding in between the molecules. This explains why ChCl:H_2O(1:3) and ChCl:H_2O(1:4) have the highest surface tension (see Table 3.1). It also suggests that the polarity minimally decreases as the water ratio increases.

The σ-potential describes the affinity of a solvent for a molecular surface of σ polarity[157]. Again, the hydrogen bond threshold (σ_{HB}) is 0.008 e/A[157-158]. As seen in Figure 4.3, the room temperature σ-potentials of the solvents and choline chloride are parabolic and indicate significant affinity for

hydrogen-bonding interaction. Thus, the σ-potentials confirm the polarity of the solvents as polar. Both the HBA (positive region) and HBD (negative region) profiles show affinity for HBD and HBA molecular-surface charges. However, the hydrogen-bond affinity of ChCl:H_2O (1:1)and ChCl:H_2O (1:2) indicate a strong effect of the electronegative chloride anion and similarities in the hydrogen bonding profiles as their surface screening charges profiles overlap. This is indicated by the overlapping of their screening charge profiles, cutting the positive and negative scales at 0.017 e/A and -0.013 e/A respectively. Similarly, the σ-potentials of ChCl:H_2O (1:3) and ChCl:H_2O (1:4) are almost the same but with reduced effect of the chloride anion. The two solvents intercept the positive scale at 0.015 e/A and on the negative scale at -0.012 e/A.

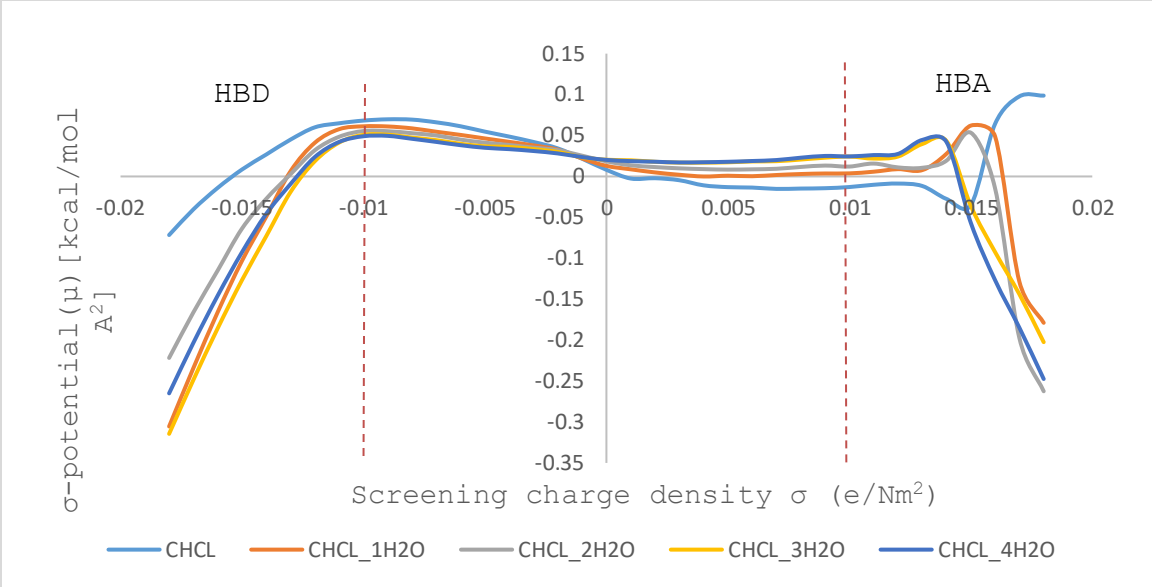

Figure 4.3. The σ-Potentials of ChCl and ChCl:H_2O solvents

4.3.4 FORCES OF INTERACTIONS WITHIN DES SOLVENTS

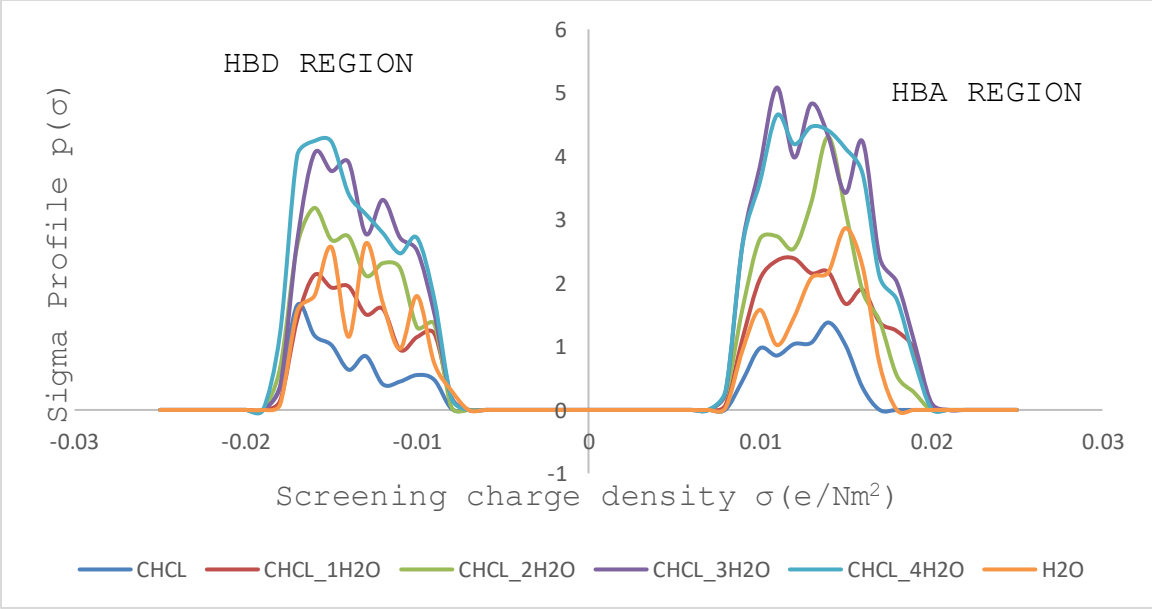

Figure 4.4. The hydrogen bonding profile within H_2O, ChCl and the ChCl:H_2O solvents. This is representative of the strength of hydrogen bonds.

The forces of interaction contributed by hydrogen bonding is seen in Figure 4.4. Figure 4.4 indicates that, except in choline chloride and water molecules, hydrogen bonding constitutes about a third of the forces of interactions within each solvent. Comparison of Figures 4.2, 4.4, and 4.5 shows that the contribution of the HBD and HBA to hydrogen bonding differs in the ChCl:H_2O (1:3) and ChCl:H_2O (1:4) solvents than the other solvents. This may be due to greater charge delocalization around the hydrogen atoms of the water molecules (HBD) from the chloride anion (HBA). If this is so, then the partial charges of hydrogen atoms in the HBD within the ChCl:H_2O (1:3) and ChCl:H_2O (1:4) solvent systems should be more positive. Charge transfer analysis should confirm this suggestion.

Confirming the observation in the σ-potentials, the hydrogen bonding and the nonhydrogen bonding forces within the ChCl:H_2O (1:3) and ChCl:H_2O (1:4) are almost the same. The hydrogen bonding profiles of ChCl:H_2O (1:1) and H_2O are the same. Therefore, at 1:1 ChCl:H_2O ratio, the group contribution of the H_2O HBD appears to be negligible in respect to hydrogen bonding donation. Weak van der Waals and electrostatic forces are the dominant interactive forces within the solvent systems.

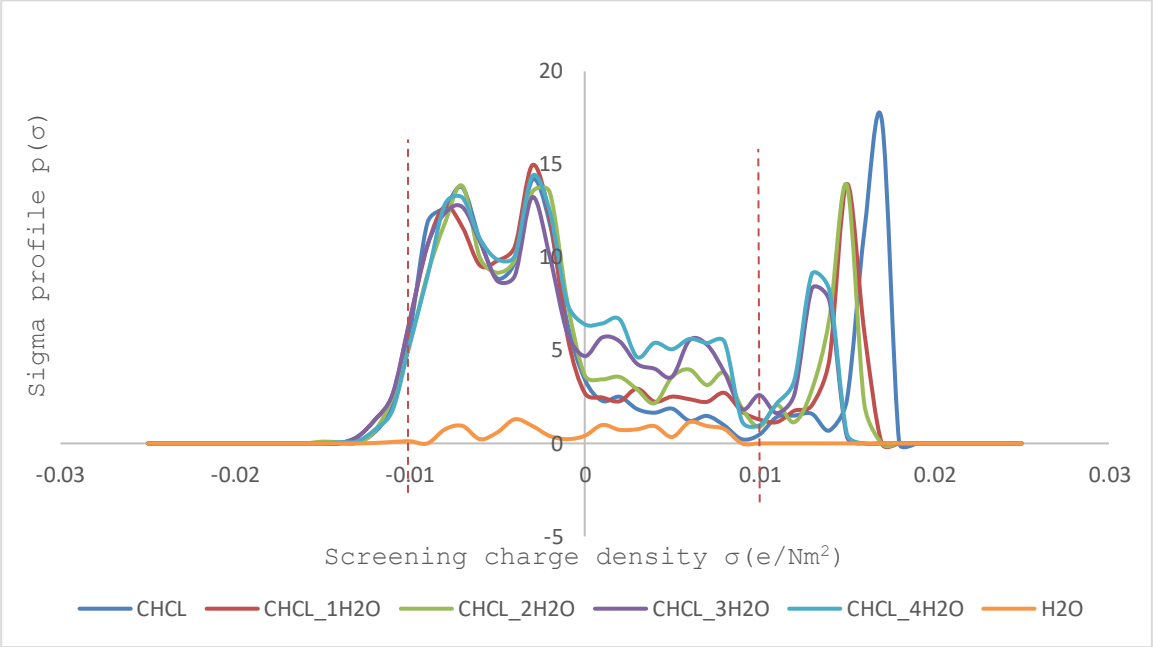

Figure 4.5. The σ-profile of all other forces within ChCl, H_2O and the ChCl:H_2O solvent systems. The profile suggests that electrostatic forces, Van der Waals, and other weak forces are the dominant forces with the solvents formulated.

4.3.5 CHARGE TRANSFER ANALYSIS

Charge delocalization has been suggested to be the underpinning cause of DES formation and their characteristically low melting points[159]. Abbot et al.(2003), first suggested charge spreading of negative charges from halides to the HBD in a study involving choline fluoride and urea[15]. Abbot observed a strong cross-correlation between the fluoride anion and the amino (-NH_2) group of urea in a HOESY-NMR spectrum. Similar cross-correlation was observed when the

F^- was substituted with Cl^-. As a result, charge spreading and charge transfer analysis continue to be used as one of the basis for explaining DES formation and their associated physical and chemical properties.

4.3.5.1 HIRSHFELD PARTIAL CHARGE ANALYSIS

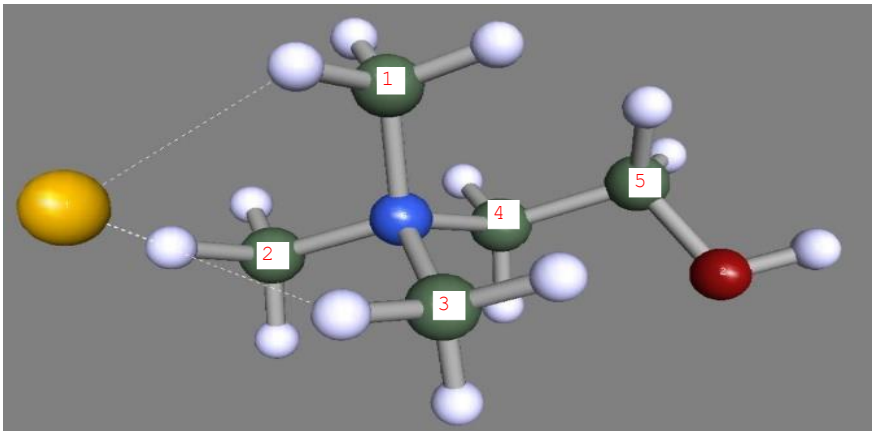

Figure 4.6. Optimized structure of Choline chloride with the carbons numbered

$$q_A = Z_A - \int \rho_A(r)dr \qquad \textit{Equation 4. 13}$$

$q_A =$ Charge of atom A

$Z_A =$ Atomic number of atom A

$\rho_A(r) =$ Electron density of atom A

Table 4.1. Hirshfeld partial charges for choline chloride and the ChCl:H_2O solvents. The five carbon atoms and nitrogen, chloride, and oxygen are presented.

	SOLVENTS				
ATOM	**ChCl**	**1:1**	**1:2**	**1:3**	**1:4**
Cl	-0.644	-0.525	-0.514	-0.42	-0.437
N	0.096	0.097	0.097	0.098	0.097
O	-0.219	-0.214	-0.219	-0.224	-0.218
C5	0.01	0.005	0.012	0.005	0.012
C4	-0.015	-0.008	-0.01	-0.008	-0.01
C3	-0.034	-0.034	-0.033	-0.032	-0.033
C2	-0.042	-0.04	-0.046	-0.046	-0.047
C1	-0.041	-0.038	-0.043	-0.036	-0.044

Table 4.2. Hirshfeld partial charges of the water molecules in the ChCl:H_2O solvents.

	SOLVENTS			
ATOM	**1:1**	**1:2**	**1:3**	**1:4**
O	-0.332	-0.27	-0.333	-0.226
H	0.054	0.063	0.066	0.098
H	0.144	0.166	0.148	0.18
O		-0.311	-0.269	-0.336
H		0.085	0.067	0.068
H		0.151	0.168	0.096
O			-0.306	-0.307
H			0.086	0.091
H			0.152	0.155
O				-0.258
H				0.173
H				0.066

The Hirshfeld population charge analysis indicates that the charge on the Cl^- anion reduces from -0.644 in choline chloride to -0.42 (see Table 4.1). More importantly, charge spreading from the Cl^- anion is greatest in ChCl:H_2O (1:3) followed by ChCl:H_2O (1:4). This charge spreading from the Cl^- supports delocalization but more onto the choline backbone than the HBD hydrogen atoms. Therefore, this enforces or

supports the suggestion by Zahn et al.(2016) that charge delocalization between the halide anions and HBD may not solely be the reason for the characteristic low melting points in DESs.

The central positive charge on the quaternary nitrogen suffers no effect from the charge spreading from the Cl^- ion. Indeed, the charge variation on the N^+ is minimal and insignificant between +0.096 and +0.098, though the largest charge was observed in ChCl:H_2O (1:3). Again, the carbons closer to the Cl^- observe the largest charge spreading in ChCl:H_2O (1:3) than the rest of the solvents (see Table 4.1). In C1, C2 and C3 of the solvents, the C1 and C3 appears to be proximally closer to the Cl^- than the C2. Thus, these two carbons express more variation in their charge. A similar trend is seen in the hydroxyl oxygen in choline chloride. The most significant charge spreading is observed in ChCl:H_2O (1:3).

Also, analysis of the charge spreading in HBD indicates that, when equivalent HBD hydrogen atoms are observed, the ChCl:H_2O(1:3) again expresses the largest charge spreading. Based on the above observations, it can be confirmed that the deep eutectic composition is the ChCl:H_2O(1:3).

4.3.5.2 VORONOI DEFORMATION DENSITY (VDD) ANALYSIS

$$Q_A = -\int_{Voronoi\ cell\ of\ A}(\rho(r) - \sum_B \rho_B(r))\, dr \qquad \text{Equation 4.14}$$

$Q_A =$ VDD charge

$\rho(r) =$ electron density of molecule

$\rho_B(r) =$ atomic density of atom B of promolecule

The Voronoi deformation density redistributions (ΔQ) of the various solvents were calculated using VDD of choline chloride as base reference (see Tables 4.3 and 4.4). VDD provides information on the direction of flow of charge and hence bond formation. A positive ΔQ ($\Delta Q>0$)indicates charge flow out of the atom/bond whiles $\Delta Q<0$ indicates charge flow into atom/bond.

Table 4.3. Voronoi deformation density charges for choline chloride and the ChCl:H_2O solvents. The five carbon atoms and nitrogen, chloride, and oxygen are presented.

	SOLVENTS				
ATOM	**ChCl**	**1:1**	**1:2**	**1:3**	**1:4**
Cl	-0.674	-0.564	-0.554	-0.472	-0.483
N	0.054	0.054	0.056	0.056	0.055
O	-0.252	-0.246	-0.252	-0.255	-0.251
C5	0.001	0	0	-0.004	0.001
C4	-0.031	-0.024	-0.03	-0.028	-0.03
C3	-0.036	-0.037	-0.036	-0.033	-0.035
C2	-0.037	-0.036	-0.038	-0.036	-0.039
C1	-0.034	-0.035	-0.037	-0.033	-0.036

From Table 4.4, the main direction and flow of charge is from the Cl^- ion. All other atoms express insignificant ΔQ out of or into the atom. This finding supports the findings of Abbot et al. (2003) that charge flow from the halide ion induces charge delocalization leading to hydrogen bonding.

Table 4.4. Voronoi deformation density electronic redistribution (ΔQ)in millielectrons of ChCl:H_2O solvents

	VDD ELECTRONIC REDISTRIBUTION(ΔQ)/me			
ATOM	**1:1**	**1:2**	**1:3**	**1:4**
Cl	110	120	202	191
N	0	2	2	1
O	6	0	-3	1
C5	-1	-1	-5	0
C4	7	1	3	1
C3	-1	0	3	1
C2	1	-1	1	-2
C1	-1	-3	1	-2

4.4 CONCLUSION

The main aims of the molecular dynamic simulation using density functional theory (DFT) were to establish the possibility of predicting the ratio of constituent compounds that would form DES and to understand the molecular basis of DES formation. When successful, it will do away with the laborious and wasteful way of preparing DES. Also, the objective was to optimize the structures of ChCl:H_2O solvents, develop Cosmo files for each solvent, and carrying out charge transfer analysis to establish whether the simulation results would confirm the experimental results.

Based on the data obtained, the structures of all the solvents were successfully optimized and Cosmo files successfully developed for each solvent. The charge transfer analysis confirmed that the eutectic ratio of choline chloride and water is 1:3 as determined experimentally. The results also showed that charge spreading or charge delocalization occurs during the formation of DESs. This charge transfer predominantly emanates from the Cl^- ion and that the spreading is bidirectional. However, most of the charge is spread over the choline cation backbone and a minority onto the HBD.

The mechanism of the formation of DES per the molecular dynamic simulations appears as follows:

i. Upon contact with the water HBD molecules, charge from the Cl^- counter anions spreads onto the choline cation backbone.
ii. The charge spreading weakens the charge density on the Cl^- ions.
iii. This causes the Cl^- ions to form weak interactions with the hydrogen atoms of the HBD
iv. These interactions between the Cl^- ions and the H atoms of the HBD lead to the formation of weak hydrogen bonding.

v. The sum of these interactions are, however, stronger than the sum of hydrogen bonding within water molecules. Hence, the solvent(DES) so formed exhibit very low freezing and melting points.

It is important to add that other weaker interactions, especially, Van der Waals forces may also be contributing to the interactions between the HBA and HBD in DESs.

The above information obtained from the simulation, it suggests that molecular dynamic simulations and DFT is a good predictive tool for the formulation of DESs.

CHAPTER FIVE

CONCLUSIONS AND RECOMMENDATIONS

The main aim of this work was to explore the use water molecules as the sole hydrogen bond donor (HBD) in the formulation of DES and to investigate the molecular basis of DES formation via molecular dynamic simulation. A set of eight solvents were prepared/formulated using choline chloride as quaternary ammonium salt (QAS) and water as HBD at varying molar ratio of water.

The solvents were subjected to physical and chemical characterization to define the eutectic point, as well as confirm the eutectic composition. The eutectic composition was defined as the solvent or formulation with the lowest melting or freezing point (eutectic point). All solvents recorded steep depression in their freezing point relative to the individual constituents. However, the ChCl:H_2O (1:3) reported the lowest freezing point. Hence, ChCl:H_2O (1:3) formulation was identified as the eutectic composition with eutectic point of -84.7^{o}C.

The characteristic low freezing and melting points observed in DES is suggestively attributed to hydrogen bond formation between the constituent groups. If this suggestion is true, then the eutectic composition should exhibit high

thermal stability characterized by high boiling and decomposition temperatures. Again, the strength of the hydrogen bonds within the eutectic composition should be relatively stronger compared to the other solvents. Thus, thermal stability studies were conducted via DSC and TGA on all the solvents. Also, the hydrogen bonding was studied spectroscopically via NMR, FTIR, and Raman.

The spectroscopic analysis indicated a weak downfield shift in the NMR spectra characteristic of hydrogen bond formation. Also, X-H stretching associated with hydrogen bond was observed in the lower energy regions of the FTIR spectra. Similar observation was made in the Raman spectra. Therefore, spectroscopic analyses of the solvents indicated the formation of hydrogen bonding other than the intramolecular hydrogen bonding within water molecules. The DFT simulation confirmed that the hydrogen bonding formed in the solvents, though weaker, were stronger than the hydrogen-bonding profile observed within water molecules. Again, the ChCl:H_2O 1:3 and ChCl:H_2O 1:4 were observed to possess relatively stronger hydrogen bonding than the other solvents.

The thermal stability studies involving DSC and TGA supported the earlier physicochemical observations in that the solvents thermal stability correlated with the observed

trend in hydrogen-bond strength. Thus, the ChCl:H_2O 1:3 and ChCl:H_2O 1:4 were found to be more thermally stable, high boiling points, and decomposition temperatures compared to the other solvents.

Viscosity and surface tension analyses also conformed to the effect of hydrogen bonding. As the hydrogen bond strength increased, the viscosity and surface tension also increased. Thus, the solvents with relatively strong hydrogen bond had relatively high viscosity and surface tension compared to the other solvents.

DFT simulation were performed via COSMO-RS to probe the underlying molecular basis of the behavior of DESs. This is particularly important as debate continues on the molecular basis for the behavior of DESs. Sigma profiles, chemical potentials and hydrogen-bond profiles as well as nonhydrogen bond profiles were simulated. Also, to explore further the nature of the interactions, charge transfer analyses were also conducted. Hirshfeld partial charges and Voronoi's deformation density charges formed the basis of the charge transfer analyses.

The Sigma, chemical potentials and hydrogen bond profiles of ChCl:H_2O 1:3 and ChCl:H_2O 1:4 were significantly higher than the rest of the solvents with their profiles almost

overlapping. The profiles confirm ChCl:H_2O 1:3 and ChCl:H_2O 1:4 to have relatively stronger hydrogen bonds. Again, the results from the charge transfer analyses suggested charge spreading across the entire organic backbone of choline cation. Also, the charge transfer across the HBD was insignificant compared to that across the organic backbone of choline cation. This is irrespective of the ratio of the HBD.

However, and probably more significant, charge flow analysis from the Voronoi's deformation density indicates that the charge spreading emanates from the chloride anion in the choline chloride. Also, the strength of the charge from the chloride anion is akin to weak hydrogen bonds and probably Van der Waals forces. Therefore, it is apparent that charge transfer or spreading occurs in the DESs formation, that the charge emanates from the halide ion, and the strength of the charge spreading is akin to hydrogen bonding. Therefore, hydrogen bonding plays a significant role in DES formation but other weaker interactions such as VDW forces may be involved. DFT, via COSMO-RS, could be used to initially predict the eutectic composition of binary DES solvents or possibly ternary DES solvents. Further studies will ascertain this.

Further work is required in the application of aqueous choline chloride DESs especially in the areas of cryo-reactions, sample preservation, pharmaceutical formulations, and biocatalysis. The quest to understand the fundamental basis of the interactions between HBDs and HBDs during DES formation require further studies.

REFERENCE

1. Brundtland, C.G. *World Commission on Environment and Development: Our Common Future;A/42/427; United Nations;* Oxford University Press: 1987; p 393.

2. Melissae F. Green Chemistry and Engineering: Towards a Sustainable Future; *American Chemical Society* 2013.

3. Anastas, P. T., *Handbook of Green Chemistry. Ionic Liquids;* Wiley-vch Verlag GmbH: Weinheim, 2010; Vol. 6; p 3

4. Tucker, J. L. Green Chemistry, a Pharmaceutical Perspective; *Organic Process Research & Development* **2006**, *10*, 2, p 315-319.

5. Jessop, P. G.; Trakhtenberg, S.; Warner, J.; The Twelve Principles of Green Chemistry. **2008**, *1000*, p 401-436.

6. Anastas, P. T.; Warner, J. C.; *Green Chemistry: Theory and Practice*. Oxford University Press: 1998.

7. Organization, U. N.; Agenda for Sustainable Development. United Nations: 2015.

8. Daniel Hoornweg, P. B.T; The World Bank, *What A Waste: A Global Review of Solid Waste Management. Urban Development Series; Knowledge Papers* **2010**,15, p 7-10.

9. Nelson, W. M.; *Green Solvents for Chemistry: Perspectives and Practice*. Oxford University Press: 2003.

10. Welton, T.; *Solvents and sustainable chemistry*. *Proc Math Phys Eng Sci.* **2015**, *471*, p 2183.

11. Ravikiran T.N; Anoop K.; Green Chemistry. *World Journal of Pharmacy and Pharmaceutical Sciences* **2015**, *4*, (04) p 353-367.

12. Seyler, C.; Capello, C.; Hellweg, S.; Bruder, C.; Bayne, D.; Huwiler, A.; Hungerbühler, K., Waste-Solvent Management as an Element of Green Chemistry: A Comprehensive Study on the Swiss Chemical Industry. *Industrial & Engineering Chemistry Research* **2006**, *45* (22) p 7700-7709.

13. Leitner, W.; Supercritical Carbon Dioxide as a Green Reaction Medium for Catalysis. *Accounts of Chemical Research* **2002**, *35* (9) p 11.

14. Licence, P.; Ke, J.; Sokolova, M.; Ross, S. K.; Poliakoff, M., Chemical reactions in supercritical carbon dioxide: from laboratory to commercial plant. *Green Chemistry* **2003**, *5* (2) p 99-104.

15. Abbott, A. P.; Capper, G.; Davies, D. L.; Rasheed, R. K.; Tambyrajah, V., Novel solvent properties of choline chloride/urea mixtures. *Chemical Communications* **2003**, (1), p 70-71.

16. Smith, E. L.; Abbott, A. P.; Ryder, K. S., Deep eutectic solvents (DESs) and their applications. *Chem Rev* **2014**, *114* (21), p 11060-82.

17. Abbott, A. P.; Capper, G.; Davies, D. L.; Munro, H. L.; Rasheed, R. K.; Tambyrajah, V., Preparation of novel, moisture-stable, Lewis-acidic ionic liquids containing quaternary ammonium salts with functional side chains. *Chemical Communications* **2001**, (19), p 2010-2011.

18. Abo-Hamad, A.; Hayyan, M.; AlSaadi, M. A.; Hashim, M. A., Potential applications of deep eutectic solvents in nanotechnology. *Chemical Engineering Journal* **2015**, *273*, p 551-567.

19. Sitze, M. S.; Schreiter, E. R.; Patterson, E. V.; Freeman, R. G., Ionic Liquids Based on $FeCl_3$ and $FeCl_2$. Raman Scattering and ab Initio Calculations. *Inorganic Chemistry* **2001**, *40* (10), p 2298-2304.

20. Abbott, A. P.; Capper, G.; Davies, D. L.; McKenzie, K. J.; Obi, S. U., Solubility of Metal Oxides in Deep Eutectic Solvents Based on Choline Chloride. *Journal of Chemical & Engineering Data* **2006**, *51* (4), p 1280-1282.

21. Abbott, A. P.; Cullis, P. M.; Gibson, M. J.; Harris, R. C.; Raven, E., Extraction of glycerol from biodiesel into a eutectic based ionic liquid. *Green Chemistry* **2007**, *9* (8), p 868.

22. Shahbaz, K.; Mjalli, F. S.; Hashim, M. A.; AlNashef, I. M., Elimination of All Free Glycerol and Reduction of Total Glycerol from Palm Oil-Based Biodiesel Using Non-Glycerol Based Deep Eutectic Solvents. *Separation Science and Technology* **2013**, *48* (8), p 1184-1193.

23. Hartley, J. M.; Ip, C. M.; Forrest, G. C.; Singh, K.; Gurman, S. J.; Ryder, K. S.; Abbott, A. P.; Frisch, G., EXAFS study into the speciation of metal salts dissolved in ionic liquids and deep eutectic solvents. *Inorg Chem* **2014**, *53* (12), p 6280-6288.

24. Wang, S.-M.; Li, Y.-W.; Feng, X.-J.; Li, Y.-G.; Wang, E.-B., New synthetic route of polyoxometalate-based hybrids in choline chloride/urea eutectic media. *Inorganica Chimica Acta* **2010**, *363* (7), p 1556-1560.

25. Lobo, H. R.; Singh, B. S.; Shankarling, G. S., Deep eutectic solvents and glycerol: a simple, environmentally benign and efficient catalyst/reaction media for synthesis of N-aryl phthalimide derivatives. *Green Chemistry Letters and Reviews* **2012**, *5* (4), p 487-533.

26. Alonso, D. A.; Baeza, A.; Chinchilla, R.; Guillena, G.; Pastor, I. M.; Ramón, D. J., Deep Eutectic Solvents: The Organic Reaction Medium of the Century. *European Journal of Organic Chemistry* **2016**, *2016* (4), p 612-632.

27. Gambino, M.; Gaune, P.; Nabavian, M.; Gaune-Escard, M.; Bros, J. P., Enthalpie de fusion de l'uree et de quelques melanges eutectiques a base d'uree. *Thermochimica Acta* **1987**, *111*, p 37-47.

28. Abbott, A. P.; Barron, J. C.; Ryder, K. S.; Wilson, D., Eutectic-based ionic liquids with metal-containing anions and cations. *Chemistry* **2007**, *13* (22), p 6495-6501.

29. Baust, J. G., Mechanisms of cryoprotection in freezing tolerant animal systems. *Cryobiology* **1973**, *10* (3), p 197-205.

30. Shin, G. G.; Richard, E. L. J.; David, L. D, Aquaporins in the Antarctic Midge, an Extremophile that Relies on Dehydration for Cold Survival. *Biol. Bull.*. **2015**, *229*, p 47–57.

31. Storey, K. B.; Storey, J. M., Freeze tolerance in animals. *Physiological Reviews* **1988**, *68* (1), p 27-84.

32. Scudellari, M., Icing Organs: Why scientists are so near and yet so far from being able to cryopreserve organs. *The Scientist[Online]* 2013. https://www.the-scientist.com/features/icing-organs-39859 (accessed Feb 07, 2013)

33. Azuma, M. M. M., Aquaporins are expressed in the columnar cells of the midgut epithelium of the silkworm, Bombyx mori. *Journal of Insect Biotechnology and Sericology* **2015**, *84*, p 55-61.

34. Campbell, E. M.; Ball, A.; Hoppler, S.; Bowman, A. S., Invertebrate aquaporins: a review. *J. Comp. Physiol. B* **2008**, *178* (8), p 935-55.

35. Walters, K. R., Jr.; Serianni, A. S.; Sformo, T.; Barnes, B. M.; Duman, J. G., A nonprotein thermal hysteresis-producing xylomannan antifreeze in the freeze-tolerant Alaskan beetle Upis ceramboides. *Proc. Natl. Acad. Sci. U S A.* **2009**, *106* (48), p 20210-20215.

36. Devries, A. L., Glycoproteins as Biological Antifreeze Agents in Antarctic Fishes. *Science* **1971**, *172* (3988), p 1152.

37. Evans, C. W.; Gubala, V.; Nooney, R.; Williams, D. E.; Brimble, M. A.; Devries, A. L., How do Antarctic notothenioid fishes cope with internal ice? A novel function for antifreeze glycoproteins. *Antarctic Science* **2010**, *23* (1), p 57-64.

38. DeVries, A. L.; Wohlschlag, D. E., Freezing Resistance in Some Antarctic Fishes. *Science* **1969**, *163* (3871), p 1073.

39. Amir, G.; Rubinsky, B.; Basheer, S. Y.; Horowitz, L.; Jonathan, L.; Feinberg, M. S.; Smolinsky, A. K.; Lavee, J., Improved viability and reduced apoptosis in sub-zero 21-hour preservation of transplanted rat hearts using anti-freeze proteins. *J. Heart Lung Transplant* **2005**, *24* (11), p 1915-1929.

40. Rinehart, J. P.; Hayward, S. A.; Elnitsky, M. A.; Sandro, L. H.; Lee, R. E., Jr.; Denlinger, D. L., Continuous up-regulation of heat shock proteins in larvae, but not adults, of a polar insect. *Proc. Natl. Acad. Sci. U S A.* **2006**, *103* (38), p 14223-14227.

41. Lannan, F. M.; Mamajanov, I.; Hud, N. V., Human telomere sequence DNA in water-free and high-viscosity solvents: G-quadruplex folding governed by Kramers rate theory. *J Am Chem Soc* **2012**, *134* (37), p 15324-15330.

42. He, C.; Gállego, I.; Laughlin, B.; Grover, M. A.; Hud, N. V., A viscous solvent enables information transfer from gene-length nucleic acids in a model prebiotic replication cycle. *Nature Chemistry* **2016**, *9*, p 318.

43. Choi, Y. H.; van Spronsen, J.; Dai, Y.; Verberne, M.; Hollmann, F.; Arends, I. W. C. E.; Witkamp, G.J.; Verpoorte, R., Are Natural Deep Eutectic Solvents the Missing Link in Understanding Cellular Metabolism and Physiology? *Plant Physiology* **2011**, *156* (4), p 1701.

44. Dai, Y.; Rozema, E.; Verpoorte, R.; Choi, Y. H., Application of natural deep eutectic solvents to the extraction of anthocyanins from Catharanthus roseus with high extractability and stability replacing conventional organic solvents. *J. Chromatogr. A* **2016**, *1434*, p 50-6.

45. Dai, Y.; van Spronsen, J.; Witkamp, G. J.; Verpoorte, R.; Choi, Y. H., Natural deep eutectic solvents as new potential media for green technology. *Anal. Chim. Acta* **2013**, *766*, p 61-8.

46. Dai, Y.; van Spronsen, J.; Witkamp, G. J.; Verpoorte, R.; Choi, Y. H., Ionic liquids and deep eutectic solvents in natural products research: mixtures of solids as extraction solvents. *J. Nat. Prod.* **2013**, *76* (11), p 2162-2173.

47. Dai, Y.; Verpoorte, R.; Choi, Y. H., Natural deep eutectic solvents providing enhanced stability of natural colorants from safflower (Carthamus tinctorius). *Food Chem.* **2014**, *159*, p 116-121.

48. Dai, Y.; Witkamp, G. J.; Verpoorte, R.; Choi, Y. H., Natural deep eutectic solvents as a new extraction media for phenolic metabolites in Carthamus tinctorius L. *Anal. Chem.* **2013**, *85* (13), p 6272-6278.

49. Dai, Y.; Witkamp, G. J.; Verpoorte, R.; Choi, Y. H., Tailoring properties of natural deep eutectic solvents with water to facilitate their applications. *Food Chem* **2015**, *187*, 14-19.

50. Hou, Y. L.; Ren, J.; Niu, S.; Wu, M., Separation of the isomers of benzene poly-carboxylic acids by quaternary ammonium salt via formation of deep eutectic solvents. *J Phys. Chem. B* **2014**, *118* (47), p 13646-50.

51. Al-Badr, A. A.; El-Obeid, H. A., Acetylcholine Chloride: Physical Profile. **2005**, *31*, p 1-19.

52. Timothy, A. I.; Marcos, S.; Eduardo, C., Case Study: Water and Ice. *Educational Researcher* **2007** p 1-33.

53. Andrew, P. A.; Ian, D.; Frank E.; Douglas R. M., Why use Ionic Liquids for Electrodeposition? In *Electrodeposition from Ionic Liquids*, 1st ed.; Wiley-VCH Verlag:Weinheim, **2008**; p 1-13.

54. Wilkes, J. S.; Zaworotko, M. J., Air and water stable 1-ethyl-3-methylimidazolium based ionic liquids. *Journal of the Chemical Society, Chemical Communications* **1992**, (13), p 965-967.

55. Qinghua, Z.; Karine, D. O. V.; Sebastien, R.; Francois J., Deep eutectic solvents syntheses: properties and applications. *Chem. Soc. Rev.* **2012**, *41* (21), p 7108-7146.

56. Tang, S.; Baker, G. A.; Zhao, H., Ether- and alcohol-functionalized task-specific ionic liquids: attractive properties and applications. *Chemical Society Reviews* **2012**, *41* (10), p 4030-4066.

57. Zhang, Y.; Bakshi, B. R.; Demessie, E. S., Life Cycle Assessment of an Ionic Liquid versus Molecular Solvents and Their Applications. *Environmental Science & Technology* **2008**, *42* (5), p 1724-1730.

58. Kudlak, B.; Owczarek, K.; Namiesnik, J., Selected issues related to the toxicity of ionic liquids and deep eutectic solvents-A review. *Environ. Sci. Pollut. Res. Int.* **2015**, *22* (16), p 11975-11992.

59. El-Harbawi, M., Toxicity Measurement of Imidazolium Ionic Liquids Using Acute Toxicity Test. *Procedia Chemistry* **2014**, *9*, p 40-52.

60. Pham, T. P.; Cho, C. W.; Yun, Y. S., Environmental fate and toxicity of ionic liquids: A review. *Water Res* **2010**, *44* (2), p 352-372.

61. Maugeri, Z.; Domínguez de María, P., Benzaldehyde lyase (BAL)-catalyzed enantioselective CC bond formation in deep-eutectic-solvents–buffer mixtures. *Journal of Molecular Catalysis B: Enzymatic* **2014**, *107*, p 120-123.

62. Sonawane, Y. A.; Phadtare, S. B.; Borse, B. N.; Jagtap, A. R.; Shankarling, G. S., Synthesis of

Diphenylamine-Based Novel Fluorescent Styryl Colorants by Knoevenagel Condensation Using a Conventional Method, Biocatalyst, and Deep Eutectic Solvent. *Organic Letters* **2010**, *12* (7), p 1456-1459.

63. Hayyan, A.; Mjalli, F. S.; AlNashef, I. M.; Al-Wahaibi, Y. M.; Al-Wahaibi, T.; Hashim, M. A., Glucose-based deep eutectic solvents: Physical properties. *Journal of Molecular Liquids* **2013**, *178*, p 137-141.

64. Pawar, P. M.; Jarag, K. J.; Shankarling, G. S., Environmentally benign and energy efficient methodology for condensation: an interesting facet to the classical Perkin reaction. *Green Chemistry* **2011**, *13* (8), p 2130-2134.

65. Mota-Morales, J. D.; Gutierrez, M. C.; Sanchez, I. C.; Luna-Barcenas, G.; del Monte, F., Frontal polymerizations carried out in deep-eutectic mixtures providing both the monomers and the polymerization medium. *Chemical Communications* **2011**, *47* (18), p 5328-5330.

66. Fernandes, P. M. V.; Campiña, J. M.; Pereira, N. M.; Pereira, C. M.; Silva, F., Biodegradable deep-eutectic mixtures as electrolytes for the electrochemical synthesis of conducting polymers. *Journal of Applied Electrochemistry* **2012**, *42* (12), p 997-1003.

67. Serrano, M. C.; Gutierrez, M. C.; Jimenez, R.; Ferrer, M. L.; del Monte, F., Synthesis of novel lidocaine-

releasing poly(diol-co-citrate) elastomers by using deep eutectic solvents. *Chem. Commun. (Camb)* **2012**, *48* (4), p 579-581.

68. Leroy, E.; Decaen, P.; Jacquet, P.; Coativy, G.; Pontoire, B.; Reguerre, A.L.; Lourdin, D., Deep eutectic solvents as functional additives for starch based plastics. *Green Chemistry* **2012**, *14* (11), p 3063-3066.

69. Ramesh, S.; Shanti, R.; Morris, E., Discussion on the influence of DES content in CA-based polymer electrolytes. *Journal of Materials Science* **2011**, *47* (4), p 1787-1793.

70. Gómez, E.; Cojocaru, P.; Magagnin, L.; Valles, E., Electrodeposition of Co, Sm and SmCo from a Deep Eutectic Solvent. *Journal of Electroanalytical Chemistry* **2011**, *658* (1), p 18-24.

71. Guillamat, P.; Cortés, M.; Vallés, E.; Gómez, E., Electrodeposited CoPt films from a deep eutectic solvent. *Surface and Coatings Technology* **2012**, *206* (21), p 4439-4448.

72. Wagle, D. V.; Zhao, H.; Baker, G. A., Deep Eutectic Solvents: Sustainable Media for Nanoscale and Functional Materials. *Accounts of Chemical Research* **2014**, *47* (8), p 2299-2308.

73. Abbott, A. P.; El-Ttaib, K.; Frisch, G.; McKenzie, K. J.; Ryder, K. S., Electrodeposition of copper composites from deep eutectic solvents based on choline chloride. *Physical Chemistry Chemical Physics* **2009**, *11* (21), p 4269-4277.

74. Hong-Gang, L.; Yan-Xia, J.; Zhi-You, Z.; Sheng-Pei, C.; Shi-Gang, S., Shape-Controlled Synthesis of Gold Nanoparticles in Deep Eutectic Solvents for Studies of Structure–Functionality Relationships in Electrocatalysis. *Angewandte Chemie International Edition* **2008**, *47* (47), p 9100-9103.

75. Dong, J.Y.; Hsu, Y.J.; Wong, D. S.H.; Lu, S.Y., Growth of ZnO Nanostructures with Controllable Morphology Using a Facile Green Antisolvent Method. *The Journal of Physical Chemistry C* **2010**, *114* (19), p 8867-8872.

76. Dong, J.Y.; Lin, C.H.; Hsu, Y.J.; Lu, S.Y.; Wong, D. S.H., Single-crystalline mesoporous ZnO nanosheets prepared with a green antisolvent method exhibiting excellent photocatalytic efficiencies. *CrystEngComm* **2012**, *14* (14), p 4732-4737.

77. Gu, C. D.; Xu, X. J.; Tu, J. P., Fabrication and Wettability of Nanoporous Silver Film on Copper from Choline Chloride-Based Deep Eutectic Solvents. *The Journal of Physical Chemistry C* **2010**, *114* (32), p 13614-13619.

78. Gutiérrez, M. C.; Rubio, F.; del Monte, F., Resorcinol-Formaldehyde Polycondensation in Deep Eutectic Solvents for the Preparation of Carbons and Carbon–Carbon Nanotube Composites. *Chemistry of Materials* **2010**, *22* (9), p 2711-2719.

79. Huang, Y.; Shen, F.; La, J.; Luo, G.; Lai, J.; Liu, C.; Chu, G., Synthesis and Characterization of CuCl Nanoparticles in Deep Eutectic Solvents. *Particulate Science and Technology* **2013**, *31* (1), p 81-84.

80. Gorke, J. T.; Srienc, F.; Kazlauskas, R. J., Hydrolase-catalyzed biotransformations in deep eutectic solvents. *Chem Commun (Camb)* **2008**, (10), p 1235-1237.

81. Lindberg, D.; de la Fuente R.M.; Widersten, M., Deep eutectic solvents (DESs) are viable cosolvents for enzyme-catalyzed epoxide hydrolysis. *J. Biotechnol* **2010**, *147* (3-4), p 169-171.

82. Hayyan, M.; Mjalli, F. S.; Hashim, M. A.; AlNashef, I. M., A novel technique for separating glycerine from palm oil-based biodiesel using ionic liquids. *Fuel Processing Technology* **2010**, *91* (1), p 116-120.

83. Gutierrez, M. C.; Ferrer, M. L.; Yuste, L.; Rojo, F.; del Monte, F., Bacteria incorporation in deep-eutectic solvents through freeze-drying. *Angew. Chem. Int. Ed. Engl.* **2010**, *49* (12), p 2158-62.

84. Mamajanov, I.; Engelhart, A. E.; Bean, H. D.; Hud, N. V., DNA and RNA in anhydrous media: duplex, triplex, and G-quadruplex secondary structures in a deep eutectic solvent. *Angew. Chem. Int. Ed. Engl.* **2010**, *49* (36), p 6310-6314.

85. Zhao, H.; Baker, G. A.; Holmes, S., Protease activation in glycerol-based deep eutectic solvents. *J. Mol. Catal. B Enzym* **2011**, *72* (3-4), p 163-167.

86. Shahbaz, K.; Mjalli, F. S.; Hashim, M. A.; AlNashef, I. M., Using Deep Eutectic Solvents Based on Methyl Triphenyl Phosphunium Bromide for the Removal of Glycerol from Palm-Oil-Based Biodiesel. *Energy & Fuels* **2011**, *25* (6), p 2671-2678.

87. Guo, W.; Hou, Y.; Ren, S.; Tian, S.; Wu, W., Formation of Deep Eutectic Solvents by Phenols and Choline Chloride and Their Physical Properties. *Journal of Chemical & Engineering Data* **2013**, *58* (4), p 866-872.

88. Guo, W.; Hou, Y.; Wu, W.; Ren, S.; Tian, S.; Marsh, K. N., Separation of phenol from model oils with quaternary ammonium saltsvia forming deep eutectic solvents. *Green Chem.* **2013**, *15* (1), p 226-229.

89. Pang, K.; Hou, Y.; Wu, W.; Guo, W.; Peng, W.; Marsh, K. N., Efficient separation of phenols from oils via forming deep eutectic solvents. *Green Chemistry* **2012**, *14* (9), p 2398-2401.

90. Kareem, M. A.; Mjalli, F. S.; Hashim, M. A.; Hadj-Kali, M. K. O.; Bagh, F. S. G.; Alnashef, I. M., Phase equilibria of toluene/heptane with tetrabutylphosphonium bromide based deep eutectic solvents for the potential use in the separation of aromatics from naphtha. *Fluid Phase Equilibria* **2012**, *333*, p 47-54.

91. Wibowo, D.; Lee, C.-K., Nonleaching antimicrobial cotton fibers for hyaluronic acid adsorption. *Biochemical Engineering Journal* **2010**, *53* (1), 44-51.

92. Habibi, E.; Ghanemi, K.; Fallah-Mehrjardi, M.; Dadolahi-Sohrab, A., A novel digestion method based on a choline chloride–oxalic acid deep eutectic solvent for determining Cu, Fe, and Zn in fish samples. *Analytica Chimica Acta* **2013**, *762*, p 61-67.

93. Degam, G. Deep Eutectic Solvents Synthesis, Characterization and Applications in Pretreatment of Lignocellulosic Biomass. PhD Dissertation, South Dakota State University, Open PRAIRIE, **2017**.

94. Fornaro, T.; Burini, D.; Biczysko, M.; Barone, V., Hydrogen-bonding effects on infrared spectra from anharmonic computations: uracil-water complexes and uracil dimers. *J. Phys. Chem. A* **2015**, *119* (18), p 4224-36.

95. Crews, P.; Rodríguez, J.; Jaspars, M., *Organic Structure Analysis*, 2nd ed.; Oxford University Press: 2010.

96. Hadj-Kali, M. K.; Al-khidir, K. E.; Wazeer, I.; El-blidi, L.; Mulyono, S.; AlNashef, I. M., Application of deep eutectic solvents and their individual constituents as surfactants for enhanced oil recovery. *Colloids and Surfaces A: Physicochemical and Engineering Aspects* **2015**, *487*, p 221-231.

97. Tang, B.; Row, K. H., Recent developments in deep eutectic solvents in chemical sciences. *Monatshefte für Chemie - Chemical Monthly* **2013**, *144* (10), p 1427-1454.

98. Hou, Y.; Gu, Y.; Zhang, S.; Yang, F.; Ding, H.; Shan, Y., Novel binary eutectic mixtures based on imidazole. *Journal of Molecular Liquids* **2008**, *143* (2), p 154-159.

99. Robles, P.A.; Valderrama, J. O. , Critical Properties, Normal Boiling Temperatures, and Acentric Factors of Fifty Ionic Liquids. *Ind. Eng. Chem. Res.* **2007**, *46*, p 1338-1344.

100. Hong-Zhen, S.; Mei, Y. J.; Qing-Shan, L.; Chang-Ping, L., Properties of four deep eutectic solvents density, electrical conductivity, dynamic viscosity and refractive index. *Acta Phys. Chim. Sin.* **2015**, *31* (8), p 1468–1473.

101. Leron, R. B.; Soriano, A. N.; Li, M.H., Densities and refractive indices of the deep eutectic solvents (choline

chloride+ethylene glycol or glycerol) and their aqueous mixtures at the temperature ranging from 298.15 to 333.15K. *Journal of the Taiwan Institute of Chemical Engineers* **2012,** *43* (4), p 551-557.

102. Abbott, A. P., Application of hole theory to the viscosity of ionic and molecular liquids. *Chem. phys. chem.* **2004,** *5* (8), p 1242-1246.

103. Abbott, A. P., Model for the conductivity of ionic liquids based on an infinite dilution of holes. *Chem. phys. chem.* **2005,** *6* (12), p 2502-2505.

104. Hansen, C. M., 50 Years with solubility parameters—past and future. *Progress in Organic Coatings* **2004,** *51* (1), p 77-84.

105. Howell, J.; Roesing, M.; Boucher, D., A Functional Approach to Solubility Parameter Computations. *The Journal of Physical Chemistry B* **2017,** *121* (16), p 4191-4201.

106. Wu, Y.; Sasaki, T.; Kazushi, K.; Seo, T.; Sakurai, K., Interactions between Spiropyrans and Room-Temperature Ionic Liquids: Photochromism and Solvatochromism. *The Journal of Physical Chemistry B* **2008,** *112* (25), p 7530-7536.

107. Abraham, M. H.; Doherty, R. M.; Kamlet, M. J.; Harris, J. M.; Taft, R. W., Linear solvation energy relationships. Part 38. An analysis of the use of solvent parameters in the correlation of rate constants, with special reference

to the solvolysis of t-butyl chloride. *Journal of the Chemical Society, Perkin Transactions 2* **1987**,(8), p 1097-1101.

108. Abraham, M. H.; Poole, C. F.; Poole, S. K., Classification of stationary phases and other materials by gas chromatography. *Journal of Chromatography A* **1999**, *842* (1), p 79-114.

109. Reichardt, C., Pyridinium N-phenolate betaine dyes as empirical indicators of solvent polarity: Some new findings. *Pure Appl. Chem.* **2004**, *76* (10), p 1903–1919.

110. Mizuguchi, J.; Tanifuji, N.; Kobayashi, K., Electronic and Structural Characterization of a Piezochromic Indigoid: 11-(3‘-Oxodihydrobenzothiophen-2‘-ylidene)cyclopenta[1,2-b:4,3-b‘]dibenzothiophene. *The Journal of Physical Chemistry B* **2003**, *107* (46), p 12635-12638.

111. Girard-Reydet, C.; Ortuso, R. D.; Tsemperouli, M.; Sugihara, K., Combined Electrical and Optical Characterization of Polydiacetylene. *The Journal of Physical Chemistry B* **2016**, *120* (14), p 3511-3515.

112. Golchoubian, H.; Moayyedi, G.; Reisi, N., Halochromism, ionochromism, solvatochromism and density functional study of a synthesized copper(II) complex containing hemilabile amide derivative ligand.

Spectrochimica Acta Part A: Molecular and Biomolecular Spectroscopy **2015**, *138*, p 913-924.

113. Marini, A.; Muñoz-Losa, A.; Biancardi, A.; Mennucci, B., What is Solvatochromism? *The Journal of Physical Chemistry B* **2010**, *114* (51), p 17128-17135.

114. Rogers, M. T.; Burdett, J. L., Keto–Enol Tautomerism in β-Dicarbonyls Studied by Nuclear Magnetic Resonance Spectroscopy: II. Solvent Effects on Proton Chemical Shifts and on Equilibrium Constants. *Canadian Journal of Chemistry* **1965**, *43* (5), p 1516-1526.

115. Laurence, C.; Nicolet, P.; Helbert, M., Polarity and basicity of solvents. Part 2. Solvatochromic hydrogen-bonding shifts as basicity parameters. *Journal of the Chemical Society, Perkin Transactions 2* **1986**, (7), p 1081-1090.

116. Nicolet, P.; Laurence, C., Polarity and basicity of solvents. Part 1. A thermosolvatochromic comparison method. *Journal of the Chemical Society, Perkin Transactions 2* **1986**, (7), p 1071.

117. Brooker, L. G. S., The Cyanine Dyes and Related Compounds. *Journal of the American Chemical Society* **1965**, *87* (4), p 937-938.

118. Kosower, E. M., The Effect of Solvent on Spectra. 1. A New Empirical Measure of Solvent Polarity: Z-Values.

Journal of the American Chemical Society **1958**, *80* (13), p 3253-3260.

119. Reichardt, C., Solvatochromic Dyes as Solvent Polarity Indicators. *Chemical Reviews* **1994**, *94* (8), p 2319-2358.

120. Reichardt, C., *Solvents and Solvent Effects in Organic Chemistry.* 3rd ed.; Wiley-VCH **2003**.

121. Zerbetto, F.; Monti, S.; Orlandi, G., Thermal and photochemical interconversion of spiropyrans and merocyanines. A semi-empirical all-valence-electron study. *Journal of the Chemical Society, Faraday Transactions 2: Molecular and Chemical Physics* **1984**, *80* (12), p 1513-1527.

122. Javuku, T., Analysis of Solvatochromism of a Biologically Active Ketocyanine Dye Using Different Solvent Polarity Scales and Estimation of Dipole Moments

International Journal of Life Science and Pharma Research **2014**, *4* (2) p 1-13.

123. Kamlet, M. J.; Abboud, J. L.; Taft, R. W., The solvatochromic comparison method. 6. The .pi.* scale of solvent polarities. *Journal of the American Chemical Society* **1977**, *99* (18), p 6027-6038.

124. Kamlet, M. J.; Abboud, J. L. M.; Abraham, M. H.; Taft, R. W., Linear solvation energy relationships. 23. A comprehensive collection of the solvatochromic parameters,

.pi.*, .alpha., and .beta., and some methods for simplifying the generalized solvatochromic equation. *The Journal of Organic Chemistry* **1983**, *48* (17), p 2877-2887.

125. Abboud, J.L. M.; Taft, R. W.; Kamlet, M. J., Linear solvation energy relationships. Part 31. On Bekarek's modifications of the solvatochromic parameters. *Journal of the Chemical Society, Perkin Transactions 2* **1985**,(6), p 815-819.

126. Lagalante, A. F.; Abdulagatov, A.; Bruno, T. J., Kamlet−Taft Thermosolvatochromic Parameters of Hydrofluoroethers and Hydrofluoroether Azeotropic Mixtures. *Journal of Chemical & Engineering Data* **2002**, *47* (1), p 47-51.

127. Cabot, R.; Hunter, C. A., Molecular probes of solvation phenomena. *Chem. Soc. Rev.* **2012**, *41* (9), p 3485-3492.

128. Christian, R.; Erwin, H. G., Über Pyridinium-N-phenolat-Betaine und ihre Verwendung zur Charakterisierung der Polarität von Lösungsmitteln, X. Erweiterung, Korrektur und Neudefinition der ET-Lösungsmittelpolaritätsskala mit Hilfe eines lipophilen penta-tert-butyl-substituierten Pyridinium-N-phenolat-Betainfarbstoffes. *Liebigs Annalen der Chemie* **1983**, *1983* (5), p 721-743.

129. Christian, R., Polarity of ionic liquids determined empirically by means of solvatochromic pyridinium N-phenolate betaine dyes. *Green Chem.* **2005**, 7 (5), p 339-351.
130. Marcus, Y., The properties of organic liquids that are relevant to their use as solvating solvents. *Chemical Society Reviews* **1993**, *22* (6), p 409.
131. Catalan, J., Toward a Generalized Treatment of the Solvent Effect Based on Four Empirical Scales:Dipolarity (SdP, a New Scale), Polarizability (SP), Acidity (SA), and Basicity (SB) of the Medium. *J. Phys. Chem. B* **2009**, *113*, p 5951–5960.

132. Cerón-Carrasco, J. P.; Jacquemin, D.; Laurence, C.; Planchat, A.; Reichardt, C.; Sraïdi, K., Solvent polarity scales: determination of new ET(30) values for 84 organic solvents. *Journal of Physical Organic Chemistry* **2014**, *27* (6), p 512-518.
133. Jefferies, D.; Khalid, S., Molecular Simulations of Complex Membrane Models A2 - Becker, Sid M. In *Modeling of Microscale Transport in Biological Processes*, Academic Press: **2017**; pp 1-18.
134. Mainberger, S.; Kindlein, M.; Bezold, F.; Elts, E.; Minceva, M.; Briesen, H., Deep eutectic solvent formation: a structural view using molecular dynamics simulations with

classical force fields. *Molecular Physics* **2017**, *115* (9-12), 1309-1321.

135. Wolfram Koch, M. C. H., *A Chemist's Guide to Density Functional Theory*. 2nd ed.; Wiley-VCH Verlag GmbH: Weinheim, Germany, **2001**.

136. Beauchamp, K. A.; Lin, Y.S.; Das, R.; Pande, V. S., Are Protein Force Fields Getting Better? A Systematic Benchmark on 524 Diverse NMR Measurements. *Journal of Chemical Theory and Computation* **2012**, *8* (4), p 1409-1414.

137. Myers, J. K.; Pace, C. N., Hydrogen bonding stabilizes globular proteins. *Biophysical Journal* **1996**, *71* (4), p 2033-2039.

138. Hospital, A.; Goni, J. R.; Orozco, M.; Gelpi, J. L., Molecular dynamics simulations: advances and applications. *Adv Appl Bioinform Chem* **2015**, *8*, p 37-47.

139. Wojnarowska, Z.; Grzybowska, K.; Hawelek, L.; Dulski, M.; Wrzalik, R.; Gruszka, I.; Paluch, M.; Pienkowska, K.; Sawicki, W.; Bujak, P.; Paluch, K. J.; Tajber, L.; Markowski, J., Molecular Dynamics, Physical Stability and Solubility Advantage from Amorphous Indapamide Drug. *Molecular Pharmaceutics* **2013**, *10* (10), p 3612-3627.

140. Zahn, S.; Kirchner, B.; Mollenhauer, D., Charge Spreading in Deep Eutectic Solvents. *Chemphyschem* **2016**, *17* (21), p 3354-3358.

141. Kempter, V.; Kirchner, B., The role of hydrogen atoms in interactions involving imidazolium-based ionic liquids. *Journal of Molecular Structure* **2010**, *972* (1-3), p 22-34.

142. Hizaddin, H. F.; Ramalingam, A.; Hashim, M. A.; Hadj-Kali, M. K. O., Evaluating the Performance of Deep Eutectic Solvents for Use in Extractive Denitrification of Liquid Fuels by the Conductor-like Screening Model for Real Solvents. *Journal of Chemical & Engineering Data* **2014**, *59* (11), p 3470-3487.

143. Mulyono, S.; Hizaddin, H. F.; Alnashef, I. M.; Hashim, M. A.; Fakeeha, A. H.; Hadj-Kali, M. K., Separation of BTEX aromatics from n-octane using a (tetrabutylammonium bromide + sulfolane) deep eutectic solvent - experiments and COSMO-RS prediction. *RSC Advances* **2014**, *4* (34), p 17597-17606.

144. García, G.; Atilhan, M.; Aparicio, S., An approach for the rationalization of melting temperature for deep eutectic solvents from DFT. *Chemical Physics Letters* **2015**, *634*, p 151-155.

145. Bagayoko, D., Understanding density functional theory (DFT) and completing it in practice. *AIP Advances* **2014**, *4* (12), 127104.

146. Becke, A. D., Perspective: Fifty years of density-functional theory in chemical physics. *J. Chem. Phys.* **2014**, *140* (18), 18A301.

147. Yu, H. S.; Li, S. L.; Truhlar, D. G., Perspective: Kohn-Sham density functional theory descending a staircase. *J Chem Phys* **2016**, *145* (13), 130901.

148. Henry, M., The Hydrogen Bond: Critical essay, Articles *International Review of Science* **2016**, *1* (2) p1-31.

149. Arunan, E.; Desiraju, G. R.; Klein, R. A.; Sadlej, J.; Scheiner, S.; Alkorta, I.; Clary, D. C.; Crabtree, R. H.; Dannenberg, J. J.; Hobza, P.; Kjaergaard, H. G.; Legon, A. C.; Mennucci, B.; Nesbitt, D. J., Definition of the hydrogen bond (IUPAC Recommendations 2011). *Pure and Applied Chemistry* **2011**, *83* (8).

150. Tapia, O., Quantum mechanics and the theory of hydrogen bond and proton transfer. Beyond a Born–Oppenheimer description of chemical interconversions. *Journal of Molecular Structure: TheoChem* **1998**, *433* (1), p 95-105.

151. Young, D. C, *Computational Chemistry: A Practical Guide for Applying Techniques to Real World Problems*. 1st edu.; Wiley: **2004**.

152. Claude, D.; Annick, G.; Pierre-Yves, M.; Jacques, W., The modeling of nucleophilic and electrophilic additions and substitutions using extended Hückel-based reaction potentials. *International Journal of Quantum Chemistry* **1990**, *38* (5), p 623-640.

153. Ratajczak, H., Charge Transfer Theory and Vibrational Properties Of The Hydrogen Bond. *Journal of Molecular Structure,* **1973**, (19), p 237-245.

154. Klamt, A., Conductor-like Screening Model for Real Solvents: A New Approach to the Quantitative Calculation of Solvation Phenomena. *The Journal of Physical Chemistry* **1995**, *99* (7), p 2224-2235.

155. Abramov, Y. A., *Computational Pharmaceutical Solid State Chemistry*. 1st edu; Wiley: **2016**.

156. Andreas, K., The COSMO and COSMO-RS solvation models. *Wiley Interdisciplinary Reviews: Computational Molecular Science* **2011**, *1* (5), p 699-709.

157. Andreas, K.; Frank, E., COSMO-RS: A novel and efficient method for the a priori prediction of thermophysical data of liquids. *Fluid Phase Equilibria 172* **2000**, *172*, p 43–72.

158. Klamt, A.; Eckert, F., Erratum to "COSMO-RS: a novel and efficient method for the a priori prediction of thermophysical data of liquids" [Fluid Phase Equilib. 172 (2000) 43–72]. *Fluid Phase Equilibria* **2003**, *205* (2), p 357.

159. Carriazo, D.; Serrano, M. C.; Gutierrez, M. C.; Ferrer, M. L.; del Monte, F., Deep-eutectic solvents playing multiple roles in the synthesis of polymers and related materials. *Chem. Soc. Rev.* **2012**, *41* (14), p 4996-5014.